AN ABSTRACT OF THE THESIS OF

Nilobon Podhipleux for the degree of Doctor of Philosophy in Bioresource Engineering presented on May 7, 1998. Title: Adsorption of the Wild Type and a Synthetic Structural Stability Variant of Bacteriophage T4 Lysozyme.

Redacted for privacy

Abstract approved: _____

Joseph McGuire

In situ ellipsometry, surfactant-mediated elution, and radioisotope labeling with ^{125}I were used in order to elucidate the effect of structural stability on the adsorption of bacteriophage T4 lysozyme at solid-water interfaces. In addition, radiolabeling with ^{14}C was used to monitor adsorption and exchange at the air-water interface. A lysozyme variant was produced by substituting a tryptophan (TRP) residue for the isoleucine residue at position 3. This resulted in a protein with a lower structural stability than that of the wild type. Adsorption at the solid-water interfaces was greatly affected by the stability of the protein. TRP apparently adsorbed at the interfaces more tightly and occupied a greater surface area. Adsorption kinetics recorded at hydrophilic and hydrophobic silica were compared to the kinetic behavior predicted by each of two models for protein adsorption, each of which allowed for adsorption into two different conformational states. A three-rate-constant model assumed that generation of the more tightly bound state does not involve an area change and only occurs through a conversion of the reversibly adsorbed state. A parallel adsorption model allows adsorbing molecules to adopt either of the states directly from the solution, with the more tighly bound state

occupying a larger interfacial area. The pattern of kinetic data indicated that adoption of the more tightly bound state was quickly achieved and did involve an area change; thus, the use of the latter model to explain the data was more appropriate. Results of ^{125}I labeling experiments suggested that exchange reactions between dissolved and adsorbed proteins were affected more by the properties of the adsorbing protein, than by the conformational state and binding strength of the already adsorbed molecules. In addition, the extent and rate of adsorption at the air-water interface was observed to be dependent on stability of the protein. In particular, surface pressure and surface concentration kinetics of the less stable variant exhibited a shorter lag period and a sharper increase than that of the wild type protein.

Adsorption of the Wild Type and a Synthetic Structural Stability Variant of Bacteriophage T4 Lysozyme.

By

Nilobon Podhipleux

A THESIS

submitted to

Oregon State University

In partial fulfillment of
the requirements for the
degree of

Doctor of Philosophy

Completed May 7, 1998
Commencement June, 1998

Doctor of Philosophy thesis of Nilobon Podhipleux
Presented on May 7, 1998

APPROVED:

Redacted for privacy

Major Professor, representing Bioresource Engineering

Redacted for privacy

Head of Department of Bioresource Engineering

Redacted for privacy

Dean of Graduate School

I understand that my thesis will become part of the permanent collection of Oregon State University libraries. My signature below authorizes releases of my thesis to any reader upon request.

Redacted for privacy

Nilobon Podhipleux, Author

ACKNOWLEDGMENT

One of the best parts of writing this dissertation is getting a chance to thank those who have helped make my graduate student life at OSU memorable and enjoyable (that's right, I said enjoyable) now that my journey through graduate school is coming to an end.

First and foremost, I am grateful for the guidance, endless patience, and consideration of Dr. Joseph McGuire, my major professor. I feel so fortunate to have Joe as my academic advisor, especially after hearing horrifying stories about many conflicts between some graduate students and their major professors. Joe's concern does not end with how well his students perform in classes and the lab, but also extends to the general well being of his students.

Next, I thank Dr. Mark Daeschel, Dr. Frank Chaplen, Dr. Michelle Bothwell, and Dr. Carol Saslow for kindly serving as committee members. Besides being a committee member, Michelle is also a friend and always available to answer all kinds of my questions. Her help, patience, dedication, cheerfulness, you name it, went way beyond the call of duty.

Aside from having to learn to compete in English (which obviously did not come naturally for me), living half a world away from home is not the easiest place to be. My personal and deep appreciation goes to Janet Scholtz (who is now Dr. Scholtz) and her mother (Jean) for taking me under their wings and making me feel almost home. A very special thanks is extended to Chartchai Krittanai, Khavinet Lourvanij, and Pinya Sarasas, for their immeasurable friendship and emotional support, plus the extra duty of taking care of my parrot (Micky) when I had to leave Corvallis for conferences and for

refreshing my mental health. New friends at BRE, June Wang, Billy Kim, Alireza Esteglalian, Abdelatif Boussaid, Ginni Lin-who have come and gone-have also made my years of graduate school much more pleasant and enjoyable. I owe thanks to Russell Bazemore, who has been my friend for so many years, for listening to all my complaints during times of stress and frustration. Thanks to my colleague, Woo-Kul Lee, and all my friends who have put up with my occasionally short temper for so long.

I also thank Dr. Cynthia Bower and her keen eyes for typos; for reviewing my chapters and giving me suggestions for improvements. Since Cindy has left, Carolyn Baker has taken on the occasional task of catching my English mistakes (any remaining mistake remains my responsibility, of course). For that and many fun times together, I thank her. An appreciation is extended to David Goode for his understanding while I spent seemingly endless hours with "the other man", my computer!

Last, but certainly not least, I remained indebted (quite literally) to my parents and my 3 sisters for providing me with loving support and understanding throughout my life, especially during the time I struggled to pursue my education. Without their support, this work would still have been possible, but it would not have nearly been worth the effort.

TABLE OF CONTENTS

TABLE OF CONTENTS (continued)

TABLE OF CONTENTS (continued)

LIST OF FIGURES

LIST OF FIGURES (continued)

LIST OF FIGURES (continued)

LIST OF TABLES

LIST OF APPENDICES

LIST OF APPENDIX FIGURES

LIST OF APPENDIX TABLES

LIST OF APPENDIX TABLES (continued)

ADSORPTION OF THE WILD TYPE AND A SYNTHETIC STRUCTURAL STABILITY VARIANT OF BACTERIOPHAGE T4 LYSOZYME

CHAPTER 1

INTRODUCTION

Protein adsorption is a process that occurs spontaneously in most systems containing synthetic materials and biological fluids. Platelet adhesion and thrombus formation following protein adsorption are major concerns in the development of biocompatible materials. Treatments by delivery of therapeutic proteins via implant systems require a prolonged contact between the proteins and the surfaces of the delivery devices. This may result in the adsorption of formulated drugs, a process that can lead to the decline in the efficacy or even harmful effects of the treatments.

In the food industry, proteins play a major role in the fouling of heat-exchange and membrane surfaces, and this can lead to increased resistance to liquid flow and heat transfer. Microbial and spore adhesion appear to be mediated by protein adsorption as well. It has been difficult to quantitatively study the protein adsorption process since the surface activity of a protein is a cumulative property influenced by its size, shape, charge, thermal stability, and other factors. The use of synthetic protein mutants obtained from site-directed mutagenesis holds promise for gaining a more quantitative understanding of protein behavior at solid surfaces, as chosen molecular properties can be related unambiguously to protein surface activity.

The primary objectives of this research were to quantify the kinetic rate constants governing the adsorption of a protein from a single component solution and to determine

the ability of a protein to replace the adsorbed molecules of another dissimilar protein, as quantified by exchange reaction rate constants.

In this research, the wild type T4 lysozyme and a structural stability variant were used to study protein adsorption kinetics at hydrophobic and hydrophilic silica surfaces, using *in situ* ellipsometry. The lysozyme variant was produced by substitution of the isoleucine at position 3 (Ile 3) with a tryptophan residue (Trp), resulting in a protein with a $\Delta G_{unfolding}$ that is 2.8 kcal/mol less than that of the wild type. Dodecyltrimethyl ammonium bromide-mediated elution studies on each type of surface were carried out for both proteins as well. Sequential adsorption kinetics were also monitored by *in situ* ellipsometry. We tested two different adsorption times with the protein first introduced and four adsorption times (at two concentrations) for the protein introduced sequentially. Similar experimental conditions were used for a separate exchange study where protein was radiolabeled with ^{125}I. Results from both the ellipsometry and radiolabeling studies were analyzed with reference to two simple kinetic models in order to estimate kinetic rate constants governing adsorption and exchange mechanisms. The influences of structural stability on adsorption behavior of lysozyme at the air-water interface were also investigated. Adsorption kinetics was followed by recording the changes in surface pressure and surface radioactivity of ^{14}C-labled protein solutions.

1.1 The significance of protein adsorption

Protein adsorption is a process of many applications. It is involved in development of biocompatible devices, solid-phase diagnostics, biosensors, and chromatographic technology. Physical and chemical adsorptions are the basis of

immobilization, which is one of the crucial factors in the biosensor technique (1). According to Chen et al. (2), hydrophobic silica and hydrophilic gold particles added to a glucose oxidase membrane can increase the response current of an enzymatic electrode. They hypothesized that besides the immobilization effect, the change in glucose oxidase activity could be enhanced by the exposure of the FAD inside the enzyme caused by adsorption.

Protein adsorption is a phenomenon of interest to food and pharmaceutical industries because of its apparent role in mediating microbial and spore adhesion. Clinicians are also interested in the process since the attachment of bacteria to a solid surface is almost always preceded by the adsorption of a protein film. It is known that inert protein-repelling materials can be obtained either by surface grafting with a non-charged, hydrophilic polymer (3), or by transformation of the surface into a very low-energy material (4). Olsson et al. (5) studied the role of surface properties in the formation of the salivary pellicle and subsequent adhesion of oral bacteria on glass slides treated with different siloxane polymers. Results showed that all compounds reduced bacterial adherence after saliva contact by up to 90%. However, different patterns of the pellicle proteins adsorption were seen on different polysiloxanes. They concluded that reduction in bacterial adherence to the surfaces was the result of changes in the composition or structure of the salivary pellicle rather than inhibition of its formation.

It is very important to identify optimal formulation and delivery techniques of drugs to maximize the therapeutic benefit while minimizing the treatment costs and the potential toxicity effects. Therefore, understanding protein adsorption is crucial for a precise control of the therapeutic peptides and proteins administered. Tzannis et al. (6)

investigated the extent of interleukin-2 (IL-2, also known as T-cell growth factor) adsorption to silicone rubber tubing, a commonly used catheter material, and its residual bioactivity after interaction with the surface. Attenuated total reflected Fourier transform infrared spectroscopy was employed to monitor the deposition rate and the conformational change of IL-2 upon adsorption. They found that after 24 h of exposure, the bulk concentration of IL-2 solution decreased by 7 to 20%, depending on the initial bulk concentration of the reconstitute IL-2 solution. The residual bioactivity assay of this potential anti-tumor immune modulator showed 97 to 99.5% reductions in the activity levels. They concluded that these activity losses were the direct result of the protein-surface interaction.

Another application of protein adsorption is the idea of adding lipases to commercial detergents to aid in the removal of fat-containing substances. Wannerberger et al. (7) investigated adsorption from lipase-surfactant solutions onto methylated silica surfaces at pH 9 to simulate what might occur during the laundry process. There were 3 surfactants used in the study; sodium dodecyl sulfate (SDS, anionic), $C_{12}E_5$ (nonionic), and a commercial alcohol ethoxylate (AE, nonionic). They concluded that surfactants dominated the adsorption of lipase-surfactant mixtures at concentrations above the critical micelle concentration. However, adsorption of lipase took place upon dilution and the amount of adsorbed lipase was higher for lipase-SDS compared to lipase-nonionic surfactants. The results suggested that lipases may not be effective during the washing cycle when a surfactant is present, but they may become more active when the surfactant concentration is reduced during the rinse cycle.

1.2 Multiple states of adsorption

Many researchers believe that proteins can adsorb onto a surface in more than one state. DeFeijter et al. (8) studied adsorption of various proteins at air-water interfaces. They found that conformational rearrangement of the adsorbed molecules at low bulk concentration was considerable compared with that of the adsorbed molecules at high bulk concentration. They concluded that the degree to which adsorbed molecules undergo conformational changes depends on the amount of adsorbed molecules at the interface. Lundström (9) proposed a simple dynamic equilibrium model that allows two forms of adsorbed protein, "native" and "denatured". Both of the two states cover a different interfacial area and can desorb into the solution. This equilibrium model also allows for the adsorbed molecules to change conformation or orientation on the surface. Later, Lundström and Elwing (10) proposed a more complex model for protein adsorption. In their model, proteins can adsorb onto a surface in several forms and are allowed to exchange with molecules from the bulk solution. Because of the model complexity, this model is not very helpful in the interpretation of experimental data and in the calculation of rate constants.

Krisdhasima et al. (11) studied the adsorption kinetics of β-lactoglobulin and recommended a modification of the model suggested by Lundström (9).
In this three-rate-constant model (Figure 1.1a), protein adsorption is a 2-step process. First, protein molecules reversibly adsorb onto the surface with the adsorption rate k_1. Secondly, the adsorbed molecules can either desorb into the bulk with the rate k_{-1}, or undergo conformational changes and/or re-orientation into the irreversibly adsorbed form

with the rate s_1. When using this model, one must assume that adsorbed proteins in either state occupy the same interfacial area.

Strong evidence supporting the presence of multiple states of adsorbed proteins comes from elutability studies. Bohnert and Horbett (12) investigated the ability of SDS to remove adsorbed fibrinogen and albumin from polymer surfaces. They found that the elutability decreased as the contact time increased for both proteins. Krisdhasima et al. (13) studied adsorption kinetics and elutability of milk proteins and found that not all adsorbed proteins can be removed. This supports the hypothesis that protein molecules can adsorb in multiple states with different levels of binding strength.

Recently, McGuire et al. (14-16) studied comparative adsorption of synthetic mutants and wild type bacteriophage T4 lysozyme. Their results indicated that molecules that adsorbed in different states occupied different interfacial areas. Therefore, they proposed a parallel adsorption model (Figure 1.1b) in which proteins can adopt one of the two states directly from the bulk. In their model, molecules in state 2 are more tightly bound to the surface and occupy a greater interfacial area than those in state 1.

Podhipleux et al. (17) studied the effects of charge on protein behavior at hydrophobic and hydrophilic surfaces and analyzed their data with reference to both the kinetic models proposed by Krisdhasima et al. (11) and by McGuire et al. (15). The pattern of the data in their study indicated that adoption of more tightly bound state may occur rather quickly, and that the molecules in the more tightly bound state may occupy a greater interfacial area.

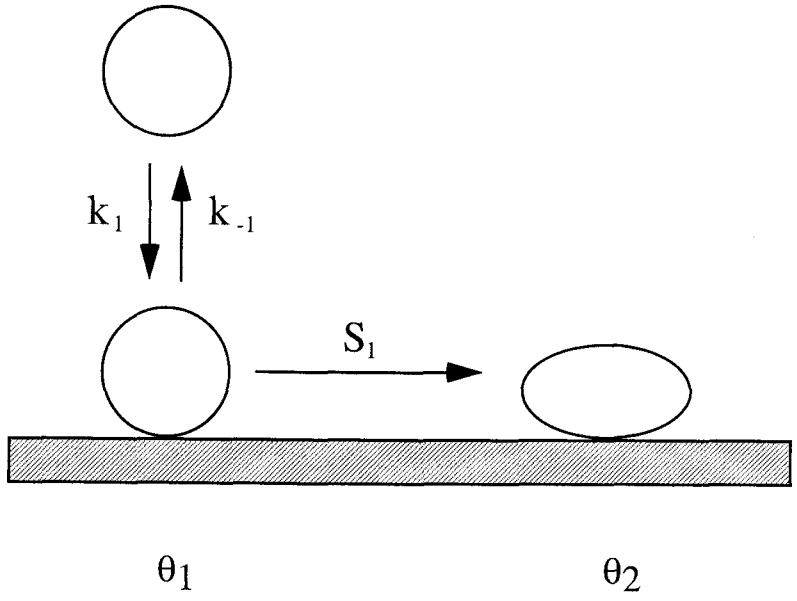

(a)

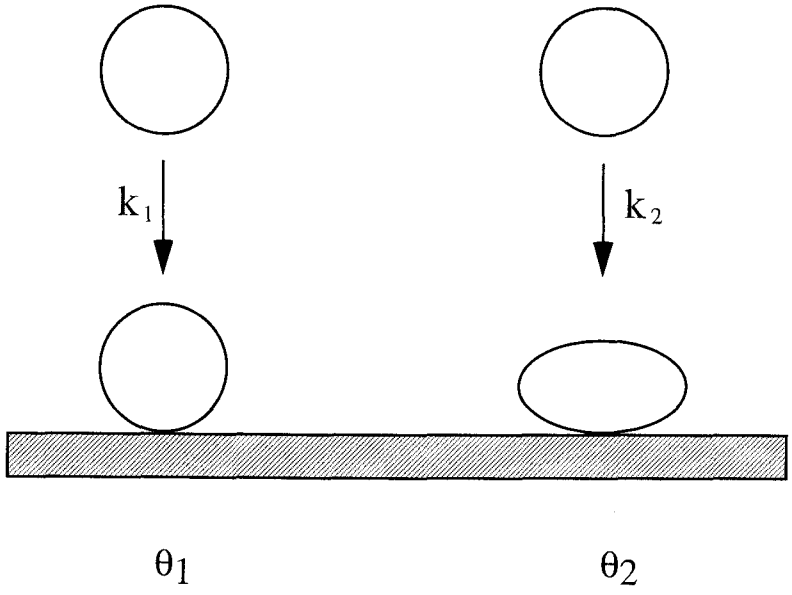

(b)

Figure 1.1. Simple mechanisms for protein adsorption. (a) three-rate-constant model proposed by Krisdhasima et al. [11] and (b) parallel adsorption kinetics proposed by McGuire et al. [15].

1.3 Sequential and competitive adsorption

Sequential adsorption is a process in which one type of protein is allowed to adsorb before a second protein is added into the system. The second protein may replace some or most of the adsorbed protein, depending on many factors, e.g. adsorption time of the first protein, adsorption time and concentration of the second protein.

Pitt et al. (18) studied adsorption of blood proteins, using ^{125}I-labeling, immunogold-labeling, and Fourier transform infrared spectroscopy techniques. They found that the protein adsorption sequence affected thrombus formation and platelet deposition. Sequential adsorption of γ-interferon and BSA on silica surfaces was investigated by Ruzgas et al. (19), using ellipsometry and radiolabeling techniques. Their data suggested that the degree of displacement of adsorbed γ-interferon by BSA increased with decreasing electrostatic interactions between the two proteins.

Elgersma et al. (20) studied both sequential and competitive adsorptions of BSA and monoclonal immuno-gamma globulins (IgG's) on polystyrene lattices. They found that IgG's was easily displaced by BSA, but not the opposite. For adsorption of the second protein to occur, however, the displacement of the first protein was not always a prerequisite. Shirahama et al. (21) monitored adsorption of lysozyme, ribonuclease, and α-lactalbumin on hydrophilic silica and hydrophobic polystyrene coated silica. They concluded that electrostatic interactions played a major role in sequential and competitive adsorption on hydrophilic silica, but these were minor on hydrophobic surfaces.

Anand and Damodaran (22) studied the dynamics of adsorption and exchange between α_{s1}-casein and β-casein at the air/water interface. They found that the

adsorptivities of both proteins in single-component systems were very similar. Studies of the binary mixture showed that β-casein was more surface active than α_{s1}-casein, with a surface load of 2:1 in favor of β-casein. Kinetic data suggested that α_{s1}-casein arrived at the interface first, but was displaced by β-casein. To a lesser extent, displacement tests showed that α_{s1}-casein was also able to displace β-casein from the interface.

In 1995, Anad and Damodaran conducted a similar study of a binary system containing lysozyme and bovine serum albumin (BSA). They found that bulk phase BSA could prevent the adsorption of lysozyme but could not displace lysozyme that already adsorbed at the interface. Lysozyme in the bulk phase, however, could not inhibit nor displace adsorbed BSA. From the analysis of the data, they were convinced that the unit cell dimensions occupied by BSA and lysozyme in the mixed monolayer were the same as those in single-component monolayers, suggesting that both proteins adsorbed independently (23).

1.4 Effects of protein stability on adsorption

By studying the genetic variants and site-directed mutants of single proteins, many researchers have shown that the structural stability of a protein influences its interfacial behaviors (15, 24-26).

Horsley et al. (24) studied adsorption isotherms of hen egg-white (HEW) and human lysozymes at hydrophobic, negatively charged hydrophilic, and positively charged hydrophilic silica surfaces. They found that human lysozyme, which is less stable than HEW lysozyme, underwent more extensive structural changes upon adsorption than

HEW lysozyme. Kato and Yutani (25) compared the surface properties of wild type and mutants of tryptophan synthase. The results suggested that mutants with higher stability exhibited greater resistance to unfolding at the interface.

Wei et al. (26) studied surface tension kinetics of superoxide dismutase, cytochrome *c*, myoglobin, lysozyme, and ribonuclease, using the Wilhelmy plate method. They found the kinetic behavior at low bulk protein concentration to be related to protein's conformational stability. Xu and Damodaran (27) followed the surface pressure of native, partially and fully denatured of hen egg-white, human, and T4 phage lysozymes. They proposed a mechanism for protein adsorption at air-water interface whereby the driving force was considered to be the combination of the interfacial force fields, contributing by hydrophobic, electrostatic, hydration, and conformational potentials.

McGuire et al. (15) studied the effect of structural stability on adsorption of T4 lysozyme at hydrophilic and methylated silica surfaces. The results from kinetic studies and surfactant-mediated elutability studies showed that proteins with lower thermal stabilities were more likely to adsorb in a non-removable form than those with higher thermal stabilities.

Wang et al. (28) studied the surface tension kinetics of various stability mutants of T4 lysozyme. They compared their experimental data to a simple adsorption kinetics model that allowed molecules to adsorb in two states, with state 2 molecule being harder to remove from the air-water interface than state 1 molecule. They found that in general the surface tension of the more stable variants was higher than that of the less stable mutants, and the rate and extent of surface tension changes decreased as $\Delta\Delta G$ increased.

$\Delta\Delta G$ was defined as the difference between $\Delta G_{unfolding}$ of wild type and that of the mutant protein. They also concluded that the contribution to changes in surface tension of state 2 molecule was higher than the contribution of state 1 molecule.

Billsten et al. (29) and Tian et al. (30) monitored changes in secondary structure of wild type and two stability mutants of T4 lysozyme upon adsorption to silica nanoparticles, using circular dichroism. They found that the extent and rate of conformational change upon adsorption varied among proteins. They concluded that the change in conformation was related to thermal stability of the proteins.

1.5 Effects of surface hydrophobicity

Many researchers have conducted studies on effects of contact surface hydrophobicity on protein surface activity (31-33). They believe that hydrophobic interaction between the contact surfaces and proteins contributes to the increase in the entropic driving force, which accompanies adsorption of protein from solution. Elwing et al. (31) used ellipsometry to study adsorption of fibrinogen on hydrophobic and hydrophilic silicon surfaces and found that adsorbed mass was greater on hydrophobic as opposed to hydrophilic surfaces. Lu and Park (32) also studied fibrinogen adsorption using germanium, poly hydroxyethyl methacrylate (poly HEMA), Biomer, and polystyrene surfaces. A weighted-peak shift method was used to determine the extent of the protein conformational changes upon adsorption to surfaces. Their results indicated that fibrinogen underwent a larger degree of conformational changes upon adsorption as the surface hydrophobicity increased.

Interestingly, it was found that the adsorption of protein did not always increase with increasing surface hydrophobicity. Adsorption isotherms, constructed by Krisdhasima et al. (11), for silicon of varying surface hydrophobicities indicated that the adsorbed mass of β-lactoglobulin increases with increasing surface hydrophobicity in the range $10.27 < W^{p}_{a,water} < 41.8$ mJ/m^2, where $W^{p}_{a,water}$ is the value of the polar component of the work of adhesion between any given solid surface and water. Outside of this range, however, the degree of surface hydrophobicity did not seem to have any effects on adsorption of β-lactoglobulin.

1.6 T4 lysozyme

Bacteriophage T4 lysozyme was chosen as the model protein for this work for many reasons: it is a well-characterized protein (34) with known amino acid sequence (35) and 3-dimensional structure (36-37); several variants have been obtained from site-directed mutagenesis, and data on their thermal stabilities (38) and enzymatic activities. (39-41) are available.

Lysozyme is a hydrolytic enzyme, which cleaves a glycosidic linkage in a complex sugar. It can destroys the cell walls of susceptible bacteria (Gram positive) by hydrolyzing the β(1→4) glycosidic linkages from N-acetylmuramic acid (NAM) to N-acetylglucosamine (NAG) in the alternating NAM-NAG hexasaccharide component of cell wall peptidoglycan (40).

T4 lysozyme, as shown in Figure 1.2, consists of 164 amino acid residues, and has a molecular weight of about 18,700 (36). It is a basic, globular protein with an isoelectric

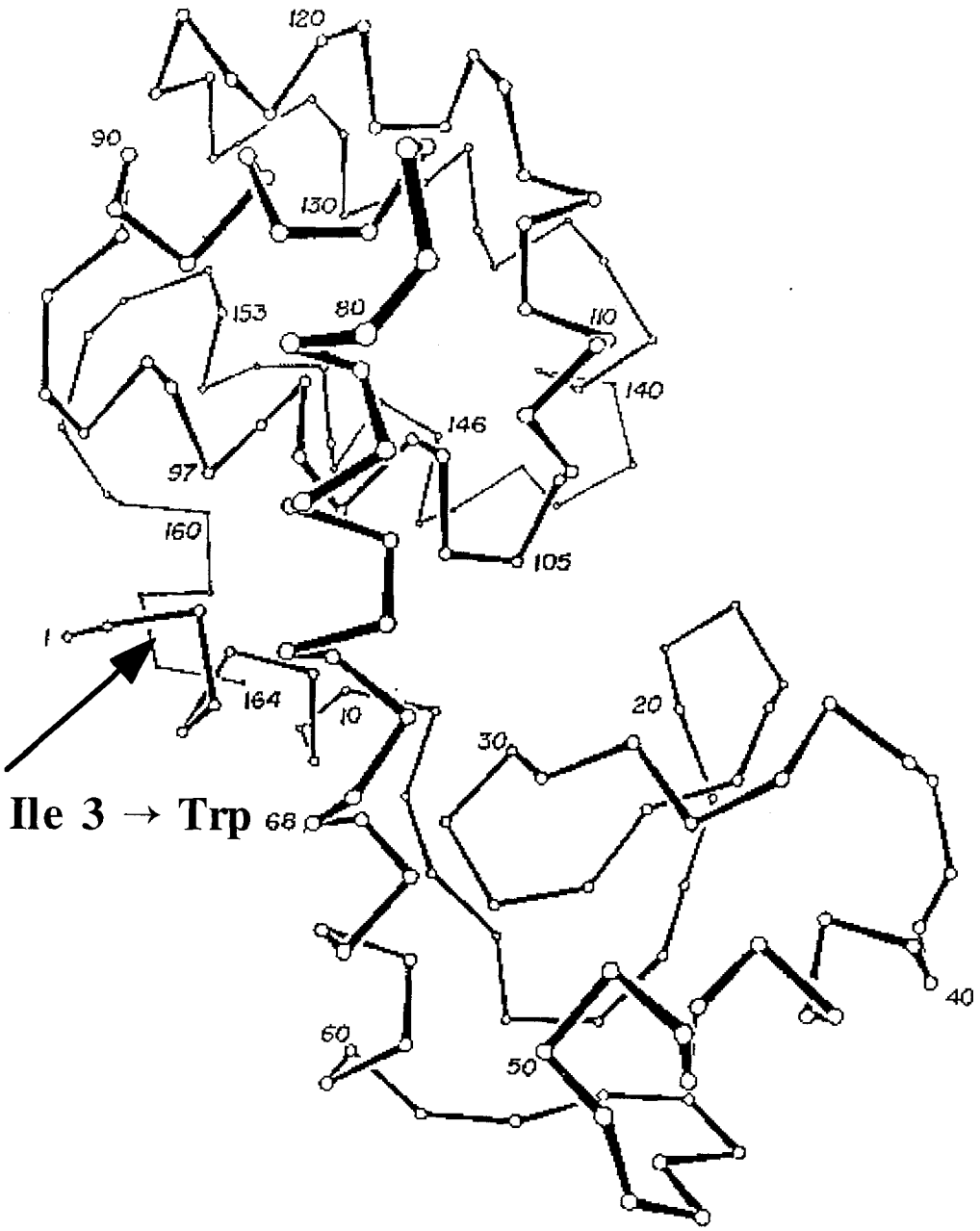

Figure 1.2. Carbon backbone of T4 lysozyme molecule. TRP variant was obtained by subsituting Ile 3 with Trp residue.

point above 9. At neutral pH, it possesses 27 positively charged groups and 18 negatively charged groups, yielding an excess of 9 positive charges (37, 42). The T4 lysozyme molecule has a bilobal structure with the active site located at the junction of the 2 domains: the C-terminal and N-terminal lobes. The C-terminal lobe is comprised of 7 short α-helices whereas the N-terminal lobe is built up from 2 α-helices and a 4-stranded anti-parallel β-sheet. These 2 domains are joined by a long α-helix structure, consisting of amino acid residues 60 to 80. There are no disulfide linkages in the wild type T4 lysozyme molecule (38, 43, 44). The secondary structure of T4 lysozyme is 68% α-helix, 11% β-sheet, 10% β-turns, 4% 3_{10} -helix, and 7% "other" structure (44). T4 lysozyme in solution is ellipsoidal. Its molecular dimensions are approximately 54 Å long, with the diameters of the C-terminal and N-terminal lobes being about 24 Å and 28 Å, respectively (36, 40). Almost all of the excess positive charges are located on the C-terminal lobe (45).

In the study done by Matsumura et al (38), isoleucine at position 3 (Ile 3) of the bacteriophage T4 lysozyme was replaced with 13 different amino acid residues, including tryptophan (Trp). Mutations were introduced into the lysozyme gene cloned in phage M13mp18, using a method developed by Kunkel (46). The mutants obtained were characterized with respect to their deviations from the wild type in terms of crystal structure and thermodynamic stability. The results showed that the overall structures of all the mutants were similar to that of the wild type (47). The difference between the free energy of unfolding (ΔΔG) of the mutant proteins and that of the wild type at the melting temperature of wild type (T_m = 64.7 °C at pH 6.5) was calculated from T_m and ΔH at T_m. The Trp mutant exhibited a ΔΔG of -2.8 kcal/mol, indicating that this mutant is less

stable than wild type. However, results from difference electron density maps (48) and crystallographic refinement (40) showed that the differences between the wild type and mutant are subtle.

1.7 Ellipsometry

Optical measurements are used extensively to study the properties of films grown on a surface. An ellipsometer is used to determine the refractive index and thickness of thin films by measuring changes in states of polarized light reflected from a sample surface. It permits *in situ* measurements of adsorption (7), therefore the kinetics of adsorption can be monitored. Ellipsometric measurements involve illuminating a sample surface with a monochromatic light of known properties, usually a low-power, helium-neon laser. This laser beam is passed through a polarizer where it is converted from a circular to a linear polarized light. After striking the surface, the reflected beam (now with altered polarization) passes through a rotating analyzer prism. A photodetector converts the light energy into an electric current proportional to the intensity of reflected beam. These measured optical properties of the film are used to calculate its refractive index and thickness. From the refractive index and thickness, the total adsorbed mass can be estimated (49).

1.8 References

1. Blum, L.J. and P.R. Coulet (Eds.). 1991. Biosensor Principles and Applications. p. 7. M. Dekker, New York.

2. Chen, Z.J., X.M. Ou, F.Q. Tang, and L. Jiang. 1996. Effect of nanometer particles on the adsorbability and enzymatic activity of glucose oxidase. *Colloids and Surfaces B: Biointerfaces* **7:** 173-179.

3. Lee, J.H. and J.D. Andrade. 1988. Polymer Surface Dynamics. p. 111. Plenum Press, New York.

4. Bruil, A., L.M. Brenneisen, J.G.A. Terlington, T. Beugling, W.G. van Aken, and J. Feijen. 1994. *In Vitro* leukocyte adhesion to modified polyurethane surfaces II: Effects of wettability., *J. Colloid Interface Sci.* **165:** 72-81.

5. Olsson, J., A. Carlén, N.L. Burns, and K. Holmberg. 1995. Modified pellicle formation and reduced *in vitro* bacterial adherence after surface treatment with different siloxane polymers., *Colloids and Surfaces B: Biointerfaces* **5:** 161-169.

6. Tzannis, S.T., W.J.M. Hrushesky, P.A. Wood, and T.M. Przybycien. 1997. Adsorption of a formulated protein on a drug delivery device surface., *J. Colloid Interface Sci.* **189:** 216-228.

7. Wannerbegger, K., M. Wahlgren, and T. Arnebrant. 1996. Adsorption from lipase- surfactant solutions onto methylated silica surfaces., *Colloids and Surfaces B:Biointerfaces* **6:** 27-36.

8. DeFeijter, J.A., J. Benjamins, and F.A. Veer. 1978. Ellipsometry as a tool to study the adsorption behavior of synthetic and biopolymers at the air-water interface., *Biopolymers* **17:** 1759-1772.

9. Lundström, I. 1985. Models of protein adsorption on solid surfaces., *Progr. Colloid Polymer Sci.* **70:**76-82.

10. Lundström I., and H. Elwing. 1990. Simple kinetic model for protein exchange reactions on solid surfaces., *J. Colloid Interface Sci.* **136:**68-84.

11. Krisdhasima, V., J. McGuire, and R.D. Sproull. 1992. Surface hydrophobic influences on β-lactoglobulin adsorption kinetics., *J. Colloid Interface Sci.* **154(2):** 337-350.

12. Bohnert, J.L. and T.A. Horbett. 1986. Changes in adsorbed fibrinogen and albumin interactions with polymers indicated by decreases in detergent elutability., *J. Colloid Interface Sci.* **111:**363-377.

13. Krisdhasima, V., P. Vinaraphong, and J. McGuire. 1993. Adsorption kinetics and elutability of α-lactalbumin, β-casein, β-lactoglobulin, and bovine serum albumin at hydrophobic and hydrophilic interfaces., *J. Colloid Interface Sci.***161:**325-334.

14. McGuire, J., V. Krisdhasima, M.C. Wahlgren, and T. Arnebrant. 1995a. Comparative adsorption studies with synthetic, structural stability and charge mutants of bacteriophage T4 lysozyme. in Proteins at Interfaces, J. Brash and T. Horbett, eds., ACS Books, Washington, D.C.

15. McGuire, J., V. Krisdhasima, M.C. Wahlgren, and T. Arnebrant. 1995. Comparative adsorption studies with synthetic, structural stability and charge mutants of bacteriophage T4 lysozyme. *in* Proteins at Interfaces II: Fundamentals and Applications. (J. Brash and T. Horbett, eds.), ACS Books, Washington, DC.

16. McGuire, J., M.C. Wahlgren, and T. Arnebrant. 1995c. The influence of net charge and charge location on the adsorption and dodecyltrimethyl ammonium bromide-mediated elutability of bacteriophage T4 lysozyme at silica surfaces., *J. Colloid Interface Sci.* **170:** 193-202.

17. Podhipleux, N., V. Krisdhasima, and J. McGuire. 1996. Molecular charge effects on protein behavior at hydrophobic and hydrophilic solid surfaces., *Food Hydrocoll.* **10:** 285-293.

18. Pitt, W.G., K. Park, and S.L. Cooper. 1986. Sequential protein adsorption and thrombus deposition on polymeric biomaterials., *J. Colloid Interface Sci.* **111:** 343-362.

19. Ruzgas, T.A., V.J. Razumas, and J.J. Kulys. 1992. Sequential adsorption of γ-interferon and bovine serum albumin on hydrophobic silicon surfaces., *J. Colloid Interface Sci.* **151:** 136-143.

20. Elgersma, A.V., R.L.J. Zsom, J. Lyklema, and W. Norde. 1992. Adsorption competition between albumin and monoclonal immuno-gamma globulins on polystyrene lattices., *J. Colloid. Interface Sci.* **152:** 410-428.

21. Shirahama, H., J. Lyklema, and W. Norde. 1990. Comparative protein adsorption in model systems. *J. Colloid. Interface. Sci.* **139:** 177-187.

22. Anand, K. and S. Damodaran. 1996. Dynamics of exchange between α_{s1}-casein and β-casein during adsorption at air-water interface. , *J. Agric. Food Chem.* **44:** 1022-1028.

23. Anand, K. and S. Damodaran. 1995. Kinetics of adsorption of lysozyme and bovine serum albumin at the air-water interface from binary mixture., *J.Colloid Interface Sci.* **176:** 63-73.

24. Horsley D., J. Herron, V. Hlady, and J.D. Andrade. 1987. Physicochemical and Biochemical Studies. *in* Proteins at Interfaces. (J.L. Brash and T.A. Horbett, eds.) p.290-304. ACS Symposium Series 343, Washington, DC.

25. Kato, A., and K. Yutani. 1988. Correlation of surface properties with conformational stabilities of wild-type and six mutant tryptophan synthase α-subunits substituted at the same position., *Protein Eng.* **2:**153-156.

26. Wei, A.-P., J.N. Herron, and J.D. Andrade. 1990. The role of protein structure in surface tension kinetics. *in* From Clone to Clinic. (D. J.A. Crommelin and H. Schellekens, Eds.), p. 305. Kluwer Academic Publishers, Amsterdam.

27. Xu, S. and S. Damodaran. 1993. Comparative adsorption of native and denatured egg-white, human, and T4 phage lysozyme at the air-water interface., *J. Colloid. Interface Sci.* **159:** 124-133.

28. Wang J., and J. McGuire. 1997. Surface tension kinetics of the wild type and four synthetic stability mutants of T4 phage lysozyme at the air-water interface., *J. Colloid. Interface Sci.* **185:** 371-323.

29. Billsten, P., M. Wahlgren, T. Arnebrant, J. McGuire, and H. Elwing. 1995. Structural changes of T4 lysozyme upon adsorption to silica nanoparticles measured by circular dichroism., *J. Colloid Interface Sci.* **175:** 77-82.

30. Tian, M., W-K Lee, M.K. Bothwell, and J. McGuire. 1998. Structural stability effects on adsorption of bacteriophage T4 lysozyme to colloidal silica., *J. Colloid Interface Sci.* **199:** In Press.

31. Elwing, H. S. Welin, A. Askendal, and I. Lundström. 1988. Adsorption of fibrinogen as a measure of the distribution of methyl groups on silicon surfaces. *J.Colloid Interface Sci.* **123:** 306-308.

32. Lu, D.R. and K. Park. 1991. Effect of surface hydrophobicity on the conformational changes of adsorbed fibrinogen. *J. Colloid Interface Sci.* **144:** 271-281.

33. McGuire, J. and V. Krisdhasima. 1993. Relating contact surface hydrophobicity to molecular events influencing biological adhesion. *J. Adhesion Sci Technol.* **7(3):**195-204.

34. Tsugita, A., M. Inouye, E. Terzaghi, and G. Streisinger. 1968. Purification of bacteriophage T4 lysozyme., *J. Biol. Chem.* **243:** 391-397.

35. Tsugita, A. and M. Inouye. 1968. Complete primary structure of phage lysozyme from *Escherichia coli* T4., *J. Mol. Biol.* **37:** 201-212.

36. Matthews, B.W., F.W. Dahlquist, and A.Y. Maynard. 1973. Crystallographic data for lysozyme from bacteriophage T4., *J. Mol. Biol.* **78:**575-576.

37. Weaver, L.H. and B.W. Matthews. 1987. Structure of bacteriophage T4 lysozyme refined at 1.7 Å resolution., *J. Mol. Biol.* **193:**189-198.

38. Matsumura, M., G. Signor, and B.W. Matthews. 1989. Sustainable increase of protein stability by multiple disulfide bonds., Nature. **342:** 291-293.

39. Dao-pin, S., E. Soderlind, W.A. Baase, J.A. Wozniak, U. Sauer, and B.W. Matthews. 1992. Cumulative site-directed charge-change replacements in bacteriophage T4 lysozyme suggest that long-range electrostatic interactions contribute little to protein stability., *J. Mol. Biol.* **221(3):**873-887.

40. Grütter, M.G. and B.W. Matthews. 1982. Amino acid substitutions far from the active site of bacteriophage T4 lysozyme reduce catalytic activity and suggest that the C-terminal lobe of the enzyme participates in substrate binding., *J. Mol. Biol.* **154:** 525-535.

41. Grütter, M.G., L.H. Weaver, T.M. Gray, and B.W. Matthews. 1983. Structure, function, and evolution of the lysozyme from bacteriophage T4. *in* Bacteriophage T4. p.356-360. (Mathews, C.K., E.M. Kutter, G. Mosig, and P.M. Berget, eds.) Am. Soc. Microbiology., Washington, DC.

42. Alber, T. and B.W. Matthews. 1987. Structure and thermal stability of phage T4 lysozyme., *Meth. Enzymol.* **154:**511-533.

43. Branden, C. and J. Tooze. 1991. Prediction, engineering, and design of protein structures. *in* Introduction to protein structure. p. 247-268. Garland Publishing, Inc., New York.

44. Arnold, G.E., J.I. Manchester, B.D. Townsend, and R.L. Ornstein. 1994. Investigation of domain motions in bacteriophage T4 lysozyme., *Biomolecular Structure and Dynamics.* **12:** 457-474.

45. Dao-pin, S., D-I. Liao, and S.J. Remington. 1989. Electrostatic fields in the active sites of lysozymes., *Proc. Natl. Acad. Sci. USA* **86:** 5361-5365.

46. Kunkel, T.A. 1985. Rapid and efficient site-specific mutagenesis without phenotype selection., *Proc. Natl. Acad. Sci. USA.* **82**: 488-492.

47. Matsumura, M., and B.W. Matthews. 1989. Control of enzyme activity by an engineered disulfide bond., *Science* **243:** 792-794.

48. Grütter, M.G., R.B. Hawkes, and B.W. Matthews. 1979. Molecular basis of thermostability in the lysozyme from bacteriophage T4., *Nature* **277:** 667-669.

49. Krisdhasima, V., J. McGuire, and R.D. Sproull. 1992. A one-film-model ellipsometry program for the simultaneous calculation of protein film thickness and refractive index., *Surf. Interface Anal.* **18:** 453-456.

CHAPTER 2

MATERIALS AND METHODS

This chapter will describe materials and methods used for all experiments in detail. It is a complete reference for materials and methods described in the following two chapters.

2.1 Materials

2.1.1 T4 Lysozyme

Synthetic mutants of T4 lysozyme were produced from transformed cultures of *E. coli* strain RR1, received from Professor Brian Matthews of the Institute of Molecular Biology, University of Oregon. For the tryptophan mutant (Trp), isoleucine at position 3 (Ile 3) was replaced with tryptophan, resulting in a less stable mutant ($\Delta\Delta G$ = -2.8 kcal/mol at pH 6.5).

Expression and purification of lysozyme followed the established procedures (1, 2). The fermentation process started with the preparation of overnight culture broth (2 g tryptone, 1 g yeast extract, 1 g NaCl, 0.2 ml of 1 N NaOH, and 200 ml deionized distilled water (DDW)). Stock cultures of T4 lysozyme, stored at -80 °C, were used to inoculate the sterilized culture broth. After incubation at 37 °C for approximately 6 h, the lysozyme culture was transferred into an autoclaved fermenter (ADI 1012, Applikon Dependable Instruments, Inc., Schiedam, Holland) containing 4.8 L of sterilized LB broth (57.6 g tryptone, 24 g yeast extract, 48 g NaCl, 4.8 g glucose, and 4.8 L DDW). Tributyl

phosphate (1.5 ml) was added as an anti-foaming agent, along with ampicillin (0.7 g) to prevent contaminant growth and to select for the desired variant (with ampicillin-resistant gene on the plasmid). The fermentation temperature was maintained at 37 °C by a water bath with a circulating system (Model 1120, VWR Scientific, Portland, OR). Agitation was maintained at 600 rpm and air flowrate was maintained at 0.8 kg/s.

When the optical density (OD at 595 nm) of the fermented fluid reached between 0.9 and 1.0 (DU 62 Spectrophotometer, Beckman Instruments, Inc., Fullerton, CA), the temperature was decreased to 30° C, and agitation was reduced to 200 rpm. Isopropyl-β-D thiogalactopyranoside (IPTG) was added to induce lysozyme expression and cell lysis. Harvesting was done 1 hour and 45 minutes after adding IPTG, by siphoning the fluid into 250 ml centrifuge bottles. From this point on, purification processes were carried out at 4 °C. The harvested liquid was centrifuged at 13,000 rpm for 25 minutes (JA-14 rotor, Model J2-MI centrifuge, Beckman Instruments, Inc., Palo Alto, CA). The resulting supernatant was re-centrifuged at 13,000 rpm for 45 minutes, and the second-spin pellet was discarded. The first-spin pellets were combined and resuspended in resuspension buffer (10 mM Tris, pH 7.4) and lysis buffer (0.1 M phosphate, 0.2 M NaCl, 10 mM $MgCl_2$). A solution of 0.5 M ethylenediamine tetraacetic acid was also added to the resuspended pellets. After stirring for about 12 hours, 1 M $MgCl_2$ and 0.01 g of deoxyribonuclease I (DNase I) were added and the solution was stirred at room temperature for 2 hours. Then, it was centrifuged at 20,000 rpm for 35 minutes (JA-20 rotor, Model J2-MI centrifuge). The pellet was discarded, and the supernatant was combined with the supernatant from the previous spins in1200 ml fleakers.

Spectrum dialysis was done against DDW, using Spectra/Por regenerated cellulose (RC) hollow fiber bundles (MWCO 11,000, Spectrum Medical Industries, Inc., Houston, TX) until the conductivity of the fluid dropped to 2 mΩ/cm, and the pH was between 6.5 and 7.5 (adjusted with 1 N NaOH or 1 N HCl if needed). Dialyzed supernatant was loaded onto a CM Sepharose CL-6B CCL-100 column (cation exchanger, Sigma Chemical Co., St. Louis, MO), and then eluted using a salt gradient of 50 mM to 0.3 M NaCl in 50 mM Tris buffer. Eluted fractions were combined in Spectra/Por molecularporous membrane tubing (MWCO 13,000, Spectrum Medical Industries, Inc.) and were dialyzed against phosphate buffer, pH 5.8, before being loaded onto SP Sephadex C50 column (cation exchanger, Sigma Chemical Co.) for concentration. To elute the concentrated protein, 0.01 M phosphate buffer, pH 6.5, containing 0.55 M NaCl and 0.02% NaN_3 was added to the column.

The concentrated protein was diluted 1:100 with phosphate buffer, pH 6.5, and its absorbance (Abs) at 280 nm was measured to determine the amount of pure protein obtained. To calculate the amount of protein obtained, Abs was divided by 1.28 for wild type and by 1.46 for the Trp mutant. Purity of the protein was routinely checked by high-pressure liquid chromatography (HPLC) and sodium dodecylsulfate polyacrylamide gel electrophoresis (SDS-PAGE). HPLC chromatogram showed the presence of only 1 peak, and SDS-PAGE gel showed only 1 protein band.

2.1.2 Surfaces

Preparation of hydrophilic and hydrophobic surfaces was done by methods similar to those described by McGuire et al. (3-5).

Hydrophilic surfaces: Silicon (Si) wafers (hyperpure, type N. phosphorous doped, plane 1-0-0) were purchased from Wacker Siltronic Corporation (Portland, OR). Oxidation of surfaces was carried out in a furnace at 1000° C (P_{O2} = 1 atm) for 18 minutes. Surfaces were cut into approximately 1.2 x 3 cm^2 plates, using a tungsten pen. Each plate was placed into a test tube, and 10 mL of 1:1:5 of NH_4OH:H_2O_2:H_2O was added. Then, they were heated to 80 °C in a water bath for 15 minutes. After rinsing with 20 ml DDW, 10 ml of 1:1:5 of HCl:H_2O_2:H_2O was added. After heating to 80 °C for 15 minutes, the silica surfaces were rinsed with 30 ml DDW, and stored in 20 ml of 50% ethanol in order to maintain their hydrophilic properties.

Hydrophobic surfaces: The hydrophilic silica plates in 50% ethanol were rinsed with 40 ml DDW, dried with N_2, and kept in a desiccator for 24 h to make sure that the surfaces were water-free. Then they were treated to be hydrophobic by immersion in a solution of dichlorodimethylsilane (DDS) in xylene for 1 h. In this research, 0.1% DDS was used. Finally, the silanized surfaces were rinsed in 100 ml each of xylene, acetone, and ethanol. Surfaces were then blown dry with N_2, and kept in desiccators until used.

Contact angles for both the hydrophilic and hydrophobic surfaces were measured with a goniometer, using a series of EtOH in water (0%, 15%, and 30%) as diagnostic liquids.

2.2 Methods employed for solid-water interface studies

2.2.1 Adsorption kinetics

A bare surface, either hydrophobic or hydrophilic, was placed into a fused quartz, trapezoid cuvette (Hellma Cells, Germany) which was placed on the sample stage of an automatic *in situ* ellipsometer (Gaertner Scientific Corp., Chicago, IL). This instrument was modified so that the surface can be placed on upright position to eliminate the gravitational effect on the protein's arrival rate to the interface. This new configuration (as depicted in Figure 2.1) also allows the solution to be thoroughly mixed by a magnetic stir bar. The ellipsometer stage was adjusted to obtain a maximum in reflected light intensity (70^{O} angle of incidence, 1 mW Helium-neon laser, wavelength 6328 Å). Fine adjustments of the sample stage were done after 5 ml of phosphate buffer (pH 7.0) was injected into the cuvette to yield steady values of Ψ and Δ (6-7). Ψ is the arctangent of the factor by which the amplitude ratio changes, and Δ is the steady value of changes in the phase of light. Final measurements of bare surface properties were recorded onto a diskette. A stock protein solution was then injected into the cuvette to yield a final concentration of 1 mg/ml. The values of Ψ and Δ were measured ellipsometrically and recorded onto a diskette every 15 s for 30, 60, 90, or 120 minutes. The surface in the cuvette was rinsed with protein-free buffer at a flow rate of 25 ml/min for 5 min, then film properties were monitored for another 25 min. Similar methods were used by McGuire et al. (3-5). A one-film-model ellipsometry program (8) was used to determine the adsorbed mass from the measured thickness and refractive index of each protein film on each surface.

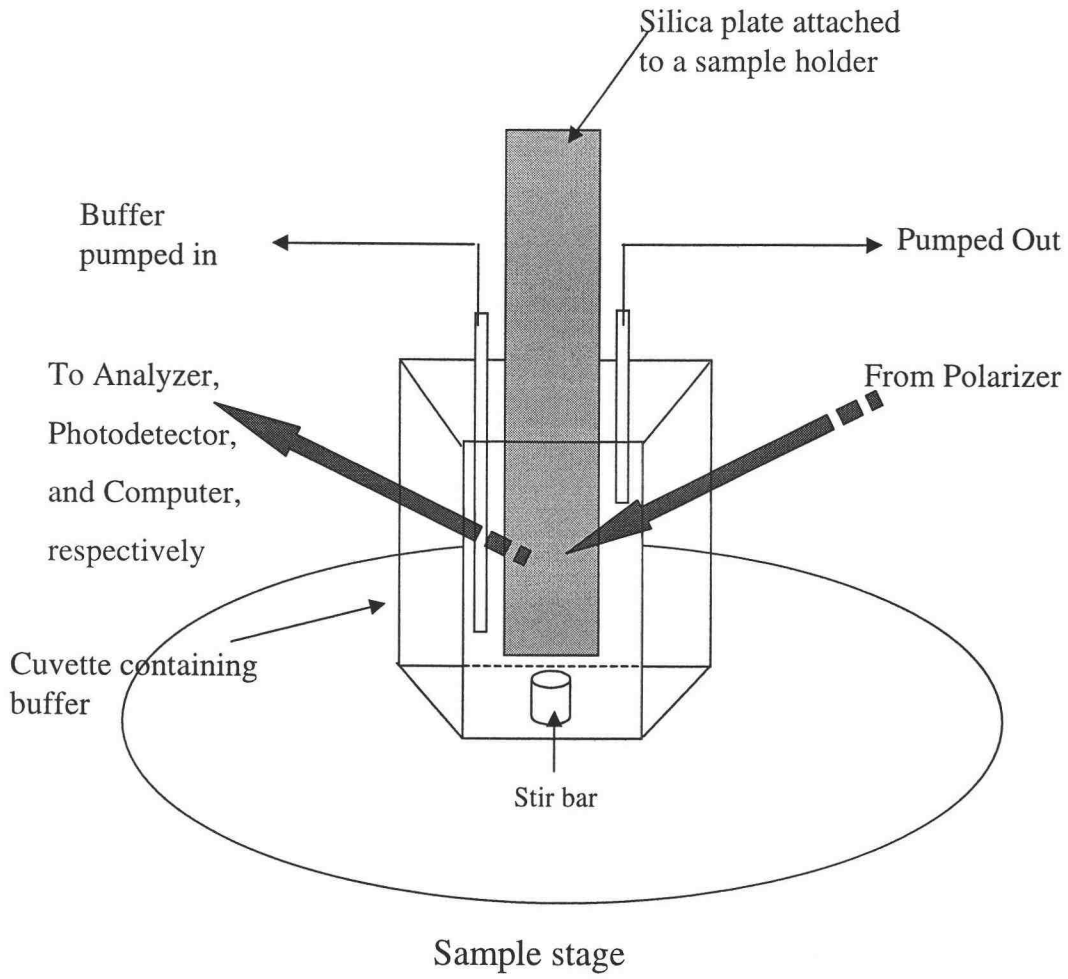

Figure 2.1. Ellipsometry setup.

2.2.2 Sequential protein adsorption kinetics

After 30 minutes (for the short time study) or two hours (for the long time study) of adsorption by the first protein and the cuvette was rinsed with a protein-free buffer at a flow rate of 25 ml/min for 5 min, the optical properties were followed for another 25 min. Then 1 ml of buffer was withdrawn from the cuvette, and 1 ml of either 0.06 mg/ml or 6

mg/ml of the second protein was added to give the final concentration of either 0.01 or 1 mg/ml. Film properties were recorded for 15, 30, 45, or 60 min. The cuvette was then rinsed with a protein-free buffer for 5 min, and the surface optical properties were monitored for another 25 min. Experiments with each protein sequence (Wild/Trp, Trp/Wild) on each type of surface were replicated at least twice.

Since ellipsometry cannot tell the differences between two proteins, the adsorbed mass collected was in the form of total adsorbed mass. To assess the reaction kinetics, a radiolabeling technique was employed to help distinguish one protein from another.

2.2.3 Surfactant-mediated elution study

This study is similar to the sequential protein adsorption study, but dodecyltrimethylammonium bromide (DTAB) was added instead of the second protein. The surfactant was allowed to contact the surface for 15 minutes, and the cuvette was rinsed with 25 ml/min of 0.01 M phosphate buffer for 5 minutes. Optical properties were monitored and recorded for another 25 minutes.

2.2.4 Sequential adsorption study by radiolabeling

This part of the research was conducted at Professor Thomas Horbett's laboratory, University of Washington. One protein (either wild type or Trp mutant) was radiolabeled with ^{125}I, using the iodine monochloride technique of Helmkamp et al. (9) as modified by Horbett (10). This technique is specific to tyrosine residues and the following reactions can be considered to occur:

$ICl + NaOH \rightarrow HOI + NaCl$

$HOI + \text{T4 lysozyme} \rightarrow \text{iodinated T4 lysozyme} + H_2O$

T4 lysozyme was radioiodinated with the iodine monochloride technique because this method is among the least disruptive to protein functions and preferential adsorption of iodinated proteins do not occur in general (10). Besides, very high specific activities can be attained (11-12). To determine whether preferential adsorption occurs, we can measure adsorption of molecules from solutions of different ratios of labeled to unlabeled protein. In the event that preferential adsorption does not occur, adsorption should be independent of these ratios.

The surfaces used in this study were glass cover slips (64% SiO_2, 13% alkali oxides, 8% boron, Fisher Scientific, Santa Clara, CA). As with the silica surfaces, acid and base treatments as well as silanization were performed on these glass cover slips to render them either hydrophobic or hydrophilic. Experiments were conducted in plastic vials containing one glass cover slip per vial (shown in Figure 2.2). A small volume of labeled protein was added to the solution of wild type or Trp lysozyme to obtained a specific activity of 200 counts per minutes (cpm)/μg.

Sequential adsorption study: adsorption was allowed to proceed for 30 minutes, and the surface was rinsed by 0.01M phosphate buffer. After incubation in a protein-free buffer for another 25 minutes, unlabeled protein (second protein) was introduced to the system. Contact time of the second protein was allowed for 4, 8, 12, 15, 30, 45, and 60 minutes. Then the surface was rinsed, followed by 25 minutes incubation in the buffer. At the end of the incubation period, the glass surface was transfer into a counting tube.

Sample radioactivity was measured with a gamma counter (Model 1185R, T.M. Analytic, Elk Grove Village, IL) and the background count was subtracted.

Spontaneous desorption or buffer-exchange study: a surface was allowed to contact a protein solution (labeled) for 30 minutes. After rinsing and incubating in a protein-free buffer for 0, 15, 30, 45, or 60 minutes, the surface radioactivity was measured.

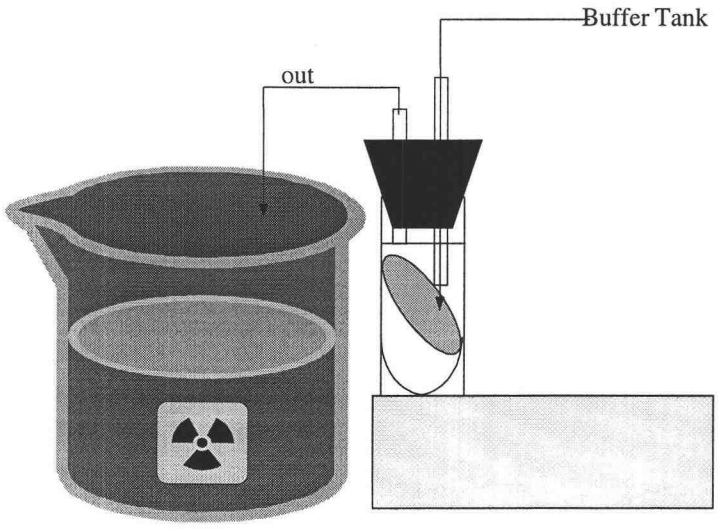

Figure 2.2. Radiolabeling study for solid-water interface setup.

Self-exchange study: this study was similar to sequential adsorption but instead of introducing a second protein to the system, the first protein was replaced with the same protein that was not labeled. The contact time for the unlabeled protein was 30 minutes.

2.3 Methods employed for air-water interface studies.

Following experiments were conducted at Dr. Srinivasan Damodaran's laboratory at the University of Wisconsin.

2.3.1. Radiolabeling of T4 lysozyme

For experiments at air-water interface, bacteriophage T4 lysozyme was radiolabeled by reductive methylation of the lysyl residues, using [^{14}C]formaldehyde and sodium cyanoborohydride ($NaCNBH_3$). Despite a lower energy and specific activity, there are advantages of using ^{14}C over ^{125}I. For examples, there are less biohazards involved in handling ^{14}C than in handling ^{125}I, and the ^{14}C isotope has a longer half-life than the ^{125}I isotope (12).

Reductive methylation of proteins with sodium borohydride ($NaBH_4$) and formaldehyde was developed first by Means and Feeney (13) as a lysine-specific protein modification procedure. The overall reaction sequence is summarized in Figure 2.3.

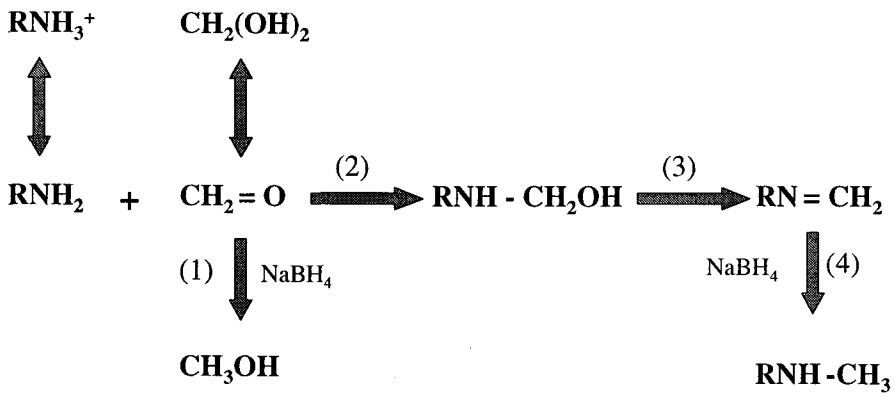

Figure 2.3. Methylation reaction of protein by formaldehyde, using $NaBH_4$ as a reducing agent.

The efficiency of the methylation is low and the strong reducing property of $NaBH_4$ may cleave disulfide bonds and peptide lingkages in protein molecules. In our case we used the method modified by Jentoft and Dearborn (12) which replace $NaBH_4$ with a milder reducing agent, $NaCNBH_3$. This method gives a much higher degree of lysyl group modification than $NaBH_4$ because $NaCNBH_3$readily reduces Schiff bases, but does not reduce aldehydes and ketones at neutral pH.

Briefly, 10 μl of [^{14}C]formaldehyde solution with a total radioactivity of 0.1 mCi (New England Nuclear Co., Boston, MA) was added to 20 ml of lysozyme solution (containing 1 mg/ml of lysozyme in phosphate buffer). After adding 25 mg of Na_2CNBH_3 (Aldrich Chemical Co., Milwaukee, WI), the solution was incubated at room temperature for 2 h. The methylated solution was dialyzed against Milli-Q water (produced by a system from Millipore Corp., Bedford, MA) for at least 24 h. The protein concentration of the ^{14}C-labeled lysozyme was measured with a spectrophotometer. The specific radioactivity was determined using a scintillation counter (14).

2.3.2. Adsorption kinetics

The rates of change in surface concentration and surface pressure of a protein solution were measured simultaneously, using a single experimental setup depicted in Figure 2.4 and 2.5. The rate of change of surface pressure was monitored by the

Wilhelmy plate method, using a Cahn electrobalance (Cahn Instruments Co., CA). A thin, sandblasted platinum plate was used as a sensor. The exact width of the platinum plate was determined by measuring the surface tension of Gold Label hexadecane (Aldrich Chemical Co., WI) to be 1.04 cm. A Teflon trough of 21cmx5.56cmx1.27cm interior dimension was used. The entire setup was housed in an incubator (Ambi-Hi-Lo-Changer, Labline) and the temperature was controlled at 24 °C.

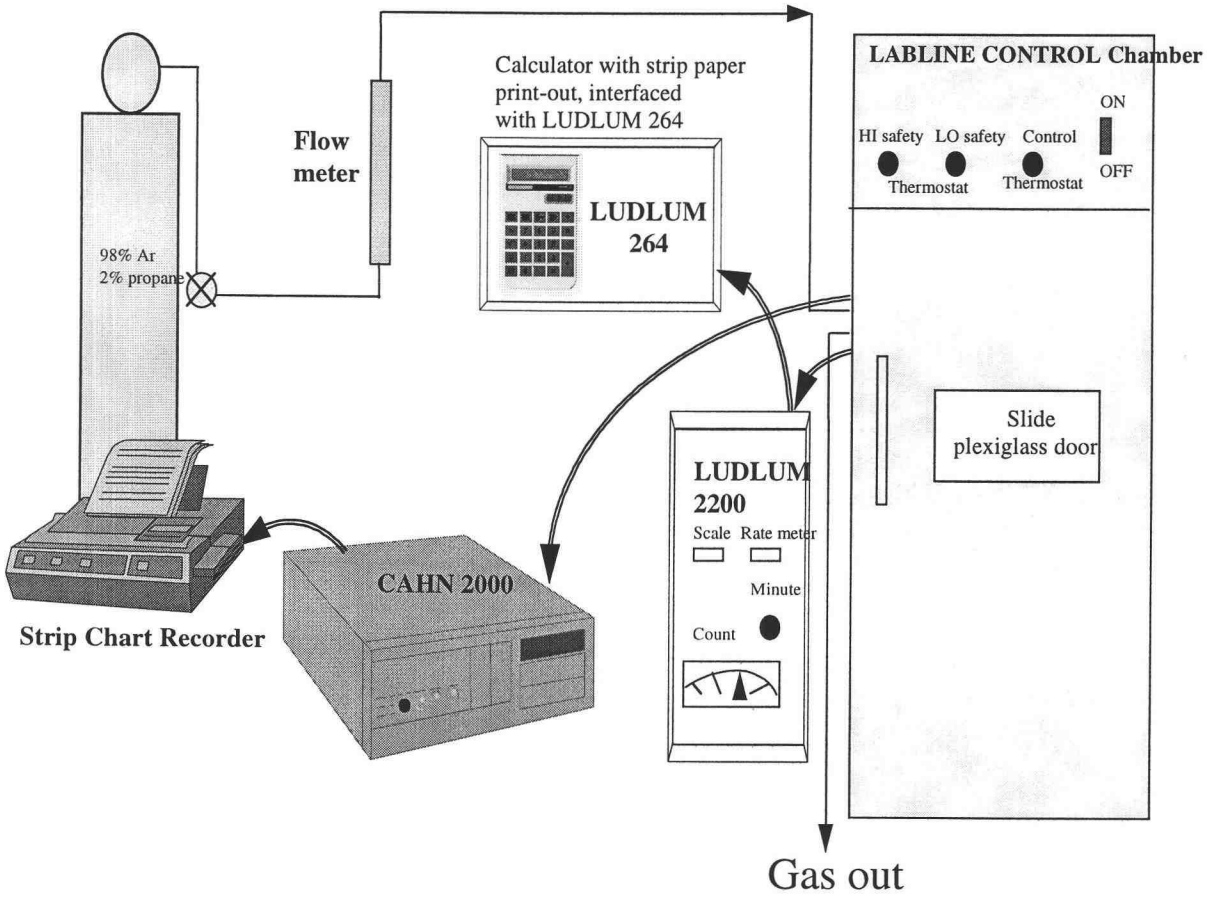

Figure 2.4. Experimental setup for air-water studies.

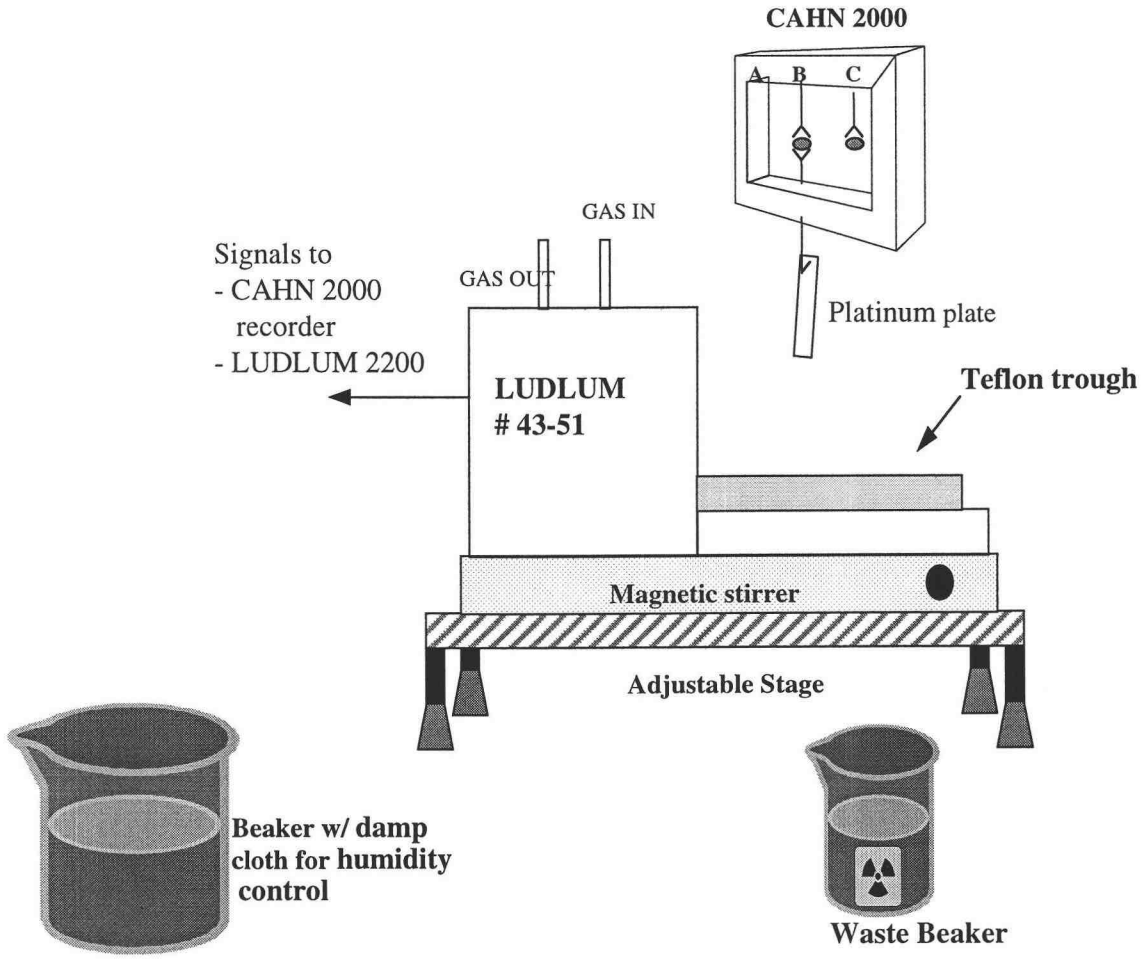

Figure 2.5. Experimental setup for air-water studies inside the chamber.

Before every experiment, the surface pressure measuring system was calibrated with 120 ml of Milli-Q water. The water was then replaced with 120 ml of 0.02 M of phosphate buffer and the surface tension of the buffer was recorded. The buffer was then replaced with 120 ml of protein solution. After the liquid surface was cleaned by gently sweeping with an aspirator until the surface tension is equal to that of the pure buffer, the protein was allowed to adsorb and the change in surface pressure was monitored continuously by a strip chart recorder (14-16).

The rate of change of protein's surface concentration was followed by measuring the surface radioactivity (14-16). A rectangular gas flow counter with an 8cmx4cm Mylar window (Ludlum Instruments, Inc., TX) was set up at the opposite end to the the electrobalance, with the air space between the Mylar window and the liquid surface of about 7 mm. A carrier gas comprised of 98% argon and 2% propane at 20ml/min was used. The counts per minute (cpm) were measured and printed out on a strip chart calculator. A calibration curve relating cpm to surface radioactivity ($\mu Ci/m^2$) constructed by spreading ^{14}C-labeled β-casein on the air-water interface was used to convert cpm to $\mu Ci/m^2$ (16).

2.4 Estimation of adsorption rate constants

According to the adsorption mechanism proposed by Krisdhasima et al. (6) shown in Figure 1.1a, differential equations describing the time-dependent fractional surface coverages of protein in states 1 (θ_1) and 2 (θ_2) are:

$$\frac{d\theta_1}{dt} = k_1 C(1-\theta_1-\theta_2) - (k_{-1}+s_1)\theta_1$$

and

$$\frac{d\theta_2}{dt} = s_1\theta_1$$

Where the total surface coverage, θ, at any time is $\theta_1 + \theta_2$, and C is the concentration of protein. By solving the above equations, the total surface coverage as a function of time can be expressed as:

$$\theta = A_1 e^{-r_1 t} + A_2 e^{-r_2 t} + A_3 \qquad \text{[Eq.2.1]}$$

where A_1, A_2, and A_3 are constants and roots r_1 and r_2 are known functions of the rate constants k_1, k_{-1}, and s_1. An expression for n expression for the total adsorbed mass as a function of time as obtained from [Eq.2.1] is:

$$\Gamma = a_1 e^{-r_1 t} + a_2 e^{-r_2 t} + a_3$$

where a_1, a_2, and a_3 are the products of the equilibrium adsorbed mass (Γ_{max}) with A_1, A_2, and A_3, respectively. The roots r_1 and r_2 are related to the kinetic rate constants as follows:

$$r_1 + r_2 = k_1 C + k_{-1} + s_1 \qquad \text{[Eq.2.2]}$$

and

$$r_1 r_2 = s_1 k_1 C . \qquad \text{[Eq.2.3]}$$

Based on the adsorption mechanism suggested and McGuire et al. (4) as shown in Figure 1.1b, protein may adopt one of two states directly from the solution. State 1 molecule is less tightly bound and occupies less interfacial area than state 2 molecule. In this model the fractional surface coverage of molecules adsorb in either state, θ_i, is defined as Γ_i/Γ_{max}, and Γ_{max} is defined as the maximum adsorbed mass allowable for monolayer coverage if all molecules adsorb in state 1.

At monolayer coverage $\theta_1 + a\theta_2 = 1$, where a is the interfacial area occupied by state 2 molecule divided by the interfacial area occupied by state 1 molecule. The total adsorbed mass is expressed by:

$$\Gamma = \Gamma_{\max}(\theta_1 + \theta_2). \qquad \text{[Eq.2.4]}$$

Solving differential equations

$$\frac{d\theta_1}{dt} = k_1 C(1-\theta_1 - a\theta_2)$$
$$\frac{d\theta_2}{dt} = k_2 C(1-\theta_1 - a\theta_2)$$

yields $\theta_1 + \theta_2 = \alpha\left[1 - e^{(-k_1 C - ak_2 C)t}\right]$,

where α is a constant. At $t = 0$, $\theta_1 + \theta_2 = 0$, and as t approaches ∞, $\theta_1 + \theta_2 = \alpha$.

Since $k_2/k_1 = \theta_2/\theta_1$ as t approaches ∞, solving for $\theta_1 + \theta_2$ as a function of rate constants yields:

$$\theta_1 + \theta_2 = \frac{\left(1 + {k_2}/{k_1}\right)}{\left(1 + {ak_2}/{k_1}\right)},$$

therefore Eq.2.4 becomes

$$\Gamma = \Gamma_{\max}\left\{\frac{\left(1 + {k_2}/{k_1}\right)}{\left(1 + {ak_2}/{k_1}\right)}\left[1 - e^{(-k_1 C - ak_2 C)t}\right]\right\}. \qquad \text{[Eq.2.5]}$$

Using non-linear regression, the values of k_1 and k_2 can be estimated.

2.5 Estimation of exchange rate constants

Based on the simple kinetic models for protein adsorption suggested by Krisdhasima et al. (6) and McGuire et al. (4), along with a kinetic model for protein exchange reactions for a binary mixture proposed by Lundström and Elwing (17), we can construct kinetic models for sequential adsorption as shown in Figure 2.6.

In Figure 2.6a, θ_{1A} is the fractional surface coverage of protein *A* that is exchangeable by protein *B* whereas θ_{2A} is the fractional surface coverage of protein A that

is not exchangeable. After a certain period of adsorption time, protein *A* is removed by rinsing with a protein-free buffer. The surface is then allowed to incubate in the protein-free buffer. When there is no spontaneous desorption, the only change in θ_{1A} is through conversion into θ_{2A} as shown by the following mathematical expression:

$$-\frac{d\theta_{1A}}{dt} = s_{1A} \cdot \theta_{1A} \qquad \text{[Eq.2.6]}$$

Rearrangement of [Eq.2.6] yields

$$-\frac{1}{\theta_{1A}} d\theta_{1A} = s_{1A} dt$$

Integration:

$$\int_{\theta_{1A,ti}}^{\theta_{1A}} \frac{1}{\theta_{1A}} d\theta_{1A} = -s_{1A} \int_{0}^{t} dt$$

$$\ln\theta_{1A} - \ln\theta_{1A,ti} = -s_{1A}(t-0)$$

$$\ln\frac{\theta_{1A}}{\theta_{1A,ti}} = -s_{1A} \cdot t$$

An exponential of the above equation yields

$$\frac{\theta_{1A}}{\theta_{1A,ti}} = e\,xp(-s_{1A} \cdot t)$$

or $$\theta_{1A} = \theta_{1A,ti} \cdot \exp(-s_{1A} \cdot t). \qquad \text{[Eq.2.7]}$$

Because $$\theta_{1A} + \theta_{2A} = 1,$$

$$\theta_{2A} = 1 - \theta_{1A}. \qquad \text{[Eq.2.8]}$$

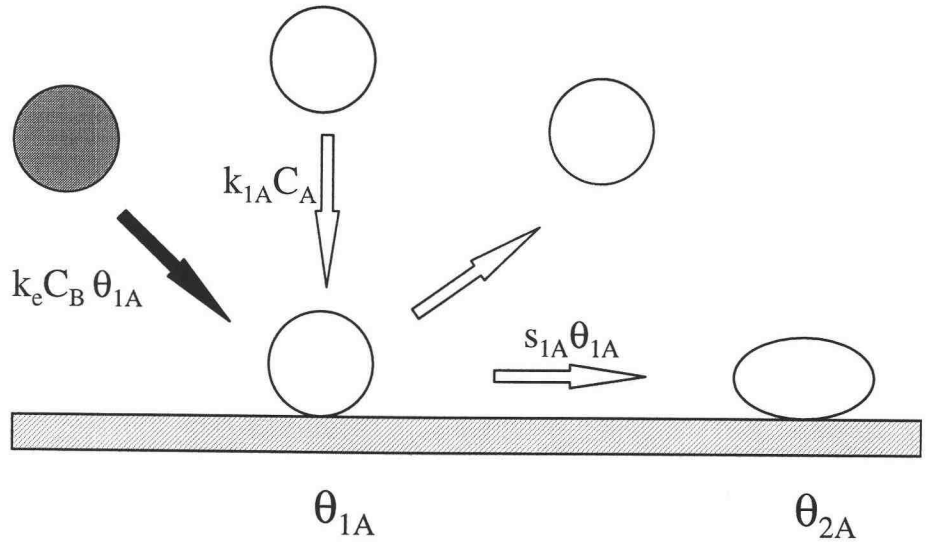

(a)

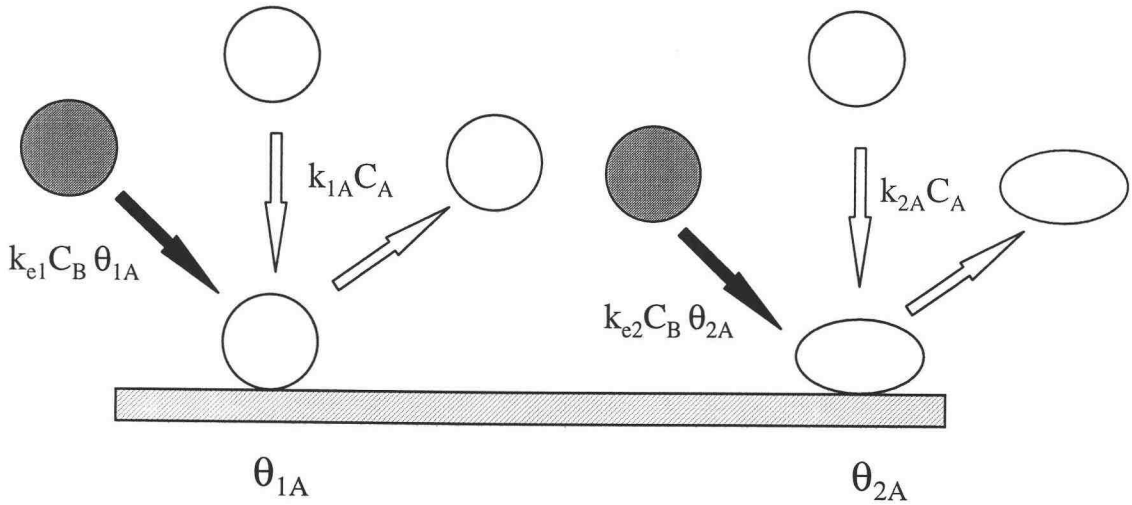

(b)

Figure 2.6. A mechanism for sequential adsorption of protein *A* followed by protein *B*, based on (a) Figure 1.1a, (b) Figure 1.1b.

If $k_{1A}>>s_{1A}$, θ_{1A} at $t = t_i$ is approximately 1. Therefore [Eq.2.8] becomes

$$\theta_{2A} = \theta_{1A,ti} - \theta_{1A}. \qquad \text{[Eq.2.9]}$$

Substitute θ_{IA} at t =t from [Eq.2.7] into [Eq.2.9],

$$\theta_{2A} = \theta_{1A} - \theta_{1A,ti} \cdot \exp(-s_{1A} \cdot t)$$

or

$$\theta_{2A} = \theta_{1A,ti}[1 - \exp(-s_{1A} \cdot t)]. \qquad \text{[Eq.2.10]}$$

At the end of incubation in the buffer (let $t = tp$), a solution of the second protein (protein B) is introduced. Therefore, the decrease in θ_{1A} can be either through the conversion into θ_{2A} or through an exchange with protein B,

$$-\frac{d\theta_{1A}}{dt} = s_{1A}\theta_{1A} + k_e[C_B]\theta_{1A} \qquad \text{[Eq.2.11]}$$

where $k_e[C_B]$ is the concentration-dependent exchange rate constant of protein A by protein B.

$$\frac{1}{\theta_{1A}} d\theta_{1A} = -(s_{1A} + k_e[C_B])dt$$

$$\int_{\theta_{1A,tp}}^{\theta_{1A}} \frac{1}{\theta_{1A}} d\theta_{1A} = -(s_{1A} + k_e[C_B]) \int_{t_p}^{t} dt$$

$$\ln \frac{\theta_{1A}}{\theta 1_{A,tp}} = (s_{1A} + k_e[C_B]) \cdot (t - t_p)$$

$$\theta_{1A} = \theta_{1A,tp} \cdot \exp\{-(s_{1A} + k_e[C_B]) \cdot (t - t_p)\} \qquad \text{[Eq.2.12]}$$

Previously at the end of incubation period $\theta_{1A,tp} = \theta_{1A}$ [Eq.2.7], therefore

$$\theta_{1A,tp} = \theta_{1A,ti} \cdot \exp(-s_{1A} t_p). \qquad \text{[Eq.2.13]}$$

Substitution of [Eq.2.13] into [Eq.2.12] gives

$$\theta_{1A} = \theta_{1A,ti} \cdot \exp(-s_{1A} t_p) \cdot \exp\{-(s_{1A} + k_e[C_B]) \cdot (t - t_p)\}. \qquad \text{[Eq.2.14]}$$

We know that the total amount of θ_{2A} equals

$$\theta_{2A,tp} + (\theta_{1A} \text{ converted} * \text{fraction of } \theta_{1A} \text{ converted into } \theta_{2A}) \qquad \text{[Eq.2.15]}$$

where fraction of θ_{1A} converted into $\theta_{2A} = \dfrac{s_{1A}\theta_{1A}}{s_{1A}\theta_{1A} + k_e C_B \theta_{1A}} = \dfrac{s_{1A}}{s_{1A} + k_e C_B}$,

and θ_{1A} converted = $\theta_{1A,tp}$ - θ_{1A} remained = [Eq.7] - [Eq.14]. Therefore,

$$\theta_{1A} \text{ converted} = \theta_{1A,ti} \cdot \exp(-s_{1A} t_p)\{1 - \exp[-(s_{1A} + k_e[C_B]) \cdot (t - t_p)]\}.$$

By using [Eq.2.10], we get

$$\theta_{2A,tp} = \theta_{1A,ti} \cdot [1 - \exp(-s_{1A} t_p)].$$

Thus, $\theta_{2A} = \theta_{1A,ti} \cdot [1 - \exp(-s_{1A} t_p)]$

$$+ \theta_{1A,ti} \exp(-s_{1A} t_p) \cdot \{1 - \exp[-(s_{1A} + k_e[C_B]) \cdot (t - t_p)]\} \cdot \frac{s_{1A}}{s_{1A} + k_e C_B}.$$

When $t >> t_p$, $\exp\{-(s_{1A} + k_e[C_B]) \cdot (t - t_p)\}$ will approach zero, so the final equation is

$$\frac{\theta_{2A}}{\theta_{1A,ti}} = 1 - \left\{ \frac{k_e[C_B]}{s_{1A} + k_e[C_B]} \cdot \exp(-s_{1A} t_p) \right\}. \qquad \text{[Eq.2.16]}$$

Results from preliminary study on elutability of adsorbed T4 lysozyme from hydrophobic and hydrophilic silica by DTAB showed no significant difference in the amount of protein eluted after 30 min and 2 h adsorption. It suggested that there was no conversion between θ_{1A} and θ_{2A} after 30 min, and that the conformational change of protein upon adsorption happened almost instantaneously (Figure 1.1b).

In the case of Figure 2.6b, protein *A* can adsorb directly from the solution in either state 1 or 2, both of which are exchangeable by protein *B* with the rates $k_{e1}[C_B]$ and $k_{e2}[C_B]$, respectively. Since no conversion between θ_{1A} and θ_{2A} is allowed, changes can be described as

$$-\frac{d\theta_{1A}}{dt} = k_{e1}[C_B]\theta_{1A} \qquad \text{[Eq.2.17]}$$

and $$-\frac{d\theta_{2A}}{dt} = k_{e2}[C_B]\theta_{2A}. \qquad \text{[Eq.2.18]}$$

From [Eq.2.17];

$$-\frac{d\theta_{1A}}{dt} = k_{e1}[C_B]\theta_{1A}$$

or $$-\frac{1}{\theta_{1A}}d\theta_{1A} = k_{e1}[C_B]dt.$$

Integration of the above equation from $\theta_{1A} = \theta_{1A,ti}$ to $\theta_{1A} = \theta_{1A}$ and from $t = 0$ to $t = t$:

$$\int_{\theta_{1A,i}}^{\theta_{1A}} \frac{1}{\theta_{1A}} d\theta_{1A} = -k_e[C_B]\int_0^t dt$$

$$\ln\frac{\theta_{1A}}{\theta_{1A,ti}} = -k_e[C_B]t$$

$$\frac{\theta_{1A}}{\theta_{1A,ti}} = \exp\{-k_e[C_B]t\}$$

yields $\theta_{1A} = \theta_{1A,ti}[\exp(-k_{e1}[C_B]\cdot t)]$. [Eq.2.19]

Similarly, integration of [Eq.2.13] yields

$$\theta_{2A} = \theta_{2A,ti}[\exp(-k_{e2}[C_B]\cdot t)]. \qquad \text{[Eq.2.20]}$$

We can solve Equations 19 and 20 based on an assumption that the exchange rates depend solely on the binding strength of the adsorbed molecules. However, our results

from radiolabeling study implied that the exchange rate constants of WT and TRP lysozymes did not depend on the binding strength of the adsorbed molecules alone, but also depend on the properties of the exchanging proteins and the interactions between the adsorbed molecules vs. the exchanging molecules.

In the case of radiolabeling study, the data suggested a combination of exchange and desorption processes. A more generalized model of exchange with desorption mechanism can be depicted as shown in Figure 2.7.

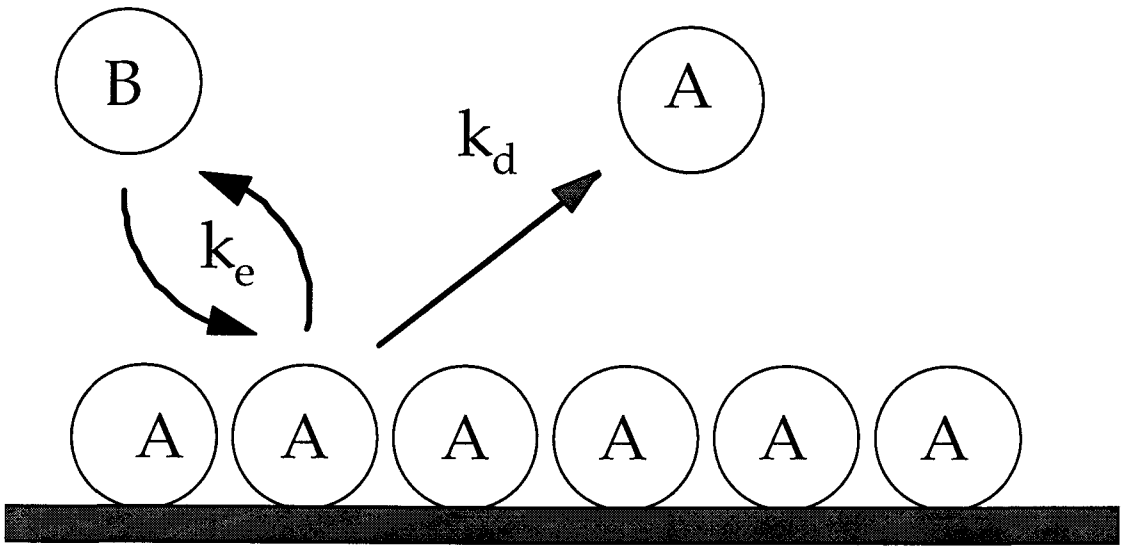

Figure 2.7. Exchange with desorption mechanism.

A differential equation describing this exchange with desorption mechanism is shown below:

$$-\frac{d\theta_A}{dt} = k_e C_B \theta_A + k_d \theta_A$$

$$-\int_{\theta_{A0}}^{\theta_A} \frac{d\theta_A}{\theta_A} = (k_e C_B + k_d)\int_0^t dt$$

$$\frac{\theta_A}{\theta_{A0}} = e^{-(k_e C_B + k_d)t}$$

Taking a natural log of the above equation results in the final form of the mathematical expression [Eq.2.21]. This equation describes the fraction of the first protein (*A*) remaining at the interface after introduction of the second protein, compared with before the introduction, as a function of the exchange rate of protein *A* by protein *B* (C_B), the rate of desorption (K_d), and the contact time of the second protein (*t*).

$$\ln\left(\frac{\theta_A}{\theta_{A0}}\right) = -(k_e C_B + K_d)t \qquad \text{[Eq.2.21].}$$

By combining the results from the ellipsometry study with the results from the radiolabeling study, the kinetic rate constants governing adsorption of WT and TRP lysozymes from solution, as well as the exchange rate constants between the two proteins at solid-water interface can be calculated.

2.6 References

1. Alber, T. and B.W. Matthews. 1987. Structure and thermal stability of phage T4 lysozyme., *Meth. Enzymol.* **154:** 511-533.

2. Muchmore, D.C., L.P. McIntosh, C.B. Russel, D.E. Anderson, and F.W. Dahlquist. 1989. Expressiom and 15N labeling of proteins for proton and nitrogen-15 NMR., *Methods Enzymol.* **177:** 44-73.

3. McGuire, J., V. Krisdhasima, M.C. Wahlgren, and T. Arnebrant. 1995a. Comparative adsorption studies with synthetic, structural stability and charge mutants of bacteriophage T4 lysozyme. *in* Proteins at Interfaces II: Fundamentals and Applications. (J. Brash and T. Horbett, eds.), ACS Books, Washington, DC.

4. McGuire, J., M.C. Wahlgren, and T. Arnebrant. 1995. Structural stability effects on the adsorption and dodecyltrimethyl ammonium bromide-mediated elutability of bacteriophage T4 lysozyme at silica surfaces., *J. Colloid Interface Sci.* **170:** 182-192.

5. McGuire, J., M.C. Wahlgren, and T. Arnebrant. 1995. The influence of net charge and charge location on the adsorption and dodecyltrimethyl ammonium bromide-mediated elutability of bacteriophage T4 lysozyme at silica surfaces., *J. Colloid Interface Sci.* **170:** 193-202.

6. Krisdhasima, V., J. McGuire, and R.D. Sproull. 1992. Surface hydrophobic influences on β-lactoglobulin adsorption kinetics., *J. Colloid Interface Sci.* **154(2):** 337-350.

7. Suttiprasit , P. and J. McGuire. 1992. The surface activity of α-lactalbumin, β-lactoglobulin, and bovine serum albumin II : Some molecular influences on adsorption to hydrophilic and hydrophobic silicon surfaces., *J. Colloid Interface Sci.* **154:** 327-336.

8. Krisdhasima, V., J. McGuire, and R.D. Sproull. 1992. A one-film-model ellipsometry program for the simultaneous calculation of protein film thickness and refractive index., *Surf. Interface Anal.* **18:** 453-456.

9. Helmkamp, R.W., R.L. Goodland, W.F. Bale, I.L. Spar, and L.E. Mutschler. 1960. High specific activity iodination of γ-globulin with iodine-131 monochloride., *CancerRes.* **20:** 1495-1500.

10. Horbett, T.A. 1981. Adsorption of proteins from plasma to a series of hydrophilic-hydrophobic copolymers. II. Compositional analysis with the prelabeled protein technique., *J. Biomed. Mater. Res.* **15:** 673-695.

11. Matthews, D.E., R.A. Hessler, N.D. Denslow, J.S. Edwards, and T.W. O'Brien. 1982. Protein composition of the bovine mitochondrial ribosome., *J. Biol. Chem.* **257(8):** 8788-8794.

12. Jentoft, N. and D.G. Dearborn. 1979. Labeling of proteins by reductive methylation using sodium cyanoborohydride., *J. Biol. Chem.* **254(4):** 4359-4365.

13. Means, G.E. and R.E. Feeney. 1968. Reductive alkylation of amino groups in proteins., *Biochemistry.* **7:** 2192-2201.

14. Xu, S. and S. Damodaran. 1992. The role of chemical potential in the adsorption of lysozyme at the air-water interface., *Langmuir.* **8:** 2021-2027.

15. Damodaran, S. and S. Xu. 1996. The role of electrostatic forces in anomalous adsorption behavior of phosvitin at the air-water interface., *J. Colloid. Interface Sci.* **178:** 426-435.

16. Xu, S. and S. Damodaran. 1993. Calibration of radiotracer method to study protien adsorption at interfaces., *J. Colloid. Interface Sci.* **157:** 485-490.

17. Lundström I., and H. Elwing. 1990. Simple kinetic model for protein exchange reactions on solid surfaces., *J. Colloid Interface Sci.* **136:** 68-84.

CHAPTER 3

SEQUENTIAL ADSORPTION BEHAVIOR OF THE WILD TYPE AND A SYNTHETIC STRUCTURAL STABILITY VARIANT OF BACTERIOPHAGE T4 LYSOZYME AT SOLID-WATER INTERFACES

3.1 Abstract

The sequential adsorption behavior of the wild type T4 lysozyme and one of its structural stability variants was studied, using ellipsometry and ^{125}I radioisotope labeling techniques. The mutant lysozyme was produced by substitution of the isoleucine residue at position 3 in the wild type with a tryptophan residue, resulting in a protein with lower structural stability. Adsorption kinetics recorded at hydrophilic and hydrophobic solid surfaces were compared to the kinetic behavior predicted by each of two mechanisms for protein adsorption, each allowing for adsorption into two different conformational states. The mutant protein apparently adsorbed at the interfaces more tightly and occupied a greater interfacial area than the wild type. However, radioisotope labeling experiments suggested that sequential adsorption and exchange of proteins occurred only in the case of the less stable mutant followed by the wild type. This suggests that, in an exchange reaction, properties of the adsorbing protein (e.g. its ability to adsorb when only a small amount of unoccupied area is exposed) may be more important than the conformational state of the protein molecules already adsorbed.

3.2 Introduction

Protein adsorption is a process that has many applications. It is involved in development of biocompatible devices, solid-phase diagnostics, and chromatographic technology. Physical and chemical adsorptions are the basis of immobilization, which is one of the crucial factors in the biosensor technique (1). Because of its apparent role in mediating microbial and spore adhesion, protein adsorption is a phenomenon of interest to food and pharmaceutical industries. In addition, clinicians are also interested since the attachment of bacteria to a solid surface is almost always preceded by the adsorption of a protein film. Adsorption of proteins to solid surfaces is largely irreversible in the sense that continued extensive soaking in buffer does not remove all the proteins, though the adsorbed proteins may be partially exchangeable with the bulk phase proteins. Since adsorption occurs more rapidly than the transport of cells to foreign materials, the cells usually end up interacting with the adsorbed protein layer on the material surfaces rather than interacting directly with the materials. Thus it is very important to study the fundamental mechanisms underlying the interactions of proteins with surfaces (2). There have been attempts to create inert protein-repelling materials by surface grafting with a non-charged, hydrophilic polymer (3), or by transformation of the surface into a very low-energy material (4). Study by Olsson et al. (5) showed that treatment of glass surfaces with siloxane polymers reduced the salivary pellicle adhesion and oral bacteria adherence after saliva contact by up to 90%.

Understanding of protein adsorption is necessary to precisely control the amount therapeutic drug administered. This is important in maximizing the therapeutic benefit while minimizing the treatment costs and the potential toxicity effects. Tzannis et al. (6)

employed an attenuated total reflected Fourier transform infrared spectroscopy techniques to investigate the extent of interleukin-2 (IL-2) adsorption to silicone rubber tubing, which is a commonly used catheter material. They also compared the residual bioactivities of different reconstituted IL-2 solutions after interaction with the surface to that of the initial solutions. After 24 h of exposure, the bulk concentration of IL-2 solutions decreased by 7 to 20% whereas the residual bioactivity level dropped by 97 to 99.5%. They concluded that these activity losses were direct results of the protein-surface interaction.

By studying the genetic variants and site-directed mutants of single proteins, many researchers have shown that the structural stability of a protein influences its interfacial behaviors (7, 8-10). Kato and Yutani (9) compared the surface properties of wild type and mutants of tryptophan synthase. Data suggested that mutants with higher stability exhibited greater resistance to unfolding at the interface. McGuire et al. (7, 11, 12) studied comparative adsorption of synthetic mutants and wild type bacteriophage T4 lysozyme on silica surfaces. Their results indicated that molecules adsorbed in different states occupied different interfacial areas. As a result, they proposed a parallel adsorption model, which allow proteins to adopt one of the two states directly from the bulk. Study performed by Elgersma et al. (13) on both sequential and competitive adsorption of BSA and monoclonal immuno-gamma globulin's (IgG's) onto polystyrene lattices showed that IgG's was easily displaced by BSA, but not the opposite. There has been considerable progress in the study of the kinetic and thermodynamics of adsorption of various proteins from single protein systems. However, the understanding in sequential adsorption and

exchange of proteins at the interface is not yet sufficient to predict or clearly explain the adsorption behavior of protein mixtures.

The primary objectives of this research were to quantify the kinetic rate constants governing the adsorption of a protein from a single component solution and to determine the ability of a second protein to displace the adsorbed molecules of the first protein (exchange constant). The wild type T4 lysozyme and its variant were used to study adsorption kinetics of proteins at hydrophobic and hydrophilic silica surfaces, using *in situ* ellipsometry and ^{125}I-radiolabeling. The lysozyme variant was produced by substitution of isoleucine at position 3 (Ile 3) with a tryptophan residue (Trp), resulting in a protein with $\Delta G_{unfolding}$ of 2.8 kcal/mol less than that of the wild type protein.

3.3 Materials and Methods

3.3.1 Proteins

Transformed cultures of *E. coli.* Strain RR1 containing bacteriophage T4 lysozyme wild type (WT) and tryptophan variant (TRP) plasmids were obtained from Professor Brian Matthews of the University of Oregon. Fermentation and purification of proteins followed the established procedures as described in Chapter 2 (14,15). Concentrated stock protein solutions were diluted with 0.01 M phosphate buffer, pH 7.0 (Sigma Chemical Co., St. Louis, MO) to yield a final concentration of 6 mg/ml ($E_{280}^{1\%}$ are 12.8 and 14.6 for the wild type and tryptophan variant, respectively). Then the solutions were passed through filters of 0.22 μm pore size (Milipore Corp., Bedford, MA), collected into cryogenic vials, and kept at –80 °C.

3.3.2 Silica surfaces

Silicon (Si) wafers (hyperpure, type N. phosphorous doped, plane 1-0-0) were purchased from Wacker Siltronic Corporation (Portland, OR). Oxidation of surfaces was carried out before the surfaces were cut into approximately 1.2 x 3 cm^2 plates, using a tungsten pen. Cleaning of silica plates was done by methods similar to those described by McGuire et al. (6-8), where plates were washed with mixtures of 1:1:5 of $NH_4OH:H_2O_2:H_2O$ then 1:1:5 of $HCl:H_2O_2:H_2O$, rinsed, and stored in 20 ml of 50% ethanol. Preparation of hydrophobic silica started with rinsing of the hydrophilic silica plates in 50% ethanol with deionized distilled water (DDW), dried with N_2, and kept in a desiccator for 24 h. Silanization took place with immersion of dried plates in a solution of 0.1% dichlorodimethylsilane (DDS) in xylene for 1 h, followed by rinsing in 100 ml each of xylene, acetone, ethanol, blown dry with N_2, and then kept in desiccators until used (16).

3.3.3 Glass surfaces

Glass cover slips (64% SiO_2, 13% alkali oxides, 8% boron) were purchased from Fisher Scientific (Santa Clara, CA). Acid and base treatments as well as silanization were performed on these glass cover slips following the same procedures performed on silica surfaces. Contact angles for both the silica surfaces and the glass cover slips were measured with a goniometer (Rame-Hart Inc., Mountain Lakes, NJ) using DDW as a diagnostic liquid.

3.3.4 Ellipsometry

A silica surface (hydrophobic or hydrophilic) was placed into a fused quartz, trapezoid cuvette (Hellma Cells, Germany) which was placed on the sample stage of an automatic *in situ* ellipsometer (Gaertner Scientific Corp., Chicago, IL). This instrument was modified so that the surface can be placed on upright position. After 5 ml of 10 mM phosphate buffer, pH 7.0 was injected into the cuvette, the ellipsometer stage was adjusted to obtain a maximum in reflected light intensity and steady optical properties (16-17). Measurements of surface properties were taken every 15 s.

Bare surface properties were recorded for 5 min before a protein solution was injected into the cuvette to yield a final protein concentration of 1 mg/ml. Surface properties were followed for another 30 min before the surface was rinsed with a protein-free buffer at a flow rate of 25 ml/min for 5 min. Film properties were monitored for another 25 min. The second protein solution was added to give the final concentration of either 0.01 or 1 mg/ml, and film properties were followed for 15, 30, 45, or 60 min. Then the cuvette was rinsed with a protein-free buffer for 5 min, and film properties were monitored for another 25 min.

At the end of the incubation period, dodecyltrimethylammonium bromide (DTAB) was added to the cuvette and was allowed to contact the surface for 15 min. The cuvette was then rinsed with 25 ml/min of 10 mM phosphate buffer for 5 minutes. Optical properties were monitored and recorded for another 25 minutes. One-film-model ellipsometry program (25) was used to determine the adsorbed mass of protein from the ellipsometrically determined values of film thickness and refractive index as explained by Cuypers et al. (26). A partial specific volume (V) of 0.78 $cm^3/\mu g$ and a molecular weight

to molar refractivity (*M/A*) ratio of 3.827 μg/cm^2 were used in the calculation (27-28). These protein-specific values were used to determine the adsorbed mass in both the presence and absence of DTAB. This is because it is impossible to assign the correct values for mixed films. This approach would overestimate the adsorbed mass of the mixed films, but would not influence any of the trends observed in these experiments.

Experiments with each protein sequence (Wild/Trp, Trp/Wild) on each type of surface were replicated at least twice.

3.3.5 Adsorption studies by radiolabeling

Concentrated T4 lysozyme stock solutions were radioiodinated with ^{125}I, using the iodine monochloride technique of Helmkamp et al. (18) as modified by Horbett (19). ^{125}I-lysozymes were mixed with unlabeled protein solutions to yield the final specific radioactivity of 200 cpm/μg. Experiments were conducted in plastic vials containing one glass cover slip per vial and 1.5 ml solution of the labeled first protein. Adsorption was allowed to proceed for 30 min, and the surface was rinsed by 10 mM phosphate buffer. After incubation in a protein-free buffer for another 25 minutes, unlabeled second protein was introduced to the system. Contact time of the second protein was allowed for 4, 8, 12, 15, 30, 45, and 60 min. Then the surface was rinsed, followed by a 25 min incubation in buffer. At the end of the incubation period, the glass surface was transfer into a counting tube and the sample radioactivity was measured with a gamma counter (Model 1185R, T.M. Analytic, Elk Grove Village, IL).

Spontaneous desorption or buffer-exchange study was carried out by contacting the surfaces with ^{125}I-labeled proteins for 30 min, rinsed, and incubated in a protein-free buffer for 0, 15, 30, 45, or 60 min. Then the surface radioactivity was measured.

Similar to the sequential adsorption study, self-exchange study was done by replacing the labeled first protein with the same protein that was not labeled. The contact time for the unlabeled protein was 30 minutes.

3.4 Results and Discussion

It is widely accepted that the amount of protein adsorbed at the solid surface is dependent on the surface hydrophobicity (20), thus the degree of hydrophobicity should be reported. We used a contact angle as an indication of surface hydrophobicity in this study. The data from contact angle measurement is reported in Table 3.1.

Table 3.1. Contact angles of hydrophobic and hydrophilic surfaces as measured with a goniometer, using deionized distilled water as a diagnostic liquid.

Surface	Contact Angle (degree ± S.D.)	
	Hydrophobic	Hydrophilic
Silica plate	80.0 ± 3.0	13.2 ± 2.7
Glass cover slip	72.8 ± 1.3	5.5 ± 1.3

3.4.1 Visual analysis of the kinetic plots

Representative plots of sequential adsorption kinetics on hydrophobic and hydrophilic silica for WT followed by TRP are shown in Figure 3.1 and 3.2, and for TRP followed by WT are shown in Figure 3.3 and 3.4, respectively. The shape of the adsorption curves of the same protein (WT or TRP) on both surfaces is very similar, but it differs among proteins on the same surface. From a quantitative point of view the adsorbed mass of TRP is approximately the same on both surfaces whereas the adsorbed mass of WT is significantly higher on hydrophobic than on hydrophilic silica. Moreover, the amount of WT adsorbed is also substantially higher than TRP on both surfaces.

Previously in the development of a parallel adsorption mechanism, McGuire et al. (7) suggested that TRP molecules tend to adsorb in a state that occupies a larger interfacial area than that of WT, thus the allowable adsorbed mass for monolayer coverage for TRP is lower than TRP. The possibility that TRP prefers to adsorb to the surfaces in a "more unfolded" state, which occupies a greater interfacial area than a "less unfolded" state, was investigated by Tian et al. using circular dichroism technique (21). Their results on adsorption study of T4L to colloidal silica particles showed that at 1:1 ratio of protein: particle, the α-helix loss after 90 min of adsorption for CYS, WT, and TRP was 10, 12, and 24%, respectively. This supported the hypothesis that the degree of unfolding upon adsorption is highly related to the thermal stability of the protein. Our results are also consistent with such behavior.

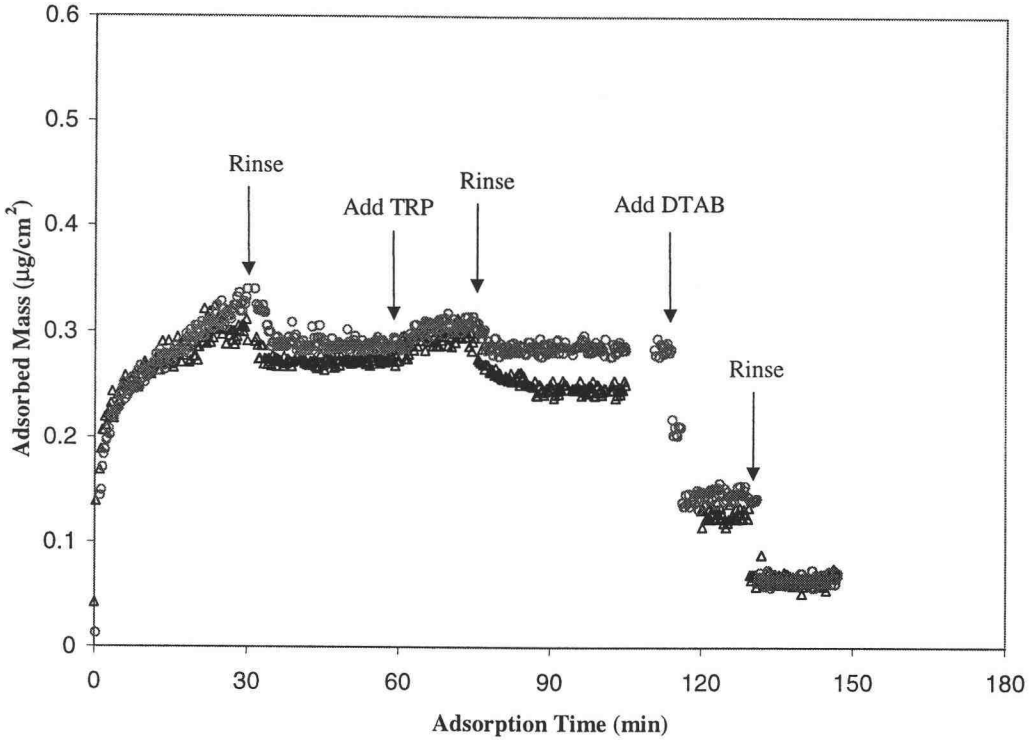

Figure 3.1. Sequential adsorption of WT follows by 0.01 mg/ml TRP (Δ), and 1 mg/ml TRP (○) on hydrophobic silica.

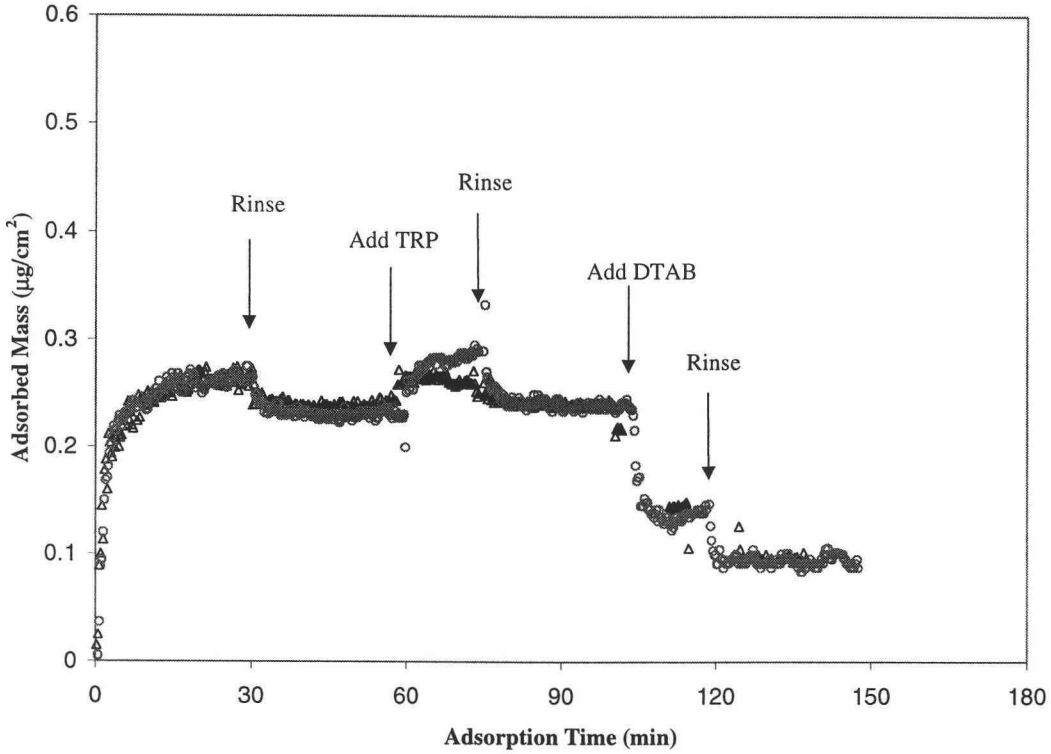

Figure 3.2. Sequential adsorption of WT follows by 0.01 mg/ml TRP (Δ), and 1 mg/ml TRP (○) on hydrophilic silica.

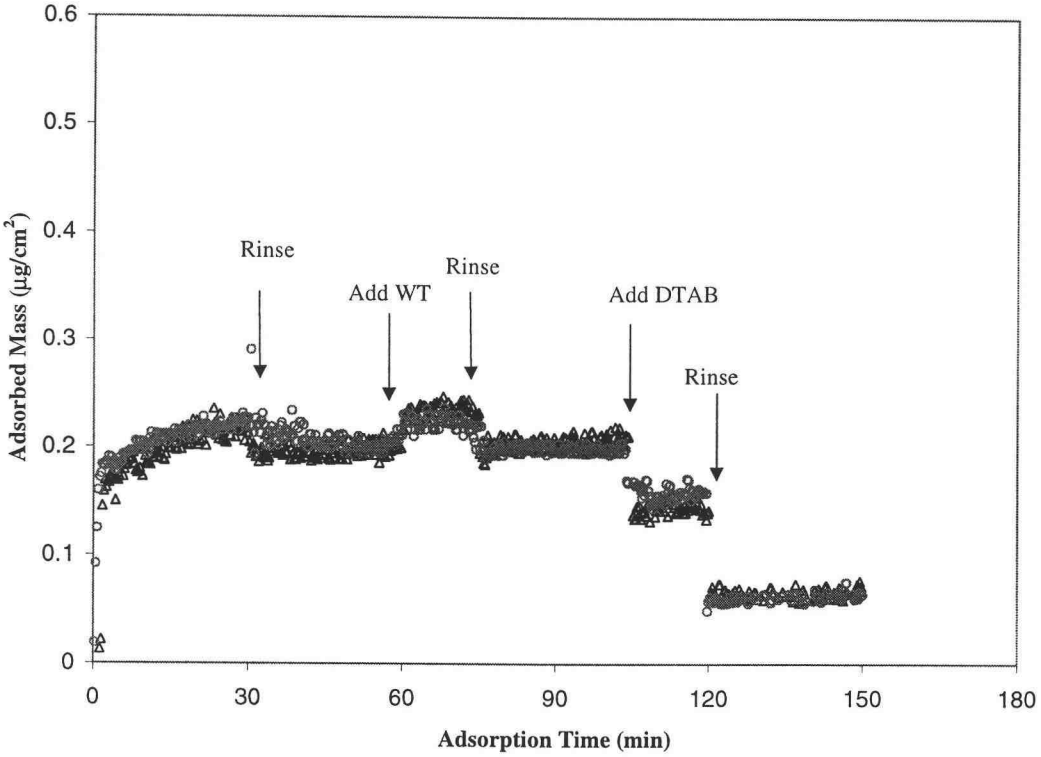

Figure 3.3. Sequential adsorption of TRP follows by 0.01 mg/ml WT (Δ), and 1 mg/ml WT (○) on hydrophobic silica.

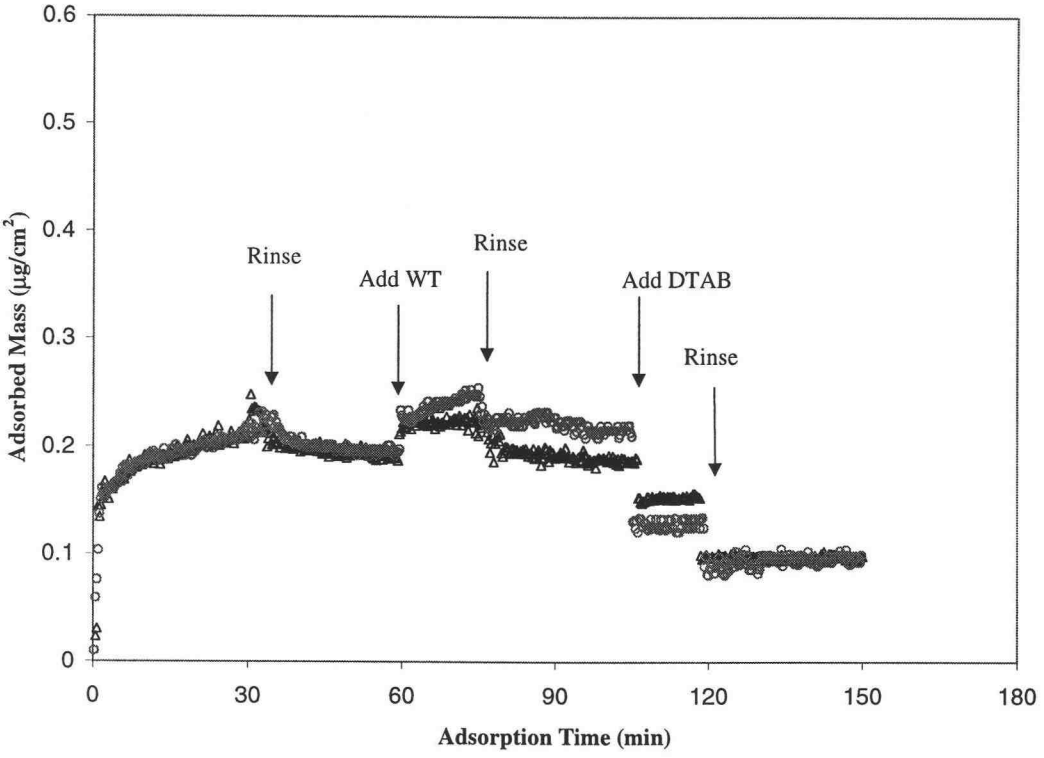

Figure 3.4. Sequential adsorption of TRP follows by 0.01 mg/ml WT (Δ), and 1 mg/ml WT (○) on hydrophilic silica.

3.4.2 Analysis with reference to adsorption kinetic models

3.4.2.1 A three-rate-constant adsorption kinetic model

Krisdhasima et al. (16) studied β-lactoglobulin adsorption kinetics, and proposed a mechanism for protein adsorption as shown in Figure 3.5. According to this three-rate-constant model, protein adsorption is a 2-step process. In the first step, protein molecules reversibly adsorb onto the surface with the kinetic rate k_1. In the second step, the adsorbed molecules can either desorb into the bulk phase with the rate k_{-1}, or undergo conformational changes and/or re-orientation into the irreversibly adsorbed form with the rate s_1. In this model, adsorbed proteins in either state are assumed to occupy the same interfacial area.

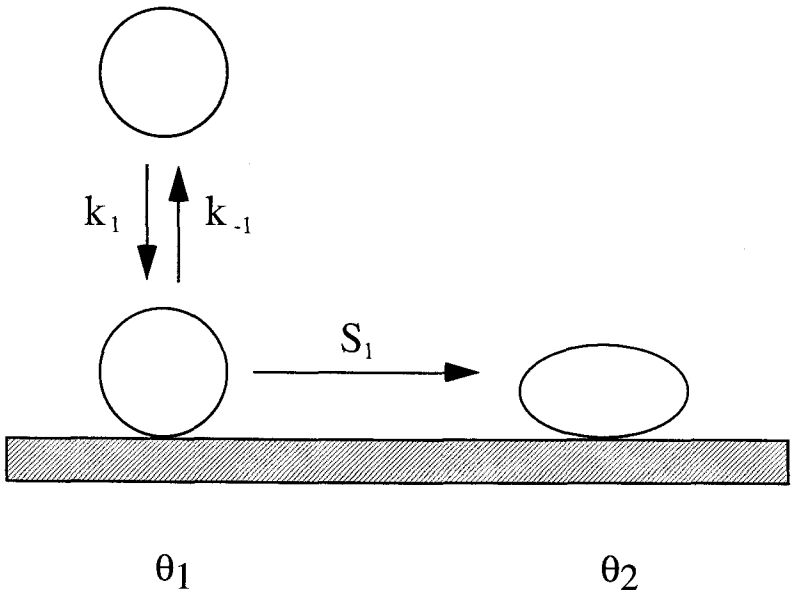

Figure 3.5. The three-rate-constant mechanism for protein adsorption proposed by Krisdhasima et al. [16].

Results from preliminary study on elutability of adsorbed T4 lysozyme by DTAB are shown in Table 3.2. According to the data there was no significant difference in the amount of protein eluted after 30 min and 2 h adsorption. It suggested that there was no conversion between θ_{1A} and θ_{2A} after 30 min, and that the conformational change of protein upon adsorption happened almost instantaneously. This is in agreement with the results obtained by Podhipleux et al. (22) on the study of the molecular charge effects on adsorption behavior of proteins, which suggested that adoption of a more tightly bound state happened rather quickly for T4L.

Table 3.2. Percent of adsorbed mass that was elutable from hydrophobic and hydrophilic silica surfaces following 15 min contact with DTAB.

Protein	Adsorbed Mass Eluted (%)	
	Hydrophobic	Hydrophilic
Wild Type		
30 min adsorption time	73.1	63.7
2 h adsorption time	75.3	66.7
TRP Mutant		
30 min adsorption time	62.2	48.6
2 h adsorption time	63.9	47.9

Since there is no evidence indicating the differences in the make-up of protein layer adsorbed for 30 min and 2 h, only 1 contact time (30 min) was used for the first protein in the study of sequential adsorption kinetics.

As previously mentioned, the three-rate-constant model assumed that generation of the irreversibly adsorbed molecules could only happen through the conversion of the reversible adsorbed molecules, and that the conversion does not involve any changes in the interfacial area occupied by the molecules. Nevertheless, the pattern of the data indicated that adoption of the more tightly bound state was achieved much faster, and molecules in that state occupy a greater interfacial area. For this reason, it is not suitable to use this model to illustrate the adsorption mechanism of T4L.

3.4.2.2 A parallel adsorption kinetic model

Since the previous model was proven insufficient to explain the adsorption kinetics of T4L, a more suitable mechanism must be adopted. The parallel adsorption kinetic model (Figure 3.6) proposed by McGuire et al. (7), a simple and similar mechanism was employed. In this model proteins can adsorb directly from the bulk solution into two states with state 2 molecules being more resistant to DTAB elution and occupy a larger interfacial area than state 1 molecules.

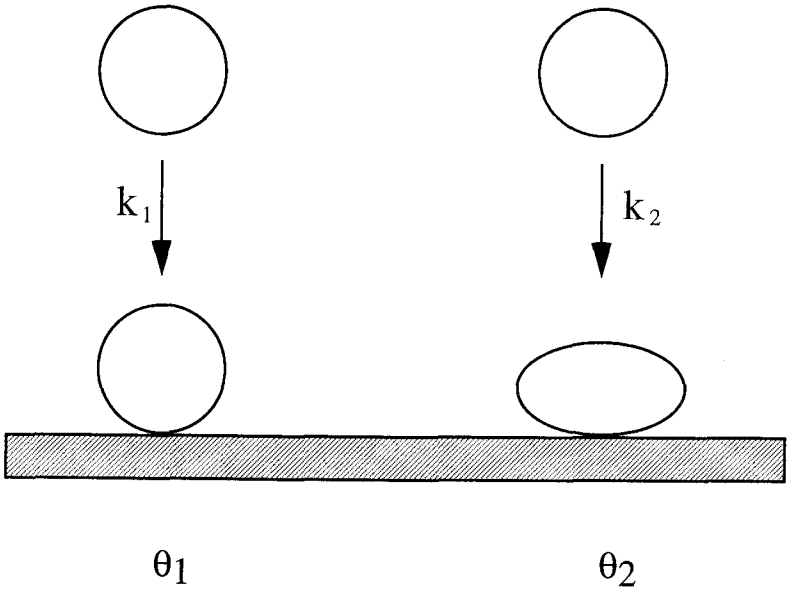

Figure 3.6. The parallel adsorption mechanisms for protein adsorption proposed by McGuire et al. [7]

Parameters k_1 and k_2 are kinetic rates governing adsorption of protein molecule into state 1 and state 2, respectively. In the absence of the diffusion-controlled process, the time-dependent fractional surface coverage of protein in each of the two states (θ_1 and θ_2) can be described as:

$$\theta_1 = \left(\frac{1}{1+(ak_2/k_1)} \right) * \left[1 - e^{-(-k_1 C - ak_2 C)t} \right]$$

$$\theta_2 = \left(\frac{k_2/k_1}{1+(ak_2/k_1)} \right) * \left[1 - e^{-(-k_1 C - ak_2 C)t} \right]$$

where a is the ratio of area occupies by a state 2 molecule to that occupies by a state 1 molecule, and C (mg/ml) is the bulk protein concentration.

If we define the maximum adsorbed mass of molecules allowable for monolayer coverage as Γ_{max} (μg/cm^2), the total adsorbed mass of protein at any time is calculated from:

$$\Gamma_{max} = \Gamma_{max}*(\theta_1+\theta_2) ,$$

and $(\theta_1+a\theta_2) = 1$ when the surface is covered. The value Γ_{max} was approximated as 0.396 μg/cm^2, corresponding to a maximum allowable monolayer adsorbed mass of molecules adsorbed in a close-packed, end-on manner (28 x 28 Å per molecule). For adsorption on hydrophobic silica, parameter a was set to 2.095 (= 0.396/0.189). The specific interfacial area occupied by state 2 molecules, 1/0.189, was based on the lowest ellipsometric data of TRP adsorption on hydrophilic surface. The specific interfacial area occupied by state 1 molecules, 1/0.396, was based on the theoretical value. Similarly in the case of hydrophobic silica, parameter a was set to 2.052 (= 0.396/0.193), where 1/0.193 was taken as the specific interfacial area occupied by state 2 molecules on hydrophobic surfaces.

Following the mechanism illustrated in Figure 3.6, the values of adsorption parameters k_1C, k_2C, and the ratio k_2/k_1 of WT and TRP were determined, using the linear regression analysis of the ellipsometric data from the single protein systems. The results are presented in Table 3.3. According to the data TRP is more likely to adsorb in state 2 on both surfaces, with k_2 approximately an order of magnitude higher than k_1. In the case of WT on hydrophilic silica the tendency is higher for molecules to adsorb in state 2, whereas the opposite is true for adsorption of WT on hydrophobic silica. Since the air-water interface can be considered as an ideal hydrophobic surface, we can compare our results to those obtained by Wang et al. (23) on spreading pressure kinetic data of

1 mg/ml T4L solutions. They found the ratio k_2/k_1 of WT and TRP to be 0.60 and 8.26, which are qualitatively similar to our findings (0.70 for WT and 12.5 for TRP).

Table 3.3. The average values of kinetic rate constants from ellipsometric measurements, based on the parallel adsorption model (Figure 1.1b).

Protein	Surface	Rate Constants		
		K_1C (min^{-1})	K_2C (min^{-1})	K_2/K_1
Wild Type	Hydrophobic	0.285	0.193	0.7
	Hydrophilic	0.140	0.215	1.5
TRP Mutant	Hydrophobic	0.035	0.436	12.5
	Hydrophilic	0.046	0.419	9.1

3.4.3 Self-exchange study

Data suggested that adsorbed WT and TRP can exchange with molecules from the bulk. Approximately 12% of WT and 16% of TRP on hydrophilic surface exchanged after 30 min. These numbers are as high as 33% for WT and 32% for TRP on hydrophobic surface. The higher numbers in percent exchanged from hydrophobic surface may be explained partly by a stronger binding strength of the adsorbed protein on hydrophilic surface. This hypothesis is supported by the results from elution study (Table 3.2) which exhibit a higher resistance to elution on hydrophilic surface for both proteins.

3.4.4 Estimation of exchange rate constants

Based on the simple kinetic models for protein adsorption suggested by McGuire et al. (7), along with a kinetic model for protein exchange reactions for a binary mixture proposed by Lundström and Elwing (24), we constructed a kinetic model for sequential adsorption which is shown in Figure 3.7. According to this model, protein *A* can adsorb directly from the solution in either state 1 or 2, both of which are exchangeable by protein *B* with the rates $k_{e1}[C_B]$ and $k_{e2}[C_B]$, respectively. No conversion between θ_{1A} and θ_{2A} is allowed, thus $-\frac{d\theta_{1A}}{dt} = k_{e1}[C_B]\theta_{1A}$, and $-\frac{d\theta_{2A}}{dt} = k_{e2}[C_B]\theta_{2A}$.

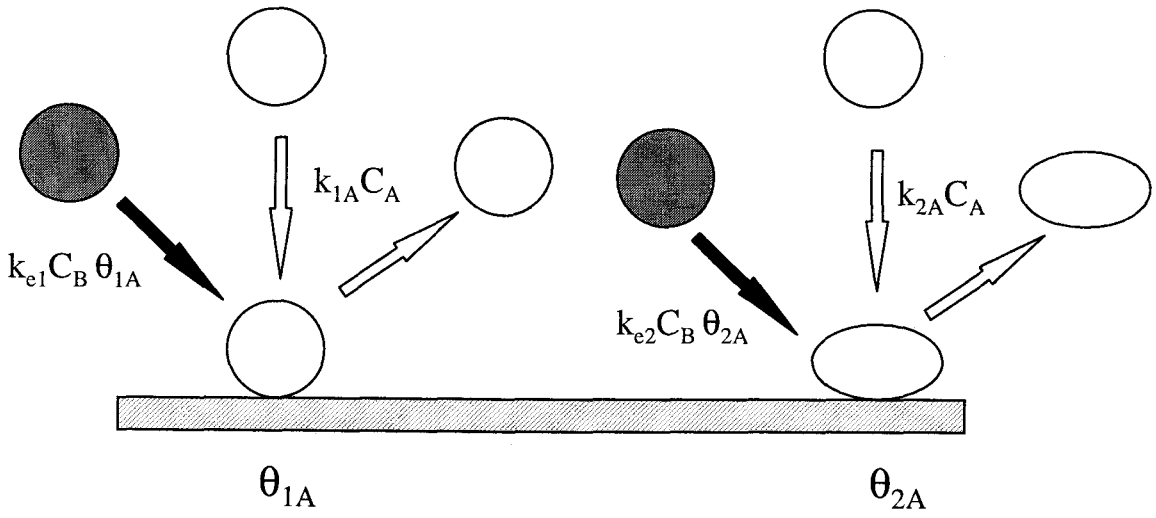

Figure 3.7. A mechanism for sequential adsorption of protein *A* followed by protein *B*, based on Figure 3.6.

Integration of the preceding equations from $\theta_{1A} = \theta_{1A,ti}$ to $\theta_{1A} = \theta_{1A}$ and from $t = 0$ to $t = t$ yields:

$$\theta_{1A} = \theta_{1A,ti}[\exp(-k_{e1}[C_B]\cdot t)],$$

and $$\theta_{2A} = \theta_{2A,ti}[\exp(-k_{e2}[C_B]\cdot t)].$$

We can solve the above equations under the condition that the exchange rates depend solely on the binding strength of the adsorbed molecules.

Unlike the self-exchainge study, our results from radiolabeling study implied that the exchange rate constants of WT and TRP lysozymes did not depend on the binding strength (determined by the resistance to DTAB elution) of the adsorbed molecules alone, but also depend on the properties of the exchanging proteins and the interactions between the adsorbed molecules vs. the exchanging molecules. Furthermore, experimental data suggested a combination of exchange and desorption processes, therefore a more generalized model of exchange with desorption mechanism was developed as depicted in Figure 3.8.

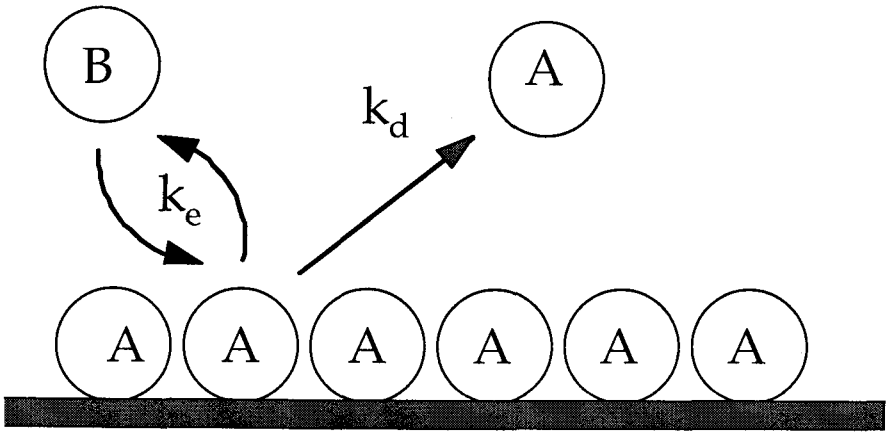

Figure 3.8. Exchange with desorption mechanism.

Equation describing this exchange with desorption mechanism are:

$$-\frac{d\theta_A}{dt} = k_e C_B \theta_A + k_d \theta_A$$

$$-\int_{\theta_{A0}}^{\theta_A} \frac{d\theta_A}{\theta_A} = (k_e C_B + k_d)\int_0^t dt$$

$$\frac{\theta_A}{\theta_{A0}} = e^{-(k_e C_B + k_d)t}$$

Taking a natural log of the above equation results in:

$$\ln\left(\frac{\theta_A}{\theta_{A0}}\right) = -(k_e C_B + K_d)t\,.$$

This is the final form of the mathematical expression describing the fraction of the first protein (A) remaining at the interface after introduction of the second protein compared with before the introduction as a function of the exchange rate of protein A by protein B (C_B), the rate of desorption (K_d), and the contact time of the second protein (t).

Linear regression analysis of the experimental data from radiolabeling study resulted in kinetic rate constants shown in Table 3.4, assuming that the values of kinetic rates were additive. Since desorption reaction is, to a certain extent, a function of the concentration difference between the interface and the bulk, it is unlikely that the desorption rate would remain the same when the bulk concentration of protein is not zero. This explains some of the negative values obtained for the exchange rate constant, $K_e C_B$ of TRP replacing WT. Nevertheless the assumption of additive kinetic rates, though may not be accurate, was necessary.

Results in Table 3.4 suggested that WT could exchange with the molecules of adsorbed TRP on both hydrophobic and hydrophilic glass surfaces, with the exchange

rate constant being higher on hydrophilic surface. The exchange rates also increased slightly as the bulk concentration of the WT increased from 0.01 mg/ml to 1 mg/ml. At a low bulk concentration of 0.01 mg/ml, TRP could not exchange with adsorbed WT on

Table 3.4. Kinetic rate constants obtained from sequential adsorption study of ^{125}I-labeled lysozyme to glass cover slips (* indicates ^{125}I-labeled protein).

Bulk conc. of second protein	Rate Constants (min^{-1})	WT*/TRP		TRP*/WT	
		Hydrophobic	Hydrophilic	Hydrophobic	Hydrophilic
0.01 mg/ml	K	0.0049	0.0088	0.0357	0.0802
	K_d	0.0062	0.0182	0.0150	0.0273
	K_eC_B	-0.0013	-0.0094	0.0207	0.0529
1 mg/ml	K	0.0051	0.0245	0.0464	0.0835
	K_d	0.0062	0.0182	0.0150	0.0273
	K_eC_B	-0.0011	0.0063	0.0314	0.0562

neither hydrophobic nor hydrophilic surfaces. However, when the bulk concentration of TRP increased to 1 mg/ml a small fraction of adsorbed WT was replaced. Nevertheless, the exchange rate constant of WT with TRP on hydrophilic surface at 1 mg/ml was still approximately an order of magnitude lower than that of TRP exchanged by WT.

Considering the percent of adsorbed mass of WT and TRP that was elutable by DTAB from hydrophobic and hydrophilic silica (Table 3.2), we can clearly see that TRP

has a higher resistance to elution by DTAB than WT on both surfaces. Part of the reason maybe due to the higher ratio of state 2 molecules to state 1 molecules that made up the adsorbed protein film, when compared TRP to WT. Thus, if TRP exchanged with part of the adsorbed WT on either of the surface, we should notice a decrease in the percent of adsorbed mass of the mixed film that was elutable by DTAB. On the contrary if WT exchanged with adsorbed TRP, we should see an increase in the percent of adsorbed mass

Table 3.5. Percent adsorbed mass eluted by DTAB after exposure to second protein.

Second protein conc. (mg/ml)	Second protein contact time (min)	First protein adsorbed mass eluted (%)			
		WT/TRP		TRP/WT	
		Hydrophobic	Hydrophilic	Hydrophobic	Hydrophilic
0.01	15	75.2	61.0	67.3	51.7
	30	-	59.3	68.0	56.2
	45	-	62.3	67.9	56.1
	60	76.1	63.2	68.0	61.2
1.0	15	76.2	63.2	68.1	44.2
	30	76.7	61.6	67.7	52.2
	45	76.2	60.9	61.4	56.7
	60	75.5	61.9	68.5	49.9

eluted. Our results from sequential adsorption study by ellipsomtery (Table 3.5) exhibit such trends, and are in agreement with the results obtained by radiolabeling study.

As mentioned earlier, data seemed to point to the same conclusion that exchange of proteins did not depend mainly on the binding strength of the adsorbed films. The properties of the adsorbing protein, e.g. its ability to adsorb when only a small amount of unoccupied area was exposed, seemed to play a major role in the exchange reaction. Data on adsorption of T4L on silica surfaces by successive loading method obtained by Singla (28) suggested that when the bulk concentration is very low, lysozyme tends to unfold more upon adsorption. For this reason, we hypothesize that the amount of molecules trying to adsorb in state 2 would decrease as the bulk concentration increases. This may elucidate a higher exchange rate of TRP by WT when the bulk concentration of WT was increased.

3.5 Summary

Adsorption kinetics shows that TRP mutant adsorbed at the interfaces more tightly and occupied a greater interfacial area than the wild type. It also exhibited a higher resistance to elution by DTAB. More WT tended to adsorb in state 2 on hydrophilic silica than on hydrophobic silica, whereas more than 90% of TRP preferred to adsorb in state 2 on both surfaces. The amount of adsobed protein exchanged by the same species seemed to be partly dependent on the binding strength of the adsorbed proteins. Data indicated that sequential adsorption of proteins occurred in the case of the less stable mutant followed by the wild type, but was not clearly observed when proteins were introduced in reversed order. It suggested that, in an exchange reaction properties of

the adsorbing protein may be more important than the conformational state of the protein molecules already adsorbed.

3.6 Acknowledgement

This study was supported by the National Science Foundation through Grant CTS 9501842. Thanks go to Woo-Kul Lee for his help in preparation of glass cover slips, and to Lei Shen for radiolabeling of T4 lysozymes.

3.7 References

1. Blum, L.J. and P.R. Coulet (Eds.). 1991. Biosensor Principles and Applications. p. 7. M. Dekker, New York.

2. Bohnert, J. and T.A. Horbett. 1986. Changes in adsorbed fibrinogen and albumin interactions with polymers indicated by decreases in detergent elutability., *J. Colloid Interface Sci.* **111:** 363-377.

3. Lee, J.H. and J.D. Andrade. 1988. Polymer Surface Dynamics. p. 111. Plenum Press, New York.

4. Bruil, A., L.M. Brenneisen, J.G.A. Terlington, T. Beugling, W.G. van Aken, and J. Feijen. 1994. *In Vitro* leukocyte adhesion to modified polyurethane surfaces II: Effects of wettability., *J. Colloid Interface Sci.* **165:** 72-81.

6. Olsson, J., A. Carlén, N.L. Burns, and K. Holmberg. 1995. Modified pellicle formation and reduced *in vitro* bacterial adherence after surface treatment with different siloxane polymers., *Colloids and Surfaces B: Biointerfaces* **5:** 161-169.

6. Tzannis, S.T., W.J.M. Hrushesky, P.A. Wood, and T.M. Przybycien. 1997. Adsorption of a formulated protein on a drug delivery device surface., *J. Colloid Interface Sci.* **189:** 216-228.

7. McGuire, J., M.C. Wahlgren, and T. Arnebrant. 1995. Structural stability effects on the adsorption and dodecyltrimethyl ammonium bromide-mediated elutability

of bacteriophage T4 lysozyme at silica surfaces., *J. Colloid Interface Sci.* **170:** 182-192.

8. Horsley D., J. Herron, V. Hlady, and J.D. Andrade. 1987. Physicochemical and Biochemical Studies. *in* Proteins at Interfaces. (J.L. Brash and T.A. Horbett, eds.) p.290-304. ACS Symposium Series 343, Washington, DC.

9. Kato, A., and K. Yutani. 1988. Correlation of surface properties with conformational stabilities of wild-type and six mutant tryptophan synthase α-subunits substituted at the same position., *Protein Eng.* **2:** 153-156.

10. Billsten, P., M. Wahlgren, T. Arnebrant, J. McGuire, and H. Elwing. 1995. Structural changes of T4 lysozyme upon adsorption to silica nanoparticles measured by circular dichroism., *J. Colloid Interface Sci.* **175:** 77-82.

11. McGuire, J., V. Krisdhasima, M.C. Wahlgren, and T. Arnebrant. 1995a. Comparative adsorption studies with synthetic, structural stability and charge mutants of bacteriophage T4 lysozyme. *in* Proteins at Interfaces II: Fundamentals and Applications. (J. Brash and T. Horbett, eds.), ACS Books, Washington, DC.

12. McGuire, J., M.C. Wahlgren, and T. Arnebrant. 1995. The influence of net charge and charge location on the adsorption and dodecyltrimethyl ammonium bromide-mediated elutability of bacteriophage T4 lysozyme at silica surfaces., *J. Colloid Interface Sci.* **170:** 193-202.

13. Elgersma, A.V., R.L.J. Zsom, J. Lyklema, and W. Norde. 1992. Adsorption competition between albumin and monoclonal immuno-gamma globulins on polystyrene lattices., *J. Colloid. Interface Sci.* **152:** 410-428.

14. Alber, T. and B.W. Matthews. 1987. Structure and thermal stability of phage T4 lysozyme., *Meth. Enzymol.* **154:** 511-533.

15. Muchmore, D.C., L.P. McIntosh, C.B. Russel, D.E. Anderson, and F.W. Dahlquist. 1989. Expressiom and 15N labeling of proteins for proton and nitrogen-15 NMR., *Methods Enzymol.* **177:** 44-73.

16. Krisdhasima, V., J. McGuire, and R.D. Sproull. 1992. Surface hydrophobic influences on β-lactoglobulin adsorption kinetics., *J. Colloid Interface Sci.* **154(2):** 337-350.

17. Suttiprasit , P. and J. McGuire. 1992. The surface activity of α-lactalbumin, β-lactoglobulin, and bovine serum albumin II : Some molecular influences on adsorption to hydrophilic and hydrophobic silicon surfaces., *J. Colloid Interface Sci.* **154:** 327-336.

18. Helmkamp, R.W., R.L. Goodland, W.F. Bale, I.L. Spar, and L.E. Mutschler. 1960. High specific activity iodination of γ-globulin with iodine-131 monochloride., *CancerRes.* **20:** 1495-1500.

19. Horbett, T.A. 1981. Adsorption of proteins from plasma to a series of hydrophilic-hydrophobic copolymers. II. Compositional analysis with the prelabeled protein technique., *J. Biomed. Mater. Res.* **15:** 673-695.

20. Brash, J.L. and T. Horbett. (Eds.)1995. Proteins at Interfaces: An overview. *in* Proteins at Interfaces II: Fundamentals and Applications. p. 1-25. ACS Books, Washington, DC.

21. Tian, M., W-K Lee, M.K. Bothwell, and J. McGuire. 1998. Structural stability effects on adsorption of bacteriophage T4 lysozyme to colloidal silica., *J. Colloid Interface Sci.* **199:** In Press.

22. Podhipleux, N., V. Krisdhasima, and J. McGuire. 1996. Molecular charge effects on protein behavior at hydrophobic and hydrophilic solid surfaces., *Food Hydrocoll.* **10:** 285-293.

23. Wang J., and J. McGuire. 1997. Surface tension kinetics of the wild type and four synthetic stability mutants of T4 phage lysozyme at the air-water interface., *J. Colloid. Interface Sci.* **185:** 371-323.

24. Lundström I., and H. Elwing. 1990. Simple kinetic model for protein exchange reactions on solid surfaces., *J. Colloid Interface Sci.* **136:**68-84.

25. Krisdhasima, V., J. McGuire, and R.D. Sproull. 1992. A one-film-model ellipsometry program for the simultaneous calculation of protein film thickness and refractive index., *Surf. Interface Anal.* **18:** 453-456.

26. Cuypers, P.A., J.W. Corsel, M.P. Janssen, J.M.M. Kop, W.T. Hermens, and H.C. Hemker. 1983. The adsorption of prothrombin to phosphatidylserine multilayers quantitated by ellipsometry., *J. Biol. Chem.* **258:** 2426-2431.

27. Podhipleux, N. 1994. Adsorption of selected charge mutants of bacteriophage T4 lysozyme at silanized silica surfaces. Master's thesis. Department of Food Science and Technology, Oregon State University, Corvallis, OR.

28. Singla, B. 1994. Adsorption of selected stability mutants of bacteriophage T4 lysozyme at silanized silica surfaces. Master's thesis. Department of Chemical Engineering, Oregon State University, Corvallis, OR.

29. Al-Makhlafi, H., M. Lakamraju, N. Podhipleux, B. Singla, and J. McGuire. 1995. Measuring surface hydrophobicity as compared to measuring hydrophobic effect on adhesion events. *J. Food Prot.*, **58(9):** 1034- 1037.

CHAPTER 4

ADSORPTION BEHAVIOR OF BACTERIOPHAGE T4 LYSOZYME VARIANTS AT AIR-WATER INTERFACE

4.1 Abstract

The kinetics of adsorption of the wild type bacteriophage T4 lysozyme and two structural stability variants at the air-water interface were studied, using a radiotracer method. The lysozyme variants were produced by substitution of the isoleucine residue at position 3 with cysteine (CYS) and tryptophan (TRP), resulting in mutant proteins with higher and lower structural stability than that of the wild type protein, respectively. The surface concentration of T4 lysozyme exhibited a brief induction period, followed by a rapid adsorption. Initially the surface pressure of lysozyme solutions exhibited a lag period, but then progressively increased for an extended period of time. Surface pressure and surface concentration kinetics of the less stable mutant showed a shorter lag time and a sharper increase than that of the wild type. Sequential adsorption experiments showed that neither of the proteins could displace the previously adsorbed molecules at the interface. Competitive adsorption of the TRP mutant and the wild type lysozymes from binary solutions were also studied. Data indicated that adsorption of lysozyme cannot be explained solely by the diffusion-limited process, and seemed to be hindered by an energy barrier at the air-water interface.

4.2 Introduction

Protein films adsorbed at interfaces are involved in situations that are important in many areas of pharmaceutical, biomedical, and bioprocess technology. Bioseparation and protein purification by chromatography and foam fractionation techniques involves competitive adsorption of proteins and enzymes at solid-liquid interface, and gas-liquid interface, respectively (1). Stabilization of foams using proteins is also a common practice in the food industry. This is highly related to the adsorption behaviors of proteins at the air-water interface (2). Adsorption of proteins at the interface and their subsequent conformational changes result in decreasing interfacial energy, therefore reducing the surface tension of the water (3). Since surface pressure is inversely proportional to the surface tension, surface pressure kinetics can be used to monitor the adsorption behavior of protein at the air-water interface.

Wei et al. (4) studied surface tension kinetics of superoxide dismutase, cytochrome *c*, myoglobin, lysozyme, and ribonuclease, using the Wilhelmy plate method. They found the kinetic behavior at low bulk protein concentration to be related to protein's conformational stability. Xu and Damodaran (5) followed the surface pressure of native, partially and fully denatured of hen egg white, human, and T4 phage lysozymes. They proposed a mechanism for protein adsorption at air-water interface whereby the driving force was considered to be the combination of the interfacial force fields, contributing by hydrophobic, electrostatic, hydration, and conformational potentials.

Kato and Yutani (6) measured the surface tension, foaming, and emulsifying properties of the wild type and six mutants of tryptophan synthase α-subunits. They

found that more stable mutants exhibited less surface activity, and concluded that protein surface properties are partly determined by their conformational stability.

In this research, we investigated the influences of structural stability on adsorption behavior of T4 phage lysozyme at the air-water interface. We recorded the surface pressure kinetics and the surface radioactivity of ^{14}C-labled protein solutions.

4.3 Materials and Methods

4.3.1 Materials

The transformed cultures of *E. coli*, containing bacteriophage T4 lysozyme (T4L) wild type (WT), cysteine (CYS) or tryptophan (TRP) variant plasmids were obtained from Professor Brian Matthews of the University of Oregon. Replacing isoleucine at position 3 (Ile 3) with CYS resulted in a protein with $\Delta G_{unfolding}$ of 1.2 kcal/mol more than that of WT protein. Substitution of Ile 3 with TRP residue resulted in a mutant protein with $\Delta G_{unfolding}$ of 2.8 kcal/mol less than that of WT protein. Circular dichroism spectra obtained by Tian et al. (7) for these proteins showed no differences in structural conformation among the variants. Purification of proteins followed the established procedures (8, 9). Ultrapure Na_2HPO_4, $NaHPO_4$, and NaCl were obtained from Aldrich Chemical Co. (Milwaukee, WI). [^{14}C]Formaldehyde was purchased from New England Nuclear Co. (Boston, MA). Milli-Q water (produced with a system from Millipore Corp., Bedford, MA) with a resistivity of 18.2 MΩ.cm was used in all experiments.

4.3.2 Radiolabeling and protein assay

Lysozymes were radiolabeled with [^{14}C] formaldehyde by reductive methylation of the lysine residues as described elsewhere (10, 11). The protein concentration of stock solutions were determined ($E^{1\%}$ at 280 nm was 12.8 for WT and CYS, and 14.6 for TRP) to be 0.726 mg/ml for WT, 0.736 mg/ml for CYS, and 0.660 mg/ml for TRP. The specific radioactivities of the labeled proteins were determined with a scintillation counter to be 0.4112 μCi/mg, 0.8995 μCi/mg, and 2.1981 μCi/mg for WT, CYS, and TRP, respectively.

4.3.3 Adsorption kinetics from single protein systems

The kinetics of adsorption of proteins at the air-water interfaces was monitored as described elsewhere (11-13). Briefly, a stock protein solution was diluted with 125 ml of 0.01 M phosphate buffer, pH 7.0 to obtain the final protein concentration of 1.5 μg/mL (1.5×10^{-4}%). The solution was poured into a Teflon trough (21x5.56x1.27 cm^3) and the surface was cleaned with an aspirator. The rate of change of surface concentration of the radiolabeled protein was monitored by measuring the surface radioactivity with a Ludlum gas proportional counter (Ludlum Measurements, Inc., Sweetwater, TX). The rate of change of surface pressure was monitored simultaneously by the Wilhelmy plate method (Cahn Instruments, Co., CA). In addition, the entire setup was housed in a chamber maintained at 24 ± 0.2 °C and 90-95% relative humidity. Finally, a calibration curve relating counts per minute (cpm) versus surface radioactivity (μCi/m^2) constructed by

spreading ^{14}C-labeled β-casein on the air-water interface was used to convert cpm to μCi/m^2 (14).

4.3.4 Competitive adsorption experiments

To monitor adsorption of the wild type from binary solution mixtures, stock solutions of [^{14}C] WT and unlabeled TRP were mixed with phosphate buffer to the required bulk concentrations. The concentration of WT was kept constant at 1.5 μg/ml whereas the concentration of TRP was varied to yield the final concentration ratio of [^{14}C]WT:TRP of 1:2, 1:1, and 2:1. Further, the binary mixtures were poured into the Teflon trough. After the surface was swept, the rates of change in surface radioactivity and surface pressure were monitored.

4.3.5 Exchange studies

The ability of WT and TRP to displace each other from the interface was studied. First, 1.5 μg/ml solution of ^{14}C-labled protein was allowed to adsorb for 8 h. Then the stock solution of unlabeled protein was injected into the subsurface to yield the unlabeled protein concentration of 1.5 μg/ml, and the surface radioactivity was followed for another 4 h.

4.3.6 Preferential adsorption studies

To investigate whether a preferential adsorption occurred, the solution mixtures of 1:1 of [^{14}C] WT: TRP, WT: [^{14}C] TRP, and [^{14}C] WT: [^{14}C] TRP were diluted with

phosphate buffer to obtain the combined bulk concentration of 1.5 μg/ml. The mixtures were poured into the Teflon trough and the rate of change in surface radioactivity was followed. Another experiment was performed out to compare the rates of change in surface radioactivity of 1.5 μg/ml [^{14}C]TRP solution to the 1.5 μg/ml solution mixture of 1:1 [^{14}C]TRP:TRP.

4.4 Results and Discussion

4.4.1 Adsorption kinetics from single protein systems

Kinetics of the surface concentration and surface pressure of the lysozyme wild type, CYS mutant, and TRP mutant during adsorption from a 1.5 μg/ml solution are shown in Figure 4.1. Similar to the study done by Xu and Damodaran (5), the surface pressure kinetics of T4L exhibited a lag period. However, the kinetics of T4L adsorbed mass showed a very brief induction period without any initial desorption from the interface. Since the surface concentration values in these figures represent the net amount of protein after correcting for the background radioactivity from the bulk phase, the slightly negative values of adsorbed mass at time zero were results of experimental deviations.

Kinetics of adsorption of WT protein (Figure 4.1a) and CYS (Figure 4.1b) are very similar. It is apparent that the surface concentration of the protein solutions increased with time and approached steady state after about 240 min of adsorption. The surface pressure of WT and CYS solutions did not increase for over 100 min and the net increase in the surface pressure was only about 6 mN/m after 1500 min of adsorption.

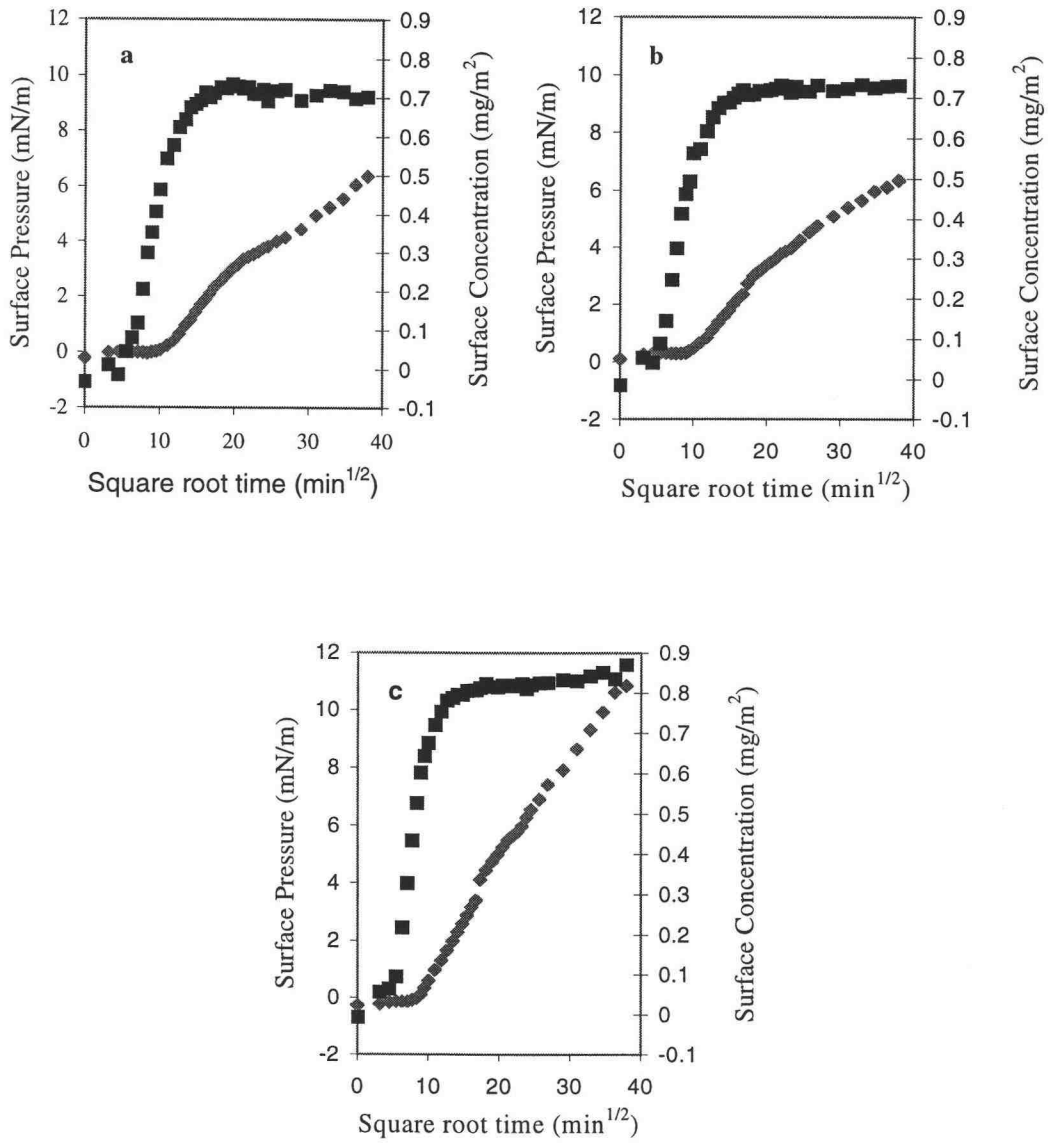

Figure 4.1. Kinetics of surface concentration (■) and surface pressure (◆) of adsorbed lysozyme at the air-water interface: (a) WT; (b) CYS; and (c) TRP. The bulk concentration of protein was 1.5 μg/ml in all cases.

Since the surface concentration seemed to reach an apparent equilibrium value well before 1500 min while the surface pressure was still changing, it suggested that WT and CYS retained much of their native structures upon initial adsorption. Then the adsorbed molecules underwent a very slow unfolding process at the interface (15).

Unlike the behavior of WT and CYS, TRP (Figure 4.1c) demonstrated a shorter surface pressure lag time, a shorter induction period for surface concentration, and a sharper increase in both the surface pressure and surface concentration. This indicated the ability of TRP to unfold more rapidly upon adsorption. However, its surface pressure also did not reach a steady-state value after 1500 min of adsorption.

Wang et al. (3) studied the surface tension kinetics of various stability mutants of T4L. In general the surface tension of the more stable variants was higher than that of the less stable mutants, and the rate and extent of surface tension changes decreased as $\Delta\Delta G$ increased. $\Delta\Delta G$ is defined as the difference between $\Delta G_{unfolding}$ of wild type and that of the mutant protein. Our results are in agreements with their findings. The results are also in agreement with data obtained by Tian et al. (7) on adsorption study of T4L to colloidal silica particles. They found that after 90 min of adsorption at 1:1 ratio of protein: particle, the α-helix loss of WT, CYS, and TRP was 12, 10, and 24%, respectively.

The adsorption process of amphiphilic molecules from a very dilute bulk phase to the air-water interface was proposed a diffusion-controlled mechanism by Ward and Tordai (16). The rate of arrival of protein molecules at an interface can be expressed as follows:

$$\Gamma = 2C_o(D_{app}/\pi)^{1/2}\, t^{1/2} \qquad \text{[Eq.4.1]}$$

where Γ, C_o, D_{app}, and t are protein adsorbed mass per surface area, bulk phase concentration, apparent diffusion coefficient, and time, respectively (3, 11, 15). The values of D_{app} for each plot were calculated from the linear portions of the plots (Figure 4.1), and tabulated in Table 4.1 (see Appendix G).

Table 4.1. Apparent diffusion coefficient (D_{app}) of bacteriophage T4 lysozyme at the air-water interface, calculated from the linear portions of the experimental data shown in Figure 4.1.

Protein	ΔΔG (kcal/mol)	Slope	R^2	D_{app} (cm^2/s)
CYS	+1.2	$1x10^{-6}$	0.9889	$3.49x10^{-7}$
WT	0	$1x10^{-6}$	0.9811	$3.49x10^{-7}$
TRP	-2.8	$2x10^{-6}$	0.9888	$1.40x10^{-6}$

* R^2 is the correlation coefficient

Diffusion coefficient of T4L in water was also estimated using the Stokes-Einstein equation (17):

$$D = \frac{kT}{6\pi\eta r_m} \qquad \text{[Eq.4.2]}$$

where D, k, T, η, *and* r_m *are* diffusion coefficient of molecule in solution, Bolzmann's constant, absolute temperature, viscosity of the solvent, and molecular radius, respectively. Estimated r_m from the hydrodynamic particle size was 1.52 nm (18, see Appendix F), therefore the diffusion coefficient of T4L is approximately $1.43x10^{-6}$ cm^2/s. We can see that the apparent diffusion coefficient of the wild type and CYS lysozyme is

at least an order of magnitude lower than the value in solution (water). However, the apparent diffusion coefficient of the more flexible mutant (TRP) is approximately equal to the value in the solution. These results are similar to Xu and Damodaran's data (5) when compared the apparent diffusion coefficient of the native T4L to that of the fully denatured lysozyme.

Our results suggested that T4 lysozyme seemed to experience an energy barrier that hinders their adsorption at the air-water interface, and that data in Table 4.1 cannot be explained solely by the theory of diffusion-limited adsorption process. This is because a less stable protein is more flexible and thus has a higher hydrodynamic size than the wild type protein. If the diffusion-limited adsorption process is true, TRP mutant should have exhibited a lower diffusion coefficient than that of the wild type. The surface concentration kinetics of T4L from experiments were compared to that predicted by [Eq.4.1] as shown in Figure 4.2. It is clearly seen that the experimental data is much lower than that predicted by the diffusion-limited process. The diffusion-controlled theory also requires that when the surface is clean, the activation energy (E_a)to adsorption at the interface is equaled to zero (15). This is not in an agreement with the experimental data from which the lag period is clearly observed. According to Xu and Damodaran (5) a diffusion-limited adsorption process is more likely for flexible proteins, but not for highly-charged and tightly folded globular proteins such as T4 lysozyme.

4.4.2 Competitive adsorption experiments

The effects of TRP concentration in the bulk phase on the kinetics of adsorption of WT are shown in Figure 4.3. By keeping bulk [^{14}C]WT concentration at 1.5 μg/ml

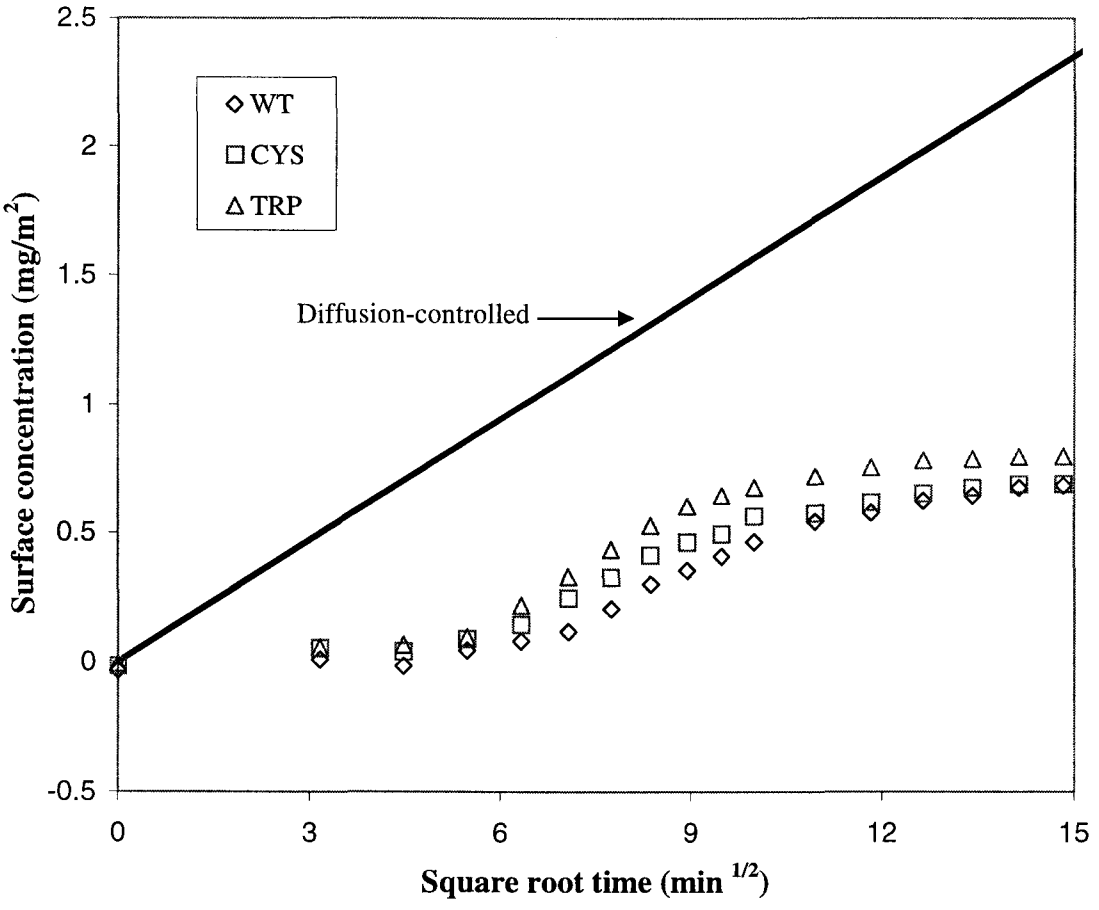

Figure 4.2. Comparison of adsorption kinetics of T4 lysozyme in single component systems to the theoretical values estimated from [Eq.4.1].

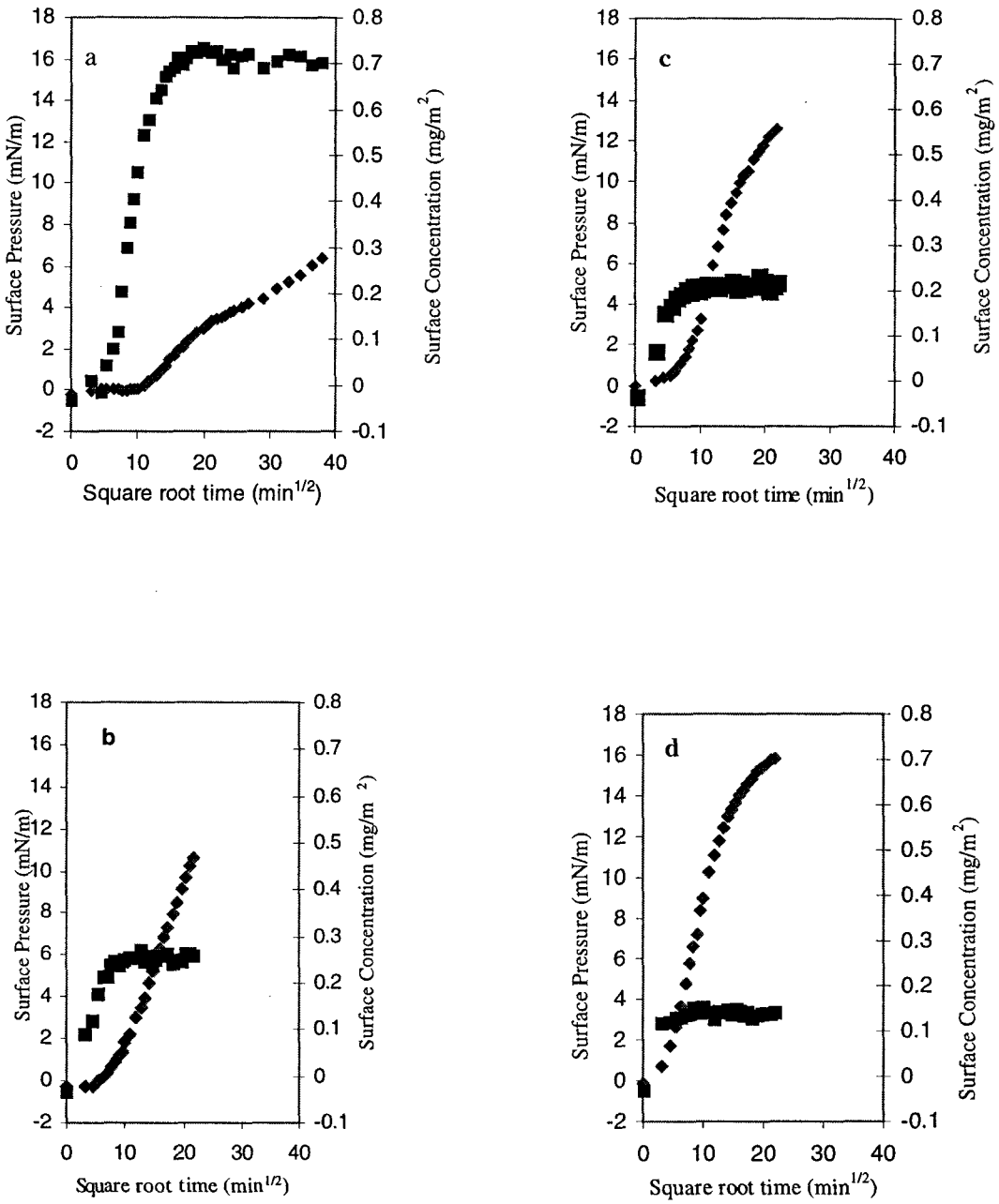

Figure 4.3. Kinetics of adsorption of [^{14}C]lysozyme from binary mixtures containing 1.5 μg/ml of [^{14}C]WT and varying concentration of unlabeled TRP. Bulk concentrations of unlabeled TRP were as follows: (a) 0, (b) 0.75 μg/ml, (c) 1.5 μg/ml, and (d) 3.0 μg/ml. Symbols ■ and ◆ represent surface concentration and surface pressure, respectively.

while changing the bulk concentration of unlabeled TRP from 0.75 to 3.0 μg/ml, the ratio of WT to TRP was varied from 2.0 to 0.5. According to the plots, an increase in TRP concentration continuously decreased the extent of WT adsorption at the air-water interface. The induction time of surface pressure kinetics of the mixture decreased with an increase in TRP concentration. No induction period was observed in the case of interfacial adsorbed mass kinetics. In the case of surface pressure kinetics, it is interesting to see that the presence of only 0.75 μg/ml TRP in the bulk phase resulted in a decrease in lag time from more than 100 to approximately 25 min. The lag time of the mixed protein solution progressively decreased with increasing concentration of TRP in the bulk phase. This may be due in part to the higher total bulk concentration which resulted in more molecule-molecule and molecule-surface collisions.

An increase in TRP concentration in the bulk phase also led to a decrease in D_{app} of WT (Figure 4.4). It implies that WT could not compress the adsorbed TRP molecules to create more adsorption sites for itself (1). This resulted in a decrease in unoccupied binding sites available at the interface as increasing numbers of TRP adsorb to the interface. If WT and TRP adsorb independently, D_{app} of WT should remain the same in all cases. Figure 4.3c and 4.3d show the surface concentration kinetics of [^{14}C]WT adsorbing from the mixtures of 1:1, and 1:2 of [^{14}C]WT:TRP, respectively. It is noticed that the adsorbed mass of [^{14}C]WT in Figure 4.3c is less than half of that shown in Figure 4.3a, and that the adsorbed mass of [^{14}C]WT in Figure 4.3d is less than one-third of that shown in Figure 4.3a. These results suggested that there is a preferential adsorption of TRP over [^{14}C]WT at the air-water interface, and that the ratio of surface concentrations

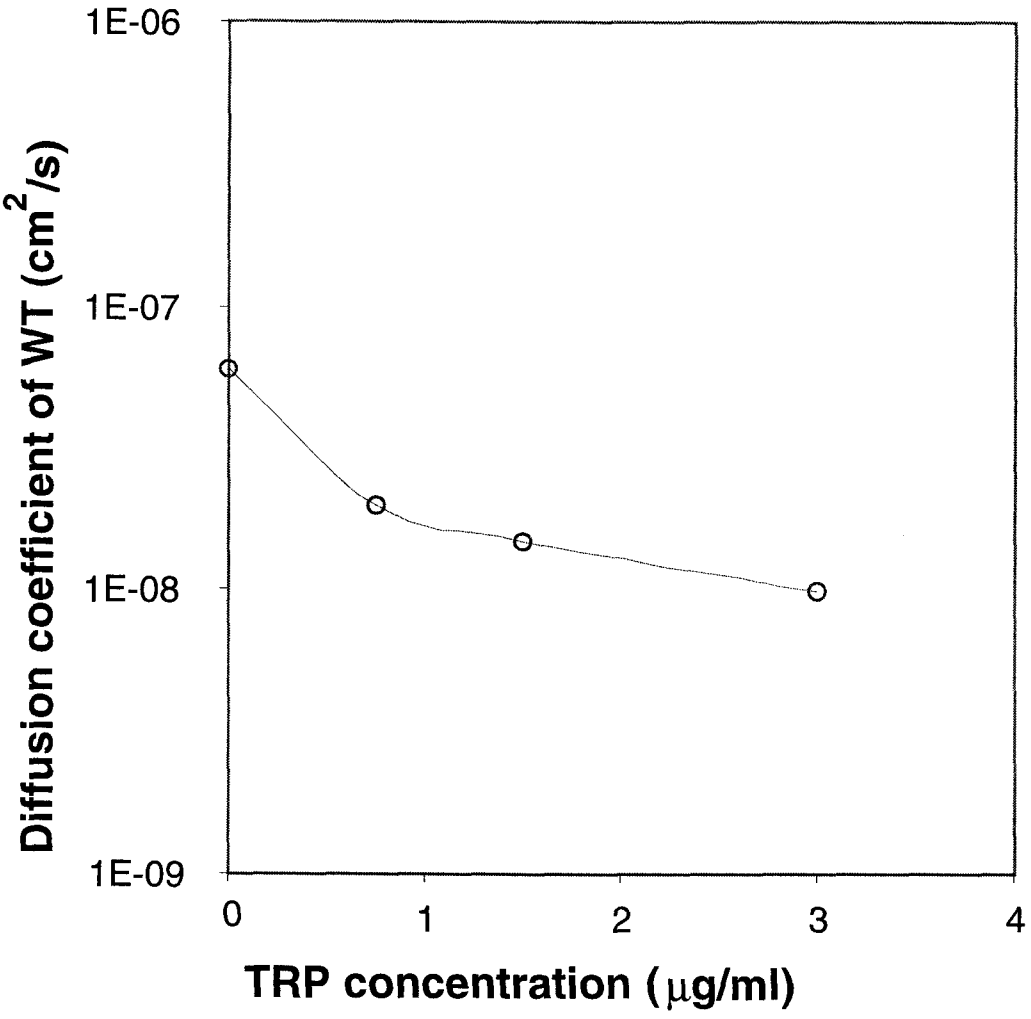

Figure 4.4. Effects of TRP concentration on the apparent diffusion coefficient of WT.

of [^{14}C]WT and TRP in the mixed film cannot be determined by the concentration ratio in the bulk phase.

4.4.3 Exchange studies

The results from displacement studies of adsorbed [^{14}C] T4L at the interface by bulk phase T4L are shown in Figure 4.5. When unlabeled WT or TRP was introduced into the subsurface of [^{14}C] WT after equilibrium adsorbed mass has been attained, there was no significant changes in surface radioactivity of the adsorbed layer. Similar results were obtained for the injections of unlabeled WT and TRP into the subsurface of [^{14}C] TRP after its adsorption equilibrium was reached.

4.4.4 Preferential adsorption studies

Results from two different studies on preferential adsorption of ^{14}C-labeled lysozyme are shown in Figure 4.6a and b. Both experiments suggested that preferential adsorption between unlabeled and labeled T4 lysozyme likely occurred. In Figure 4.6a, the surface cpm of molecules adsorbing from the mixture of 1:1 of [^{14}C]WT:[^{14}C]TRP is higher than the arithmetic sum of molecules adsorbing from the 1:1 ratio mixtures of [^{14}C]WT:TRP and WT:[^{14}C]TRP. Considering the surface cpm of molecules adsorbing from the binary mixture of [^{14}C]TRP and unlabeled TRP (Figure 4.6b), it is much lower than what would be expected for adsorption from a 1:1 mixture solution if radiolabeling has no effects on adsorption behavior of lysozyme. Though we suspect that radiolabeling

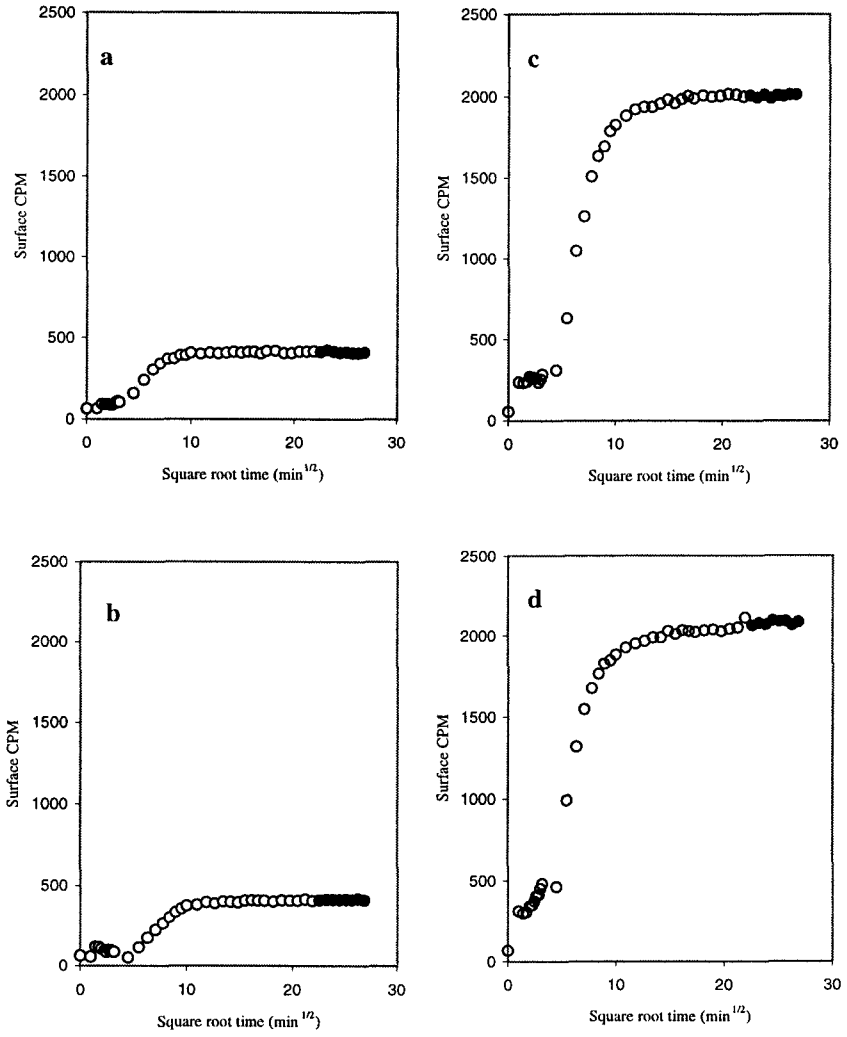

Figure 4.5. Exchange of adsorbed [^{14}C]lysozyme by unlabeled lysozyme. Opened circles (○)and closed circles (●) represent: (a) surface cpm of [^{14}C]WT before and after injection of unlabeled WT; (b) surface cpm of [^{14}C]WT before and after injection of unlabeled TRP; (c) surface cpm of [^{14}C]TRP before and after injection of unlabeled WT; and (d) surface cpm of [^{14}C]TRP before and after injection of unlabeled TRP, respectively.

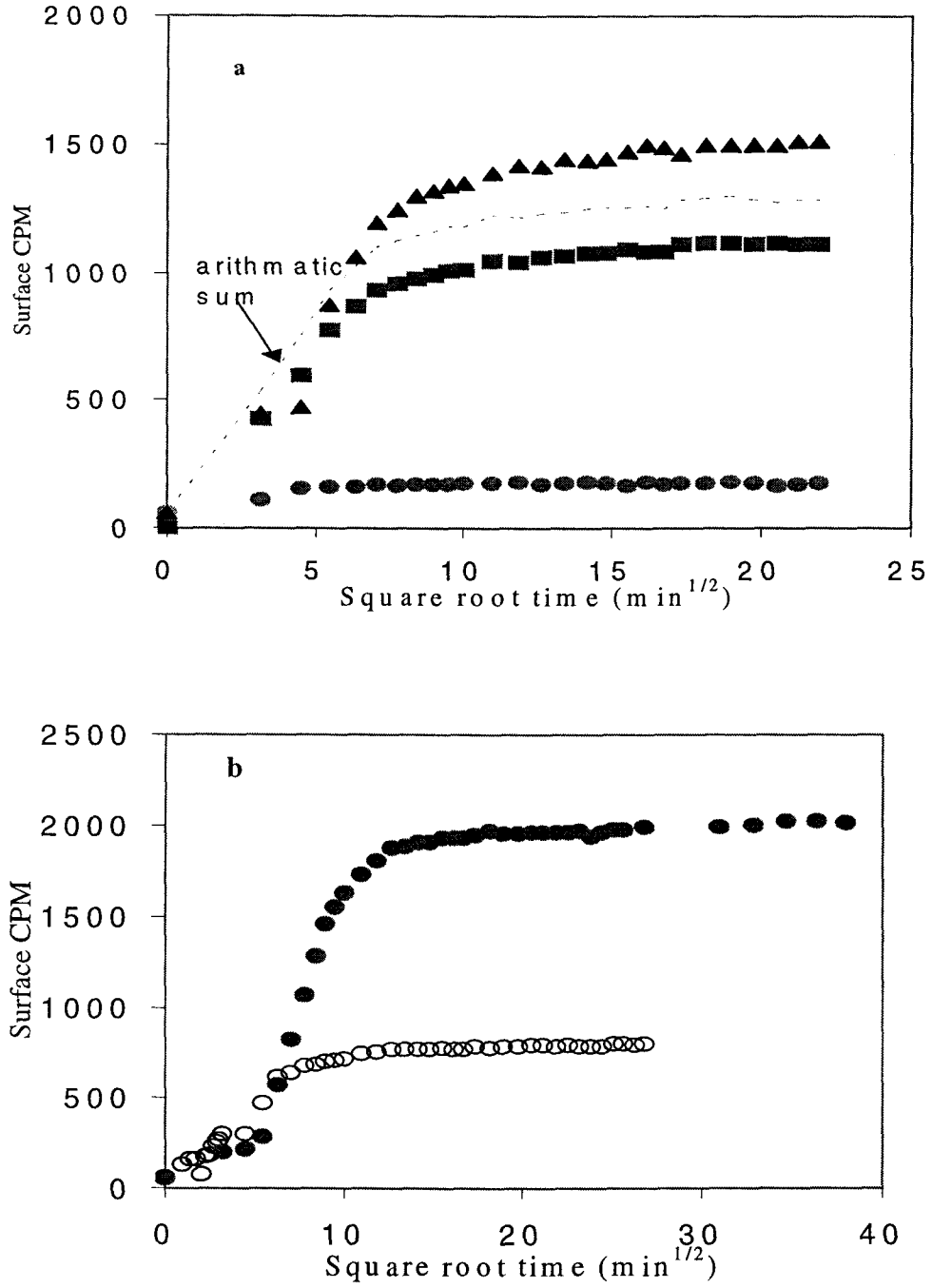

Figure 4.6. Kinetics showing a slight preferential adsorption of unlabeled lysozyme over [^{14}C]lysozyme. The surface cpm was represented with: (a) ▲, for 0.75 μg/ml [^{14}C]WT + 0.75 μg/ml [^{14}C]TRP; ●, for 0.75 μg/ml [^{14}C]WT + 0.75 μg/ml unlabeled TRP; ■, for 0.75 μg/ml unlabeled WT + 0.75 μg/ml [^{14}C]TRP; (b) ○, for 0.75 μg/ml [^{14}C]TRP + 0.75 μg/ml [^{14}C]TRP; and ●, for 1.5 μg/ml [^{14}C]TRP.

with ^{14}C isotope slightly altered the interfacial behavior of T4 lysozyme, resulting in a lower adsorbed mass of labeled proteins at the interface.

4.5 Summary

The results of this study suggested that the adsorption process of T4 lysozyme is affected by the structural stability of the protein. Data from adsorption kinetics of single protein systems indicated that adsorption of T4 lysozyme from the dilute bulk phase to the air-water interface is not diffusion-limited. The adsorption behavior of the more stable proteins (WT and CYS) seem to experience a higher energy barrier to adsorption at the interface than the adsorption behavior of the less stable protein (TRP).

4.6 Acknowledgement

This study was supported by the National Science Foundation through Grant CTS. 9501842. We acknowledge the use of experimental facilities at Dr. Srinivasan Damodaran's Laboratory, at the University of Wisconsin.

4.7 References

1. Anand, K. and S. Damodaran. 1995. Kinetics of adsorption of lysozyme and bovine serum albumin at the air-water inteface from a binary mixture., *J. Colloid. Interface Sci.* 176: 63-73.

2. Kitabatake, N. and E. Doi. 1982. Surface tension and foaming of protein solutions., *J. Food Sci.* **47:** 1218-1569.

3. Wang J., and J. McGuire. 1997. Surface tension kinetics of the wild type and four synthetic stability mutants of T4 phage lysozyme at the air-water interface., *J. Colloid. Interface Sci.* **185:** 371-323.

4. Wei, A.-P., J.N. Herron, and J.D. Andrade. 1990. The role of protein structure in surface tension kinetics. *in* From Clone to Clinic. (D. J.A. Crommelin and H. Schellekens, Eds.), p. 305. Kluwer Academic Publishers, Amsterdam.

5. Xu, S. and S. Damodaran. 1993. Comparative adsorption of native and denatured egg-white, human, and T4 phage lysozyme at the air-water interface., *J. Colloid. Interface Sci.* **159:** 124-133.

6. Kato, A. and K. Yutani. 1988. Correlation of surface properties with conformational stabilities of wild type and six mutant tryptophan synthase α-subunits substituted at the same position., *Protein Eng.* **2:** 153-156.

7. Tian, M., W-K Lee, M.K. Bothwell, and J. McGuire. 1998. Structural stability effects on adsorption of bacteriophage T4 lysozyme to colloidal silica., *J. Colloid Interface Sci.* **199:** In Press.

8. Alber, T. and B.W. Matthews. 1987. Structure and thermal stability of phage T4 lysozyme., *Meth. Enzymol.* **154:** 511-533.

9. Muchmore, D.C., L.P. McIntosh, C.B. Russel, D.E. Anderson, and F.W. Dahlquist. 1989. Expressiom and 15N labeling of proteins for proton and nitrogen-15 NMR., *Methods Enzymol.* **177:** 44-73.

10. Damodaran, S. and K.B. Song. 1991. Diffusion and energy barrier controlled adsorption of proteins at the air-water interface. *in* Interactions of Food Proteins. (N. Parris and R. Barferd, Eds.), ACS Symp Ser., Vol.454, p.104-121. American Chemical Society, Washington, DC.

11. Xu, S. and S. Damodaran. 1992. The role of chemical potential in the adsorption of lysozyme at the air-water interface., *Langmuir.* **8:** 2021-2027.

12. Damodaran, S. and S. Xu. 1996. The role of electrostatic forces in anomalous adsorption behavior of phosvitin at the air-water interface., *J. Colloid. Interface Sci.* **178:** 426-435.

13. Anand, K. and S. Damodaran. 1996. Dynamics of exchange between α_{s1}-casein and β-casein during adsorption at air-water interface., *J. Agric. Food Chem.* **44:** 1022-1028.

14. Xu, S. and S. Damodaran. 1993. Calibration of radiotracer method to study protien adsorption at interfaces., *J. Colloid. Interface Sci.* **157:** 485-490.

15. Graham, D.E. and M.C. Phillips. 1979. Proteins at liquid interfaces I: Kinetics of adsorption and surface denaturation., *J. Colloid. Interface Sci.* **70(3):** 403-414

16. Ward, A.F.H. and L. Tordai. 1946. Time-dependence of boundary tensions of solutions I: The role of diffusion in time-effects., *J. Chem. Phys.* **14:** 453-466.

17. Krijgsman, J. 1992. Chapter 7: Purification in Product Recovery. *in* Bioprocess Technology. (R.O. Jenkins, editor). p. 183. Butterworth-Heinemann Ltd., Oxford, England.

18. Levenspiel, O. 1986. Chapter 6: Flow through packed beds. *in* Engineering Flow and Heat Exchange. p. 120. Plenum Press, New York.

CHAPTER 5

CONCLUSIONS

Adsorption at solid-water interfaces were monitored with *in situ* ellipsometry and ^{125}I-radiolabeling. A comparison of the adsorption behavior to a simple model allowing parallel, irreversible adsorption into two conformational states directly from the single protein solution suggested that the extent and rate of adsorption are dependent on the conformational stability of the protein. The less stable variant adsorbed at the solid surface in a more tightly bound state and occupied more surface area.

According to the ^{125}I-radiolabeled data, the amount of adsorbed protein exchanged by the same species from the bulk (self-exchange), is to some extent dependent on the binding strength of the adsorbed protein. However, when the protein is exchanged with a dissimilar protein, the exchange reaction seems to be affected by the properties of the adsorbing protein rather than the binding strength of the adsorbed molecules. This phenomenon was also supported by results from ellipsometrically monitored sequential protein adsorption kinetics.

The kinetics of adsorption at the air-water interface of T4 lysozyme were monitored by measuring the surface radioactivity of ^{14}C-radiolabled protein, and by simultaneously measuring the change in surface pressure with the Wilhelmy plate method. Results indicated that adsorption of T4 lysozyme from a dilute bulk phase to the air-water interface is not diffusion-limited, contrary to normal assumptions relevent to this kind of experiment. The adsorption process is determined largely by the

conformational stability of the protein, and the more stable protein seems to experience a higher energy barrier to adsorption.

Competitive adsorption experiments suggested that there is a preferential adsorption of the less stable variant over the wild type at the air-water interface, and that the ratio of surface concentrations of each species in the mixed film cannot be determined from the concentration ratio in the bulk phase. Unlike the behavior exhibited at the solid-water interface, neither of the species adsorbed at the air-water interface can be replaced once the steady state was achieved. This may not be a fair comparison because the time needed for protein to reach steady state in these experiments is much longer at the air-water interface.

Bibliography

Alber, T. and B.W. Matthews. 1987. Structure and thermal stability of phage T4 lysozyme., *Meth. Enzymol.* **154:** 511-533.

Al-Makhlafi, H., A. Nasir, J. McGuire, and M. Daeschel. 1995. Adhesion of *Listeria monocytogenes* to silica surfaces after sequential and competitive adsorption of bovine serum albumin and β-lactoglobulin., *Appl. Environ. Microbiol.* **61(5):** 2013-2015.

Anand, K. and S. Damodaran. 1995. Kinetics of adsorption of lysozyme and bovine serum albumin at the air-water interface from binary mixture., *J.Colloid Interface Sci.* **176:** 63-73.

Anand, K. and S. Damodaran. 1996. Dynamics of exchange between α_{s1}-casein and β-casein during adsorption at air-water interface. , *J.Agric.Food Chem.* **44:** 1022-1028.

Arnold, G.E., J.I. Manchester, B.D. Townsend, and R.L. Ornstein. 1994. Investigation of domain motions in bacteriophage T4 lysozyme., *Biomolecular Structure and Dynamics.* **12:** 457-474.

Billsten, P., M. Wahlgren, T. Arnebrant, J. McGuire, and H. Elwing. 1995. Structural changes of T4 lysozyme upon adsorption to silica nanoparticles measured by circular dichroism., *J. Colloid Interface Sci.* **175:** 77-82.

Blum, L.J. and P.R. Coulet (Eds.). 1991. Biosensor Principles and Applications. p. 7. M. Dekker, New York.

Bohnert, J.L. and T.A. Horbett. 1986. Changes in adsorbed fibrinogen and albumin interactions with polymers indicated by decreases in detergent elutability., *J. Colloid Interface Sci.* **111:** 363-377.

Branden, C. and J. Tooze. 1991. Prediction, engineering, and design of protein structures. *in* Introduction to Protein Structure. p. 247-268. Garland Publishing, Inc., New York.

Brash, J.L. and T. Horbett. (Eds.)1995. Proteins at Interfaces: An overview. *in* Proteins at Interfaces II: Fundamentals and Applications. p. 1-25. ACS Books, Washington, DC.

Bruil, A., L.M. Brenneisen, J.G.A. Terlington, T. Beugling, W.G. van Aken, and J. Feijen. 1994. *In Vitro* leukocyte adhesion to modified polyurethane surfaces II: Effects of wettability., *J. Colloid Interface Sci.* **165:** 72-81.

Chen, Z.J., X.M. Ou, F.Q. Tang, and L. Jiang. 1996. Effect of nanometer particles on the adsorbability and enzymatic activity of glucose oxidase. *Colloids and Surfaces B: Biointerfaces* **7:** 173-179.

Cuypers, P.A., J.W. Corsel, M.P. Janssen, J.M.M. Kop, W.T. Hermens, and H.C. Hemker. 1983. The adsorption of prothrombin to phosphatidylserine multilayers quantitated by ellipsometry., *J. Biol. Chem.* **258:** 2426-2431.

Damodaran, S. and K.B. Song. 1991. Diffusion and energy barrier controlled adsorption of proteins at the air-water interface. *in* Interactions of Food Proteins. (N. Parris and R. Barferd, Eds.), ACS Symp Ser., Vol.454, p.104-121. American Chemical Society, Washington, DC.

Damodaran, S. and S. Xu. 1996. The role of electrostatic forces in anomalous adsorption behavior of phosvitin at the air-water interface., *J. Colloid. Interface Sci.* **178:** 426-435.

Dao-pin, S., D-I. Liao, and S.J. Remington. 1989. Electrostatic fields in the active sites of lysozymes., *Proc. Natl. Acad. Sci. USA* **86:** 5361-5365.

Dao-pin, S., E. Soderlind, W.A. Baase, J.A. Wozniak, U. Sauer, and B.W. Matthews. 1992. Cumulative site-directed charge-change replacements in bacteriophage T4 lysozyme suggest that long-range electrostatic interactions contribute little to protein stability., *J. Mol. Biol.* **221(3):** 873-887.

DeFeijter, J.A., J. Benjamins, and F.A. Veer. 1978. Ellipsometry as a tool to study the adsorption behavior of synthetic and biopolymers at the air-water interface., *Biopolymers* **17:** 1759-1772.

Elgersma, A.V., R.L.J. Zsom, J. Lyklema, and W. Norde. 1992. Adsorption competition between albumin and monoclonal immuno-gamma globulins on polystyrene lattices., *J. Colloid. Interface Sci.* **152:** 410-428.

Elwing, H. S. Welin, A. Askendal, and I. Lundström. 1988. Adsorption of fibrinogen as a measure of the distribution of methyl groups on silicon surfaces. *J. Colloid Interface Sci.* **123:** 306-308.

Graham, D.E. and M.C. Phillips. 1979. Proteins at liquid interfaces I: Kinetics of adsorption and surface denaturation., *J. Colloid. Interface Sci.* **70(3):** 403-414

Grütter, M.G., R.B. Hawkes, and B.W. Matthews. 1979. Molecular basis of thermostability in the lysozyme from bacteriophage T4., *Nature* **277:** 667-669.

Grütter, M.G. and B.W. Matthews. 1982. Amino acid substitutions far from the active site of bacteriophage T4 lysozyme reduce catalytic activity and suggest that the C-terminal lobe of the enzyme participates in substrate binding., *J. Mol. Biol.* **154:** 525-535.

Grütter, M.G., L.H. Weaver, T.M. Gray, and B.W. Matthews. 1983. Structure, function, and evolution of the lysozyme from bacteriophage T4. *in* Bacteriophage T4. p.356-360.

(Mathews, C.K., E.M. Kutter, G. Mosig, and P.M. Berget, eds.) Am. Soc. Microbiology., Washington, DC.

Helmkamp, R.W., R.L. Goodland, W.F. Bale, I.L. Spar, and L.E. Mutschler. 1960. High specific activity iodination of γ-globulin with iodine-131 monochloride., *Cancer Res.* **20:** 1495-1500.

Horbett, T.A. 1981. Adsorption of proteins from plasma to a series of hydrophilic-hydrophobic copolymers. II. Compositional analysis with the prelabeled protein technique., *J. Biomed. Mater. Res.* **15:** 673-695.

Horsley D., J. Herron, V. Hlady, and J.D. Andrade. 1987. Physicochemical and Biochemical Studies. *in* Proteins at Interfaces. (J.L. Brash and T.A. Horbett, eds.) p.290-304. ACS Symposium Series 343, Washington, DC.

Jentoft, N. and D.G. Dearborn. 1979. Labeling of proteins by reductive methylation using sodium cyanoborohydride., *J. Biol. Chem.* **254(4):** 4359-4365.

Kato, A., and K. Yutani. 1988. Correlation of surface properties with conformational stabilities of wild-type and six mutant tryptophan synthase α-subunits substituted at the same position., *Protein Eng.* **2:**153-156.

Kitabatake, N. and E. Doi. 1982. Surface tension and foaming of protein solutions., *J. Food Sci.* **47:** 1218-1569.

Krisdhasima, V., J. McGuire, and R.D. Sproull. 1992a. A one-film-model ellipsometry program for the simultaneous calculation of protein film thickness and refractive index., *Surf. Interface Anal.* **18:** 453-456.

Krijgsman, J. 1992. Chapter 7: Purification in Product Recovery. *in* Bioprocess Technology. (R.O. Jenkins, editor). p. 183. Butterworth-Heinemann Ltd., Oxford, England.

Krisdhasima, V., J. McGuire, and R.D. Sproull. 1992b. Surface hydrophobic influences on β-lactoglobulin adsorption kinetics., *J. Colloid Interface Sci.* **154(2):** 337-350.

Krisdhasima, V., P. Vinaraphong, and J. McGuire. 1993. Adsorption kinetics and elutability of α-lactalbumin, β-casein, β-lactoglobulin, and bovine serum albumin at hydrophobic and hydrophilic interfaces., *J. Colloid Interface Sci.***161:** 325-334.

Kunkel, T.A. 1985. Rapid and efficient site-specific mutagenesis without phenotype selection., *Proc. Natl. Acad. Sci. USA.* **82**: 488-492.

Kunkel, T.A. 1985. The mutational specificity of DNA polymerase-β during *in vitro* DNA synthesis. Production of frameshift, base substitution, and deletion mutations., *J. Biol. Chem.* **260:** 5787-5796.

Lee, J.H. and J.D. Andrade. 1988. Polymer Surface Dynamics. p. 111. Plenum Press, New York.

Levenspiel, O. 1986. Chapter 6: Flow through packed beds. *in* Engineering Flow and Heat Exchange. p. 120. Plenum Press, New York.

Lu, D.R. and K. Park. 1991. Effect of surface hydrophobicity on the conformational changes of adsorbed fibrinogen., *J. Colloid Interface Sci.* **144:** 271-281.

Lundström, I. 1985. Models of protein adsorption on solid surfaces., *Progr. Colloid Polymer Sci.* **70:** 76-82.

Lundström I., and H. Elwing. 1990. Simple kinetic model for protein exchange reactions on solid surfaces., *J. Colloid Interface Sci.* **136:** 68-84.

Matsumura, M., G. Signor, and B.W. Matthews. 1989. Sustainable increase of protein stability by multiple disulfide bonds., Nature. **342:** 291-293.

Matsumura, M., and B.W. Matthews. 1989. Control of enzyme activity by an engineered disulfide bond., *Science* **243:** 792-794.

Matthews, B.W., F.W. Dahlquist, and A.Y. Maynard. 1973. Crystallographic data for lysozyme from bacteriophage T4., *J. Mol. Biol.* **78:**575-576.

Matthews, D.E., R.A. Hessler, N.D. Denslow, J.S. Edwards, and T.W. O'Brien. 1982. Protein composition of the bovine mitochondrial ribosome., *J. Biol. Chem.* **257(8):** 8788-8794.

Means, G.E. and R.E. Feeney. 1968. Reductive alkylation of amino groups in proteins., *Biochemistry.* **7:** 2192-2201.

McGuire, J. and V. Krisdhasima. 1993. Relating contact surface hydrophobicity to molecular events influencing biological adhesion., *J. Adhesion Sci Technol.* **7(3):** 195-204.

McGuire, J., V. Krisdhasima, M.C. Wahlgren, and T. Arnebrant. 1995a. Comparative adsorption studies with synthetic, structural stability and charge mutants of bacteriophage T4 lysozyme. *in* Proteins at Interfaces II: Fundamentals and Applications. (J. Brash and T. Horbett, eds.), ACS Books, Washington, DC.

McGuire, J., M.C. Wahlgren, and T. Arnebrant. 1995b. Structural stability effects on the adsorption and dodecyltrimethyl ammonium bromide-mediated elutability of bacteriophage T4 lysozyme at silica surfaces., *J. Colloid Interface Sci.* **170:** 182-192.

McGuire, J., M.C. Wahlgren, and T. Arnebrant. 1995c. The influence of net charge and charge location on the adsorption and dodecyltrimethyl ammonium bromide-mediated elutability of bacteriophage T4 lysozyme at silica surfaces., *J. Colloid Interface Sci.* **170:** 193-202.

Muchmore, D.C., L.P. McIntosh, C.B. Russel, D.E. Anderson, and F.W. Dahlquist. 1989. Expressiom and 15N labeling of proteins for proton and nitrogen-15 NMR., *Methods Enzymol.* **177:** 44-73.

Olsson, J., A. Carlén, N.L. Burns, and K. Holmberg. 1995. Modified pellicle formation and reduced *in vitro* bacterial adherence after surface treatment with different siloxane polymers., *Colloids and Surfaces B: Biointerfaces* **5:** 161-169.

Pitt, W.G., K. Park, and S.L. Cooper. 1986. Sequential protein adsorption and thrombus deposition on polymeric biomaterials., *J. Colloid Interface Sci.* **111:** 343-362.

Podhipleux, N. 1994. Adsorption of selected charge mutants of bacteriophage T4 lysozyme at silanized silica surfaces. Master's thesis. Department of Food Science and Technology, Oregon State University, Corvallis, OR.

Podhipleux, N., V. Krisdhasima, and J. McGuire. 1996. Molecular charge effects on protein behavior at hydrophobic and hydrophilic solid surfaces., *Food Hydrocoll.* **10:** 285-293.

Ruzgas, T.A., V.J. Razumas, and J.J. Kulys. 1992. Sequential adsorption of γ-interferon and bovine serum albumin on hydrophobic silicon surfaces., *J. Colloid Interface Sci.* **151:** 136-143.

Shirahama, H., J. Lyklema, and W. Norde. 1990. Comparative protein adsorption in model systems., *J. Colloid. Interface. Sci.* **139:** 177-187.

Singla, B. 1994. Adsorption of selected stability mutants of bacteriophage T4 lysozyme at silanized silica surfaces. Master's thesis. Department of Chemical Engineering, Oregon State University, Corvallis, OR.

Suttiprasit , P. and J. McGuire. 1992. The surface activity of α-lactalbumin, β-lactoglobulin, and bovine serum albumin II : Some molecular influences on adsorption to hydrophilic and hydrophobic silicon surfaces., *J. Colloid Interface Sci.* **154:** 327-336.

Tian, M., W-K Lee, M.K. Bothwell, and J. McGuire. 1998. Structural stability effects on adsorption of bacteriophage T4 lysozyme to colloidal silica., *J. Colloid Interface Sci.* **199: In Press.**

Tsugita, A. and M. Inouye. 1968. Complete primary structure of phage lysozyme from *Escherichia coli* T4., *J. Mol. Biol.* **37:** 201-212.

Tsugita, A., M. Inouye, E. Terzaghi, and G. Streisinger. 1968. Purification of bacteriophage T4 lysozyme., *J. Biol. Chem.* **243:** 391-397.

Wang J., and J. McGuire. 1997. Surface tension kinetics of the wild type and four synthetic stability mutants of T4 phage lysozyme at the air-water interface., *J. Colloid. Interface Sci.* **185:** 371-323.

Wannerbegger, K., M. Wahlgren, and T. Arnebrant. 1996. Adsorption from lipase-surfactant solutions onto methylated silica surfaces., *Colloids and Surfaces B: Biointerfaces* **6:** 27-36.

Ward, A.F.H. and L. Tordai. 1946. Time-dependence of boundary tensions of solutions I: The role of diffusion in time-effects., *J. Chem. Phys.* **14:** 453-466.

Weaver, L.H. and B.W. Matthews. 1987. Structure of bacteriophage T4 lysozyme refined at 1.7 Å resolution., *J. Mol. Biol.* **193:**189-198.

Wei, A.-P., J.N. Herron, and J.D. Andrade. 1990. The role of protein structure in surface tension kinetics. *in* From Clone to Clinic. (D. J.A. Crommelin and H. Schellekens, Eds.), p. 305. Kluwer Academic Publishers, Amsterdam.

Xu, S. and S. Damodaran. 1992. The role of chemical potential in the adsorption of lysozyme at the air-water interface., *Langmuir.* **8:** 2021-2027.

Xu, S. and S. Damodaran. 1993a. Calibration of radiotracer method to study protien adsorption at interfaces., *J. Colloid. Interface Sci.* **157:** 485-490.

Xu, S. and S. Damodaran. 1993b. Comparative adsorption of native and denatured egg white, human, and T4 phage lysozyme at the air-water interface., *J. Colloid. Interface Sci.* **159:** 124-133.

APPENDICES

APPENDIX A

Determination of surface contact angles

Contact angles of silica surfaces and glass cover slips were measured with a goniometer. Deionized distilled water was used as a diagnostic liquid when measuring contact angles of hydrophilic and hydrophobic glass cover slips. A series of EtOH in water solutions was used as diagnostic liquids when measuring the contact angles of hydrophobic and hydrophilic silica. Measurements were repeated at least 3 times and the average values as well as the standard deviations were calculated and tabulated in Table A1 and A2.

Table A1. Contact angles of hydrophobic and hydrophilic glass cover slips as measured with a goniometer, using deionized distilled water as a diagnostic liquid.

Surface	Contact Angle (degree)			
	Sample #1	Sample #2	Sample #3	Average (± SD)
Hydrophobic	74.0	73.0	71.5	72.8 ± 1.3
Hydrophilic	5.0	7.0	4.5	5.5 ± 1.3

Table A2. Contact angles of hydrophobic and hydrophilic silica as measured with a goniometer, using deionized distilled water, 15% ethanol, and 30% ethanol as diagnostic liquids.

Surface	Diagnostic Liquid	Contact Angle (degree)				
		#1	#2	#3	#4	Average (± SD)
Hydrophobic	DDW	82.0	77.0	78.0	83.0	80.0 ± 1.3
	15% EtOH	58.0	59	58.0	60.5	58.9 ± 1.2
	30% EtOH	55.0	53.5	52.0	53.0	53.4 ± 1.2
Hydrophilic	DDW	12.5	10.0	14.0	16.5	13.2 ± 2.7
	15% EtOH	8.0	6.5	5.5	6.0	6.5 ± 1.1
	30% EtOH	0	0	0	0	0

APPENDIX B

Determination of percent adsorbed mass eluted by DTAB
from single protein systems

In order to calculate the amount of protein adsorbed that is elutable by DTAB, the average values of the adsorbed mass after the first rinse and the adsorbed mass after the second rinse were estimated (see Figure B1). Then the percent mass eluted was calculated from:

$$\%Eluted = \frac{(R_1 - R_2)}{R_1} * 100$$

where R_1 = the average adsorbed mass after the first rinse,

and R_2 = the average adsorbed mass after the second rinse.

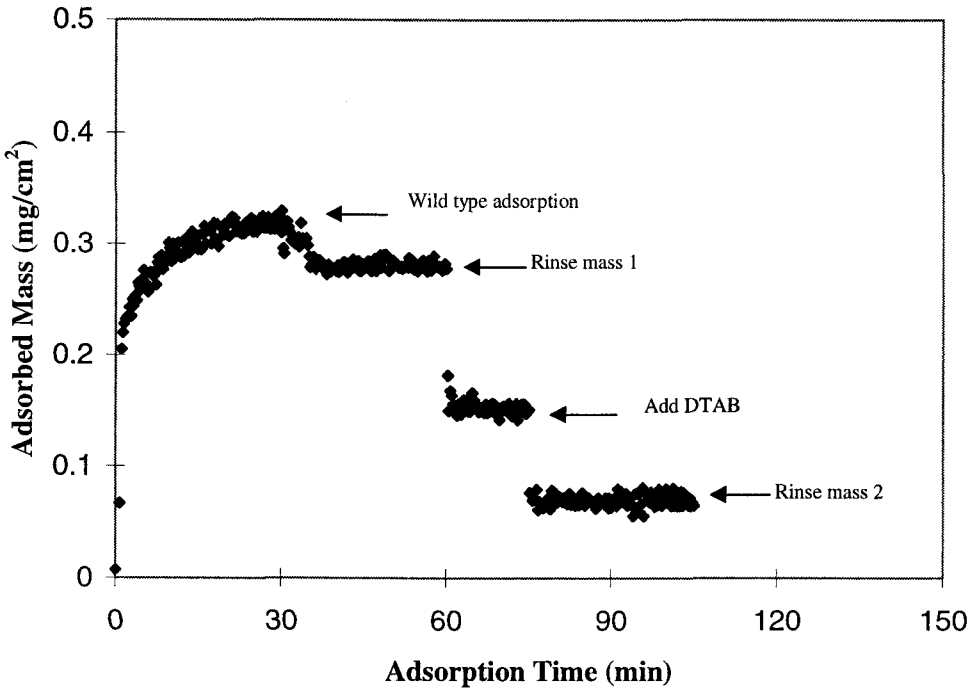

Figure B1. Adsorption kinetics of wild type on hydrophobic silica, follows by elution with DTAB.

The average values of percent adsorbed mass eluted by DTAB for wild type and TRP mutant from hydrophobic and hydrophilic silica after 30 min and 2 h adsorption are shown in Table B1.

Table B1. Percent adsorbed mass eluted by DTAB from hydrophobic and hydrophilic silica surfaces after 30 min and 2 h adsorption.

Protein	Surface					
	Hydrophobic			Hydrophilic		
	Rinsed Mass (mg/m^2)	After DTAB (mg/m^2)	% Eluted	Rinsed Mass (mg/m^2)	After DTAB (mg/m^2)	% Eluted
30 min						
Wild Type	2.809	0.755	73.1	2.401	0.871	63.7
TRP Mutant	2.034	0.769	62.2	2.035	1.045	48.6
2 h						
Wild Type	2.952	0.728	75.3	2.561	0.853	66.7
TRP Mutant	2.135	0.770	63.9	2.097	1.090	47.9

APPENDIX C

Determination of percent adsorbed mass eluted by DTAB
from sequential adsorption systems

In order to calculate the amount of protein adsorbed that is elutable by DTAB after contacting the pre-adsorbed surface with the second protein, average values of the adsorbed mass after the first rinse and the adsorbed mass after the third rinse were estimated (see Figure C1). Then the percent mass eluted was calculated from:

$$\%Eluted = \frac{(R_1 - R_3)}{R_1} * 100$$

where R_1 = the average adsorbed mass after the first rinse,

and R_3 = the average adsorbed mass after the third rinse.

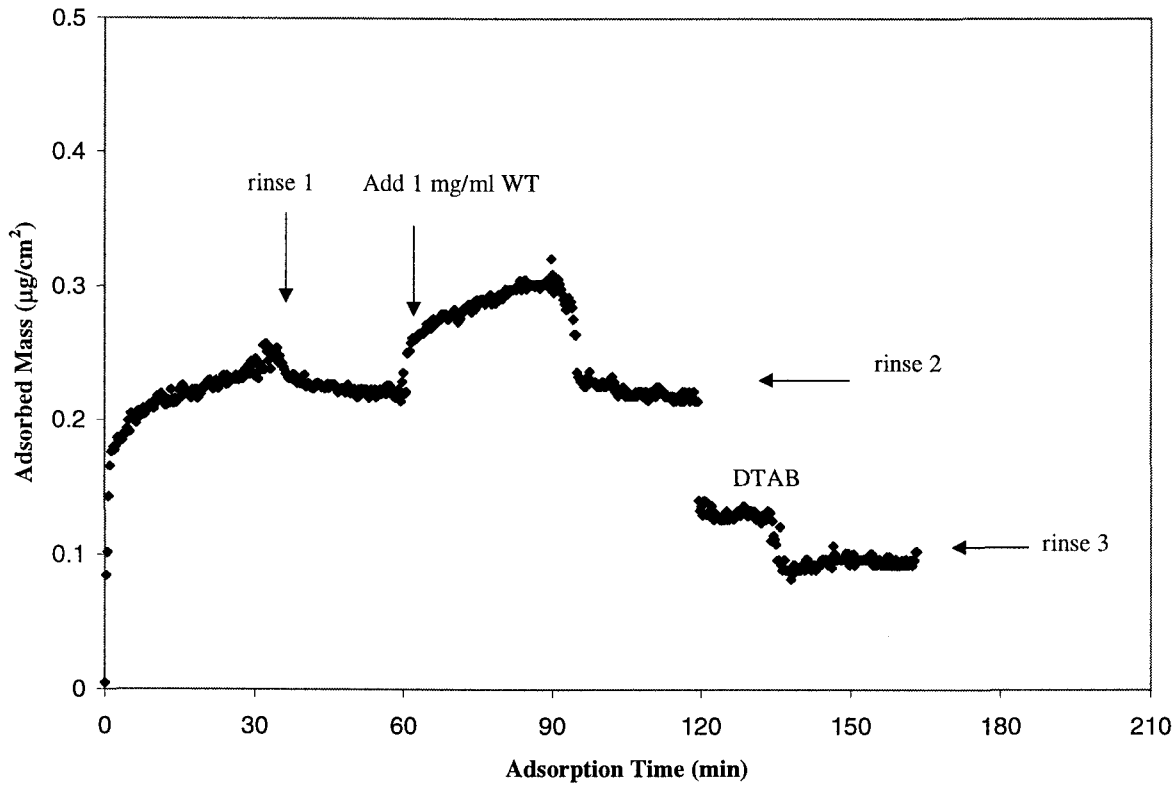

Figure C1. Sequential adsorption kinetics of TRP on hydrophilic silica, follows by WT and DTAB, respectively.

The average values of percent adsorbed mass eluted by DTAB for sequential adsorption experiments of wild type followed by TRP, and of TRP followed by wild type from hydrophobic and hydrophilic silica are shown in Table C1.

Table C1. Percent adsorbed mass eluted by DTAB after exposure to second protein.

Second protein conc. (mg/ml)	Second protein contact time (min)	First protein adsorbed mass eluted (%)			
		WT/TRP		TRP/WT	
		Hydrophobic	Hydrophilic	Hydrophobic	Hydrophilic
0.01	15	75.2	61.0	67.3	51.7
	30	-	59.3	68.0	56.2
	45	-	62.3	67.9	56.1
	60	76.1	63.2	68.0	61.2
1.0	15	76.2	63.2	68.1	44.2
	30	76.7	61.6	67.7	52.2
	45	76.2	60.9	61.4	56.7
	60	75.5	61.9	68.5	49.9

APPENDIX D

Determination of kinetic rate constants of T4 lysozyme adsorption from the parallel adsorption model

Parameters k_1C and k_2C are directly determined by non-linear regression analysis of the ellipsometric data fit to the parallel adsorption kinetic model proposed by McGuire et al. (1995b), shown in Figure 1.1b. Only the first part of the data (first protein adsorption and rinse) was used to calculate the kinetic rate constants governing the adsorption behavior of lysozyme from single protein systems. In using this model, the values of a (the ratio of the interfacial area occupied by a molecule adsorbed in state 2 to that occupied by a molecule adsorbed in state 1) for hydrophilic and hydrophobic silica surfaces were 2.095 and 2.052, respectively. These are values estimated from experimental data, assuming a monolayer coverage. Values of parameters k_1C, k_2C, from each replication, as well as their standard deviations for adsorption to hydrophobic silica are shown in Table D1 and D2. Same parameters for adsorption to hydrophilic silica are shown in Table D3 and D4. The average values of k_1C, k_2C, and the ratio k_2/k_1 are tabulated in Table D5.

Table D1. Kinetic model parameters from the parallel adsorption model (Figure 1.1b) for the wild type lysozyme on hydrophobic silica, using non-linear regression analysis.

Filenames	Rate Constants (min^{-1})	
	K_1C	K_2C
614w4	0.366642	0.232713
623w	0.443681	0.253004
417w	0.383093	0.200706
522w	0.241898	0.199917
526w	0.285738	0.23385
97917w3	0.302108	0.155932
97703w1	0.241676	0.152363
97704w2	0.296356	0.172943
518w	0.255423	0.161364
519w2	0.216213	0.135898
97820w1	0.246342	0.295066
97820w2	0.113198	0.160301
97915w1	0.314244	0.177755
97915w2	0.289578	0.172021
Average ± SD	0.285 ± 0.077	0.193 ± 0.044

Table D2. Kinetic model parameters from the parallel adsorption model (Figure 1.1b) for TRP mutant lysozyme on hydrophobic silica, using non-linear regression analysis.

Filenames	Rate Constants (min^{-1})	
	K_1C	K_2C
605tt	0.050416	0.356392
0103ttt	0.040544	0.246094
1105t1	-0.01709	0.589522
1103t1	0.000908	0.208752
408t2	0.007728	0.234845
501t	-0.00143	0.421505
97108t1	0.01114	0.367361
97918t1	0.090827	0.417913
97108t2	0.008121	0.313855
410tt	0.041159	0.377368
412t	0.133342	0.508685
97102t1	0.019575	0.499347
97102t2	-0.00812	0.519334
412t2	0.067254	0.469416
97103t1	0.0024016	0.52073
97107t1	0.018212	0.553393
97831t1	0.035098	0.410696
97920t	0.057493	0.546008
97921t	0.07507	0.331437
97828t1	0.04534	0.508546
97829t1	-0.00674	0.590857
97829t2	0.027014	0.619316
97827t1	-0.0098	0.643827
97827t2	0.086428	0.353243
97922t	0.038615	0.490365
97901t1	0.020611	0.367116
97923t	0.048503	0.346554
97924t	0.099915	0.406402
Average ± SD	0.035 ± 0.037	0.436 ± 0.115

Table D3. Kinetic model parameters from the parallel adsorption model (Figure 1.1b) for the wild type lysozyme on hydrophilic silica, using non-linear regression analysis.

Filenames	Rate Constants (min^{-1})	
	K_1C	K_2C
614w	0.130021	0.195726
621w	0.176867	0.282039
0107w2	0.179966	0.211671
514w	0.10508	0.237127
502w2	0.14155	0.219036
502w	0.136862	0.155279
612w	0.13205	0.181664
514w2	0.15172	0.239688
502w3	0.223448	0.198912
515w	0.124199	0.201622
612w2	0.096447	0.142924
97524w1	0.16322	0.250185
97602w	0.221837	0.245983
97603w	0.120519	0.170698
97605w	0.175666	0.176304
97818w1	0.14599	0.244772
97721w1	0.158599	0.279741
97722w1	0.134026	0.256065
97722w2	0.128953	0.187836
97723w1	0.1033	0.312672
97819w1a	0.156699	0.25785
97731w1	0.087208	0.190828
97723w2	0.127611	0.184086
97819w2	0.170573	0.269758
97911w	0.1214809	0.2099234
9765w1	0.110767	0.232347
97730w1	0.107054	0.1226
97818w2	0.098692	0.165871
Average ± SD	0.140 ± 0.034	0.215 ± 0.045

Table D4. Kinetic model parameters from the parallel adsorption model (Figure 1.1b) for TRP mutant lysozyme on hydrophilic silica, using non-linear regression analysis.

Filenames	Rate Constants (min^{-1})	
	K_1C	K_2C
603t3	0.00833	0.382621
621t2	0.024435	0.355072
417t2	-0.00588	0.420634
409tt	0.015176	0.400064
409t3	0.126127	0.264535
97831t2	0.016926	0.419623
410t	-0.00935	0.368781
410t2	0.075571	0.39605
425t	0.013141	0.370297
429t	0.031711	0.407076
429t2	0.01841	0.444115
501t3	0.007285	0.398333
430t	0.005918	0.389469
430t2	0.035344	0.418695
501t2	0.017271	0.349276
97528t1	0.148541	0.40957
97528t2	0.04335	0.333295
97801t2	0.095671	0.277784
97801t1	0.084679	0.370229
97524t2	-0.02492	0.762942
97524t1	0.15277	0.410964
97530t1	0.051232	0.465088
9763t1	0.011075	0.46004
9763t2	0.07446	0.239578
97525t1	0.069503	0.416163
97526t1	0.101214	0.97654
97526t2	0.066377	0.40984
Average ± SD	0.0464 ± 0.047	0.419 ± 0.141

Table D5. The average values of kinetic rate constants from ellipsometric measurements, based on the parallel adsorption model (Figure 1.1b).

Protein	Surface	Rate Constants		
		K_1C (min^{-1})	K_2C (min^{-1})	K_2/K_1
Wild Type	Hydrophobic	0.285	0.193	0.7
	Hydrophilic	0.140	0.215	1.5
TRP Mutant	Hydrophobic	0.035	0.436	12.5
	Hydrophilic	0.046	0.419	9.1

APPENDIX E

Determination of kinetic rate constants from radiolabeling experiments

The exchange rate constants of ^{125}I-labeled lysozyme were obtained by combining the data from 2 experiments; sequential adsorption, and spontaneous desorption studies. Radioactivity data was compared to the ellipsometric adsorbed mass of lysozyme. The changes in radioactivity of the labeled protein after contacting with the unlabeled second protein with respect to the original radioactivity were plot as a function of the second protein contact time. Only the initial data was used in the linear regression analysis of the plots. Rate constants K and K_d can be obtained by modifying [Eq. 2.21] to be fit to the plots shown in Figure E1, E2, E3, and E4.

In the presence of second protein in sequential adsorption experiement, [Eq.2.21] becomes:

$$\ln\left(\frac{\theta_A}{\theta_{A0}}\right) = -Kt$$

where

$$K = K_e C_B + K_d. \qquad \text{[Eq.E1]}$$

Without the second protein in the bulk concentration (spontaneous desorption experiment), $K_e C_B$ becomes zero. Therefore,

$$\ln\left(\frac{\theta_A}{\theta_{A0}}\right) = -K_d t. \qquad \text{[Eq.E2]}$$

Rate constant $K_e C_B$ can be calculated by subtracting K_d from K as shown in [Eq.E1].

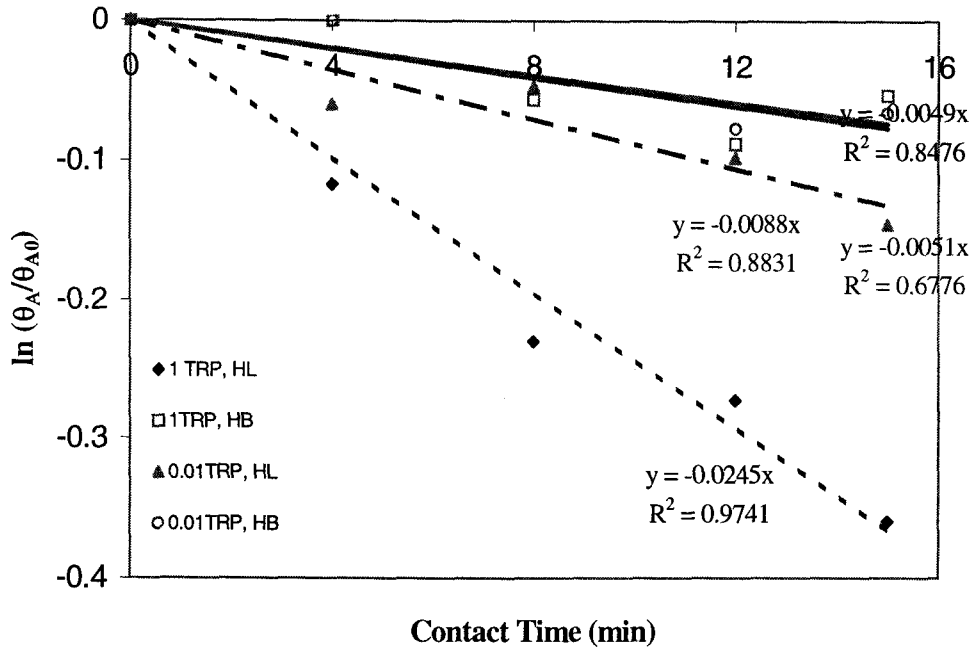

Figure E1. Exchange kinetic plot of ^{125}I-labeled WT on glass surfaces.

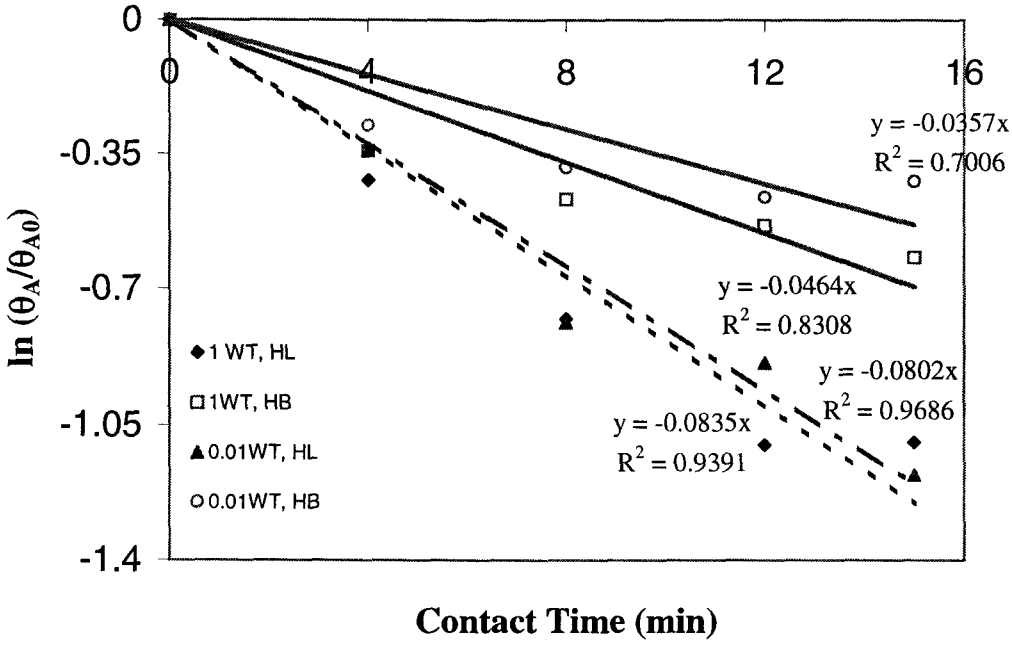

Figure E2. Exchange kinetic plot of ^{125}I-labeled TRP on glass surfaces.

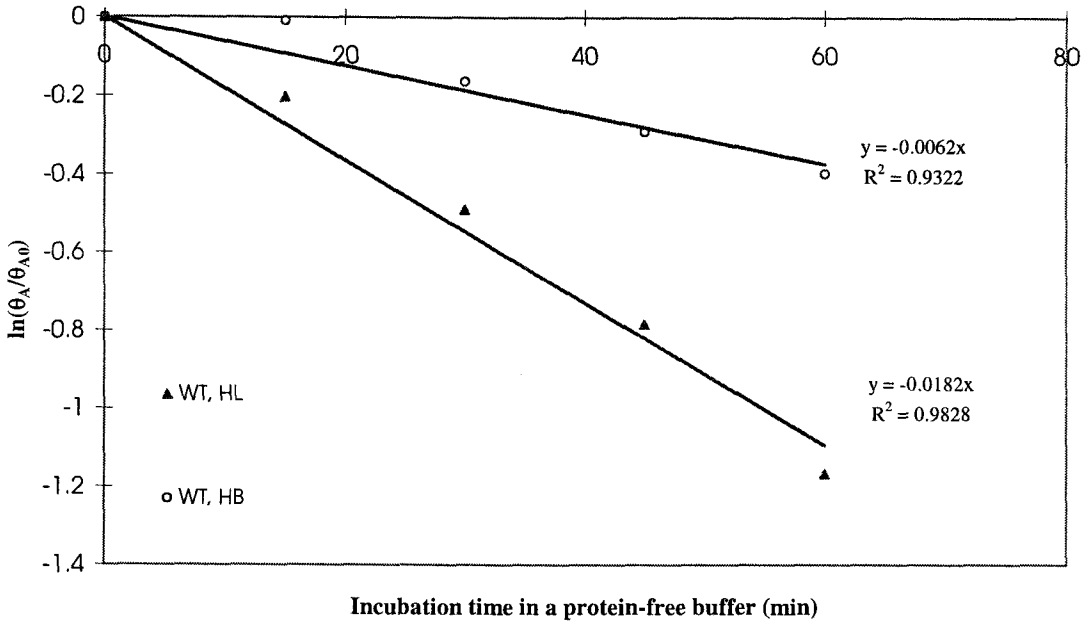

Figure E3. Desorption kinetic plot of ^{125}I-labeled WT on glass surfaces.

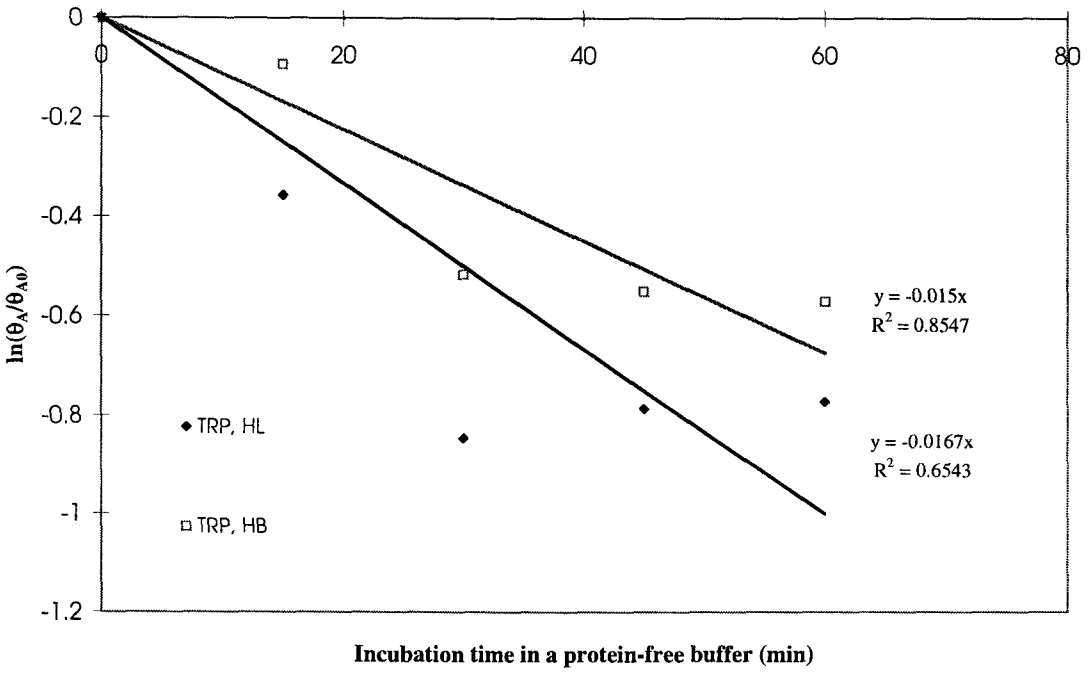

Figure E4. Desorption kinetic plot of ^{125}I-labeled TRP on glass surfaces.

Rate constants K, K_d, and K_eC_B from sequential adsorption of WT followed by TRP, and of TRP followed by WT on hydrophilic and hydrophilic glass cover slips are tabulated in Table E1.

Table E1. Kinetic rate constants obtained from sequential adsorption study of ^{125}I-labeled lysozyme to glass cover slips (* indicates ^{125}I-labeled protein).

Bulk conc. of second protein	Rate Constants (min^{-1})	WT*/TRP		TRP*/WT	
		Hydrophobic	Hydrophilic	Hydrophobic	Hydrophilic
0.01 mg/ml	K	0.0049	0.0088	0.0357	0.0802
	K_d	0.0062	0.0182	0.0150	0.0273
	K_eC_B	-0.0013	-0.0094	0.0207	0.0529
1 mg/ml	K	0.0051	0.0245	0.0464	0.0835
	K_d	0.0062	0.0182	0.0150	0.0273
	K_eC_B	-0.0011	0.0063	0.0314	0.0562

APPENDIX F

Determination of diffusion coefficient for T4 lysozyme in water

Diffusion coefficient of T4 lysozyme in water can be estimated using the Stokes-Einstein equation (Krijgsman, 1992):

$$D = \frac{kT}{6\pi\eta r_m} \qquad \text{[Eq.F1]}$$

where D = diffusion coefficient (m^2/s),

k = Bolzmann's constant ($1.38x10^{-23}$ J/K),

T = absolute temperature (K),

$\pi = 3.1416$,

η = viscosity of the solvent (Pa-s),

and r_m = molecular radius or Stokes radius (m).

The adsorption experiments at air-water interface were carried out 24 °C. We assumed the viscosity of the diluted protein solution to be equal to that of pure water, which is 10^{-3} Pa-s. Substituting $T = 24+273 = 297$ K into [Eq.F1]:

$$D = \frac{\left[\left(1.38x10^{-23}\right)*(297)\right]}{\left[6*(3.1416)*\left(10^{-3}\right)\right]} * r_m$$

or $$D = \frac{2.17\times10^{-19}}{r_m} \qquad \text{[Eq.F2].}$$

T4 lysozyme molecule is a cylinder with N-terminal lobe diameter of 2.4 nm, and C-terminal lobe diameter of 2.8 nm. The cylinder is 5.4 nm in height. Since the molecule is non-spherical, we need to estimate r_m from the hydrodynamic particle size by using the following equation:

$$d_p = \phi \cdot d_{sph} \qquad \text{[Eq.F3]}$$

where d_p = hydrodynamic particle diameter (m),

ϕ = sphericity of the particle (dimensionless),

and d_{sph} = diameter of a sphere having the same volume as the particle.

According to Levenspiel (1986), the sphericity of particles in cylinder shape is equal to 0.87 when the cylinder height (h) is equal to the cylinder diameter (d), and equal to 0.70 when h is equal to $5d$. In our case, the average cylinder diameter (average from N- and C-terminal lobes) is equal to 2.6 nm, and h is equal to $2.08d$. Therefore the sphericity of T4 lysozyme is approximately 0.80.

Volume of T4 lysozyme cylinder (V_c) can be calculated from:

$$V_c = \pi r_c^2 h$$

$$V_c = \frac{\pi d_c^{\,2} h}{4}$$

$$V_c = \frac{\left[3.1416 * \left(2.6\times10^{-9}\right) * \left(5.4\times10^{-9}\right)\right]}{4}$$

$$V_c = 2.87\times10^{-26} m^3.$$

Volume of a sphere (V_{sph}) is calculated by:

$$V_{sph} = \frac{4}{3}\pi r_{sph}^3$$

$$2.87\times10^{-26} = \frac{4}{3} * (3.1416) * r_{sph}^3$$

$$r_{sph}^3 = 6.85\times10^{-27}$$

$$r_{sph} = 1.90\times10^{-9}$$

or $$d_{sph} = 3.80\times10^{-9}.$$

Substitution of d_{sph} = 3.80x10^{-9} m, and ϕ = 0.80 into [Eq.F3] yields d_p = 3.04x10^{-9} m. [Eq.F2] can be modified as:

$$D = \frac{2.17 \times 10^{-9}}{d_p/2} \qquad \text{[Eq.F4].}$$

Substituting d_p into the above equation results in diffusion coefficient of 1.43×10^{-10} m^2/s or 1.43×10^{-6} cm^2/s.

APPENDIX G

Determination of diffusion coefficient for T4 lysozyme at air-water interface

According to Xu and Damodaran (1992) the apparent diffusion coefficient of lysozyme at the air-water interface can be estimated from the experimental data, using the following equation:

$$\Gamma = 2C_o\left(D_{app}/\pi\right)^{0.5} t^{0.5} \qquad \text{[Eq.G1]}$$

where Γ = surface concentration (mg/cm^2),

C_o = bulk concentration (1.5 mg/ml),

D_{app} = apparent diffusion coefficient (cm^2/s),

$\pi = 3.1416$,

and t = square root time (s$^{0.5}$).

Since [Eq.G1] is a linear relationship and does not apply for lag and plateau periods, only the straight portions of experimental data (Table G1) can be used to estimate the apparent diffusion coefficient (see Figure G1).

Figure G1 shows the relationship between the surface concentration of lysozyme and the square root time. We can use [Eq.G1] to fit the data and find D_{app} from:

$$D_{app} = 3.1416 * \left(slope / 3\times10^{-3} \right)^2 \qquad \text{[Eq.G2].}$$

The results are presented in Table G2.

Table G1. Surface concentration of bacteriophage T4 lysozyme at the air-water interface.

Time (min)	Square root time ($s^{0.5}$)	Surface concentration (mg/cm^2)		
		WT	CYS	TRP
40	48.99	8.02×10^{-6}	1.44×10^{-5}	2.18×10^{-5}
50	54.77	1.17×10^{-5}	2.46×10^{-5}	3.28×10^{-5}
60	60	2.04×10^{-5}	3.25×10^{-5}	4.33×10^{-5}
70	64.81	2.99×10^{-5}	4.13×10^{-5}	5.27×10^{-5}
80	69.28	3.52×10^{-5}	4.62×10^{-5}	6.02×10^{-5}
90	73.48	4.06×10^{-5}	4.93×10^{-5}	6.43×10^{-5}
100	77.46	4.63×10^{-5}	5.63×10^{-5}	6.75×10^{-5}

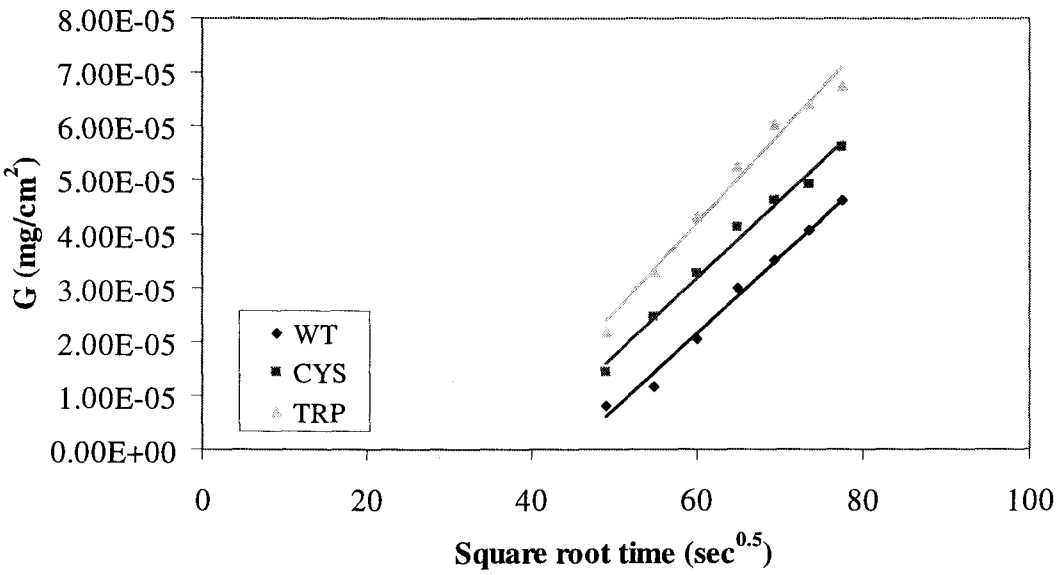

Figure G1. Relationship between the surface concentration of lysozyme and the square root time.

Table G2. Apparent diffusion coefficient of bacteriophage T4 lysozyme at the air-water interface, using [Eq.G2].

Protein	ΔΔG (kcal/mol)	Slope	R^2	D_{app} (cm^2/s)
CYS	+1.2	$1x10^{-6}$	0.9889	$3.49x10^{-7}$
WT	0	$1x10^{-6}$	0.9811	$3.49x10^{-7}$
TRP	-2.8	$2x10^{-6}$	0.9888	$1.40x10^{-6}$

APPENDIX H

Determination of surface oxidation time

Before the silica plates were cut and treated, they were oxidized in a furnace under 1 atm O_2 and 1,000 ^{o}C until the oxide layer on the surface is approximately 300 Å to reduce signals originated from refraction of the light due to the original oxide layer (about 20 Å). This number is arbitrarily chosen. In order to determine the oxidation time, silica plates are baked in a furnace under the specified conditions for 5, 10, 15, 20, 25, 30, and 35 min. After cooling down to the room temperature the thickness of oxide layer was measured, and the relationship between the thickness of the oxide layer and the oxidation time was shown in a semi-log scale (Figure H1). From this relationship, the oxidation time that will result in a 300 Å thickness of oxide layer is approximately 17 min.

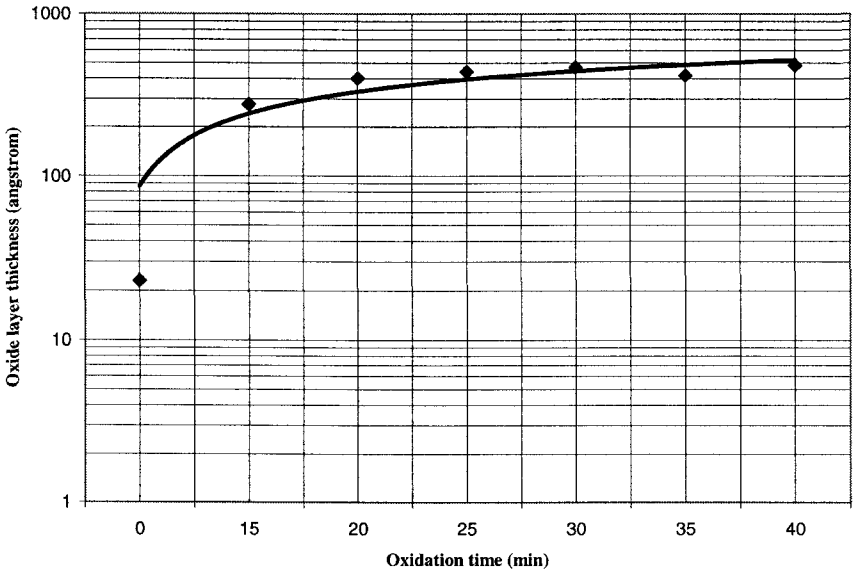

Figure H1. Relationship between oxidation time of the silica plate and the resulted thickness of oxide layer.